

ANTIBIOFILM ACTIVITIES AND PROTEOMIC ANALYSIS OF *CANDIDA TROPICALIS* IN RESPONSE TO TERPENES

Ph.D. THESIS

by

APURVA CHATRATH



**DEPARTMENT OF BIOTECHNOLOGY
INDIAN INSTITUTE OF TECHNOLOGY ROORKEE
ROORKEE - 247667, INDIA
SEPTEMBER, 2019**



ANTIBIOFILM ACTIVITIES AND PROTEOMIC ANALYSIS OF *CANDIDA TROPICALIS* IN RESPONSE TO TERPENES

A THESIS

*Submitted in partial fulfilment of the
requirements for the award of the degree
of*

DOCTOR OF PHILOSOPHY

in

BIOTECHNOLOGY

by

APURVA CHATRATH



**DEPARTMENT OF BIOTECHNOLOGY
INDIAN INSTITUTE OF TECHNOLOGY ROORKEE
ROORKEE – 247 667 (INDIA)
SEPTEMBER, 2019**







**©INDIAN INSTITUTE OF TECHNOLOGY ROORKEE, ROORKEE- 2019
ALL RIGHTS RESERVED**



INDIAN INSTITUTE OF TECHNOLOGY ROORKEE ROORKEE

STUDENT'S DECLARATION

I hereby certify that the work presented in the thesis entitled “**ANTIBIOFILM ACTIVITIES AND PROTEOMIC ANALYSIS OF *CANDIDA TROPICALIS* IN RESPONSE TO TERPENES**” is my own work carried out during a period from January, 2014 to September, 2019 under the supervision of Prof. Ramasare Prasad, Professor, Department of Biotechnology, Indian Institute of Technology Roorkee, Roorkee.

The matter presented in this thesis has not been submitted for the award of any other degree of this or any other Institute.

Dated: _____

(APURVA CHATRATH)

SUPERVISOR'S DECLARATION

This is to certify that the above mentioned work is carried out under my supervision.

Dated: _____

(Ramasare Prasad)

The Ph.D. Viva-Voce examination of **Apurva Chatrath**, Research Scholar, has been held on **December 04, 2019**.

Chairperson, SRC

Signature of External Examiner

This is to certify that the student has made all the corrections in the thesis.

Signature of Supervisor

Head of the Department

Dated: _____



ABSTRACT

Candida albicans and the emerging threats caused by non-*albicans Candida* species have started to show resistance which calls for identification of new alternatives or modification of the existing antifungal agents to defy the dominant tendency of infection. Presently, available anti-*Candida* drugs exhibit a high frequency of resistance, low specificity and toxicity at a higher dosage. In addition, the discovery of natural or synthetic anti-*Candida* drugs is slow-paced and often does not pass clinical trials. Among non-*albicans Candida* species, *Candida tropicalis* is frequently emerging fungal pathogen in the Asia-Pacific region, causing a high mortality rate due to candidiasis. The preponderance of *C. tropicalis* in clinically isolated strains is recorded as higher as 42.1%. Also, the resistance in isolated *C. tropicalis* strains towards fluconazole is observed to be 38.5%. This increased rate of fluconazole resistance and frequent isolation of *C. tropicalis* makes it a major concern. *C. tropicalis* is an opportunistic human pathogen with an ability to cause superficial as well as systemic infections in immunocompromised patients. The formation of biofilm by *C. tropicalis* can cause dreadful and persistent infections which are difficult to treat due to acquired resistance. Azole drugs including fluconazole are enormously used in several antifungal treatments. However, *C. tropicalis* isolates showing significant azole drug resistance attributed to the point mutations in cytochrome P-450 lanosterol 14- α -demethylase (Erg11p) protein. Therefore, alternative drugs against Erg11p are immensely required to combat the acquired resistance. Owing to the potential of essential oils in terms of their antimicrobial activities as well as traditional usage has emphasized their applicability in various fields ranging from agriculture to food technology and as natural alternatives alongside synthetic drugs. However, more clinical studies are required to confirm and verify the true potency of these natural substances for their safe applications in human health and the environment. Essential oils are found to be rich in terpenes which are known to have good antimicrobial properties along with their explicit aroma. Various terpenes have shown multiple antifungal activities against planktonic cells in *Candida* species. However, their effects on the biofilm formation and its eradication are still in infancy. Previous studies have revealed antifungal activities of these terpenes at multiple levels in different organisms. Therefore, the effect of antifungal agents could not be specified by studying it over one organism or even on established targets. More studies are required to be done in respect to finding probable genes, proteins and metabolites responsible for resistance against antifungal agents. Furthermore, many terpenes have been tried as antifungal agents against *Candida* species. These are found as a potent anti-*Candida* compound with a broad

range of antimicrobial properties. Thus, the exploitation of antifungal and antibiofilm properties could serve as a bridge between traditional uses and rational utilization of essential oils and citral. In the present thesis entitled “**Antibiofilm activities and proteomic analysis of *Candida tropicalis* in response to terpenes**”, an extensive study has been done to elaborate on the effects of terpenes on *C. tropicalis* biofilm.

Firstly, *in vitro* growth and development of *C. tropicalis* biofilm were recognized and antifungal activities of the seven terpenes, namely, geraniol, menthol, citral, cinnamaldehyde, carvacrol, eugenol and thymol were screened. They were further checked for the abilities of biofilm inhibition and eradication. The calculated MIC₅₀, BIC₅₀ and BEC₅₀ values for citral and thymol were lesser than other terpenes, therefore, observed to be more effective against *C. tropicalis*. The morphological changes have also shown damaged surface in the presence of these terpenes. These results clearly indicated that among these terpenes; citral and thymol were significantly effective against both planktonic and biofilm forms of *C. tropicalis*, compared to others.


Secondly, the comparative potentials of citral and thymol against *C. tropicalis* were explored. The administration of citral and thymol on *C. tropicalis* biofilm leads to a fungicidal effect. The relative fold change in the expression of certain key genes which are involved in major pathways followed by *C. tropicalis*, to reduce the effect of well-known drugs, has also been investigated to get the insights in the plausible mechanism for its survival in the presence of these two components. Citral and thymol have formed indentations in the cells depicting distorted surface and decreased viability. Also, the cell membrane and DNA damage were determined in *C. tropicalis* biofilm cells when treated with citral and thymol as antifungal agents. The cells membrane integrity was compromised and DNA damage was observed. Quantitative real-time PCR analysis showed augmented expression of the cell membrane biosynthesis genes including *ERG11/ CYT450* against citral and the cell wall-related tolerance genes involving *CNBI* against thymol thus, depicting their differential mode of actions.

Next, the homology model of well-known azole drug target Erg11p of *C. tropicalis* was employed to unravel the interaction between citral and lanosterol-14- α -demethylase (Erg11p). The molecular interactions of two isomers of citral namely neral and geranial, with *CtErg11p*, were evaluated. The three-dimensional structure of *CtErg11p* was prepared through *in silico* structural modelling approach. The best-generated model was validated and further used for the molecular docking studies with citral. The molecular docking studies provide insights into citral-*CtErg11p* interactions, which could be helpful for further optimization and development of other inhibitory analogues of citral asserting the expansion of proficient broad-spectrum antifungals. The molecular interactions between citral, heme group and participating amino

acid residues of *CtErg11p* protein have been identified that could lead to understanding the protein-ligand interaction.

Furthermore, insights into the changes in the biofilm cell proteome and the extracellular matrix of *C. tropicalis* in the presence of citral were obtained. One-dimensional polyacrylamide gel electrophoresis (1D-PAGE), two-dimensional polyacrylamide gel electrophoresis (2D-PAGE) and matrix-assisted laser desorption ionization-time of flight mass spectrometry (MALDI-TOF/TOF-MS) were employed to identify the changes in the protein expression of *C. tropicalis* in response to the sub-lethal concentration of citral. The results revealed citral-induced proteins of *C. tropicalis* biofilm. In 1D-PAGE, a total of six differential proteins, involved in oxidative stress, amino acid biosynthesis, heme biosynthesis and glucose metabolism pathways were detected. However, in 2D-PAGE, the differential expression of proteome has revealed a total of twenty-five proteins in *C. tropicalis* biofilm which were induced in the presence of citral. Among these, amino-acid biosynthesis (Met6p, Gln1p, Pha2p); nucleotide biosynthesis (Xpt1p); carbohydrate metabolism (Eno1p, Fba1p, Gpm1p); sterol biosynthesis (Mvd1p/ Erg19p, Hem13p); energy metabolism (Dnm1p, Coa1p, Ndk1p, Atp2p, Atp4p, Hts1p); oxidative-stress (Hda2p, Gre22p, Tsa1p, Pst2p, Sod2p); and biofilm specific (Adh1p, Ape1p, Gsp1p) proteins were identified. The overexpression of oxidative-stress related proteins indicates the response of biofilm cell in combating oxidative-stress during citral treatment. Moreover, the upregulation of Adh1 is of particular interest because it subsidises the biofilm inhibition through ethanol production as a cellular response. The augmented expression of Mvd1/ Erg19 signifies the effect of citral on ergosterol biosynthesis. The overall sugar and protein moieties were diminished in the treated extracellular matrix; however, ergosterol and cell wall content e.g. hexosamine were relatively increased. Therefore, it is clearly indicated that the cellular response towards citral acts through multifactorial processes.





This thesis work is dedicated to my Late Grandmother (Nani Maa) Smt. Kailash Devi and my Late Grandfather (Nana Jee) Shri Anand Swarup Lekhi as they always loved me unconditionally and supported me through my endeavours.



ACKNOWLEDGEMENT

At this moment of immense pleasure and satisfaction, as I have completed my thesis entitled “Antibiofilm activities and proteomic analysis of Candida tropicalis in response to terpenes” first, I would like to thank the Almighty with gratitude for providing me with this great opportunity. The strength and ability to come this far was all the blessings bestowed during my struggling times. This thesis is an outcome of my rigorous and dedicated five and a half years of continuous work whereby I thrived to get better each day. I am greatly obliged to the people who have knowingly or unknowingly accompanied me during this journey.

I am grateful to my supervisor Prof. Ramasare Prasad (Chairman, DRC) for his expert guidance, encouraging attitude and positive critics. I am deeply thankful to him for his time and efforts in my research work. His valuable suggestions and scientific approach helped me to accomplish this.

I am thankful to the members of my advisory committee Prof. A. K. Sharma (Internal Expert and Head of the Department) Department of Biotechnology, Prof. U. P. Singh (External Expert) Department of Chemistry and Prof. Bijan Chaudhary (Chairman, SRC) Department of Biotechnology for their valuable advice made during scientific meetings. I would also like to thank and convey my sincere regards to all the faculty members of the Department of Biotechnology, IIT Roorkee for their constant help, support and encouragement during my research work.

I sincerely acknowledge the Council of Scientific and Industrial Research (CSIR), Government of India, New Delhi for providing me with the financial support in the form of fellowship which made this journey little easier.

I am grateful to my labmates Dr Rajbala Yadav, Ms Poonam Kumari, Ms Rashmi Gangwar and Mr Pankaj Kumar Chaudhary for their sincere support, positive attitude and cooperation during my experimental work. I am also thankful to all my M. Sc. students; Mr Awadhesh Chauhan, Mr Ankit Pal, Ms Priyanka Verma, Mr Plaban Buragohain and Ms Debjani Das for their assistance, help and support in the completion of this research. I would also like to acknowledge the love, support and care of my dear friends Dr Savita Budania, Dr Anchal Sharma and Ms Neha Chaubey who made my journey memorable in IITR.

A special thanks to all the technical and non-teaching staff of the Department of Biotechnology for their help and support.

My deepest sense of gratitude goes to my family; Bade Mama, Mami, Raju Mama, Mami, Mummy, Papa, both my sisters; Somya and Swasti, and Chloe for their constant support during my highs and lows. Words are not enough to thank them for their love and affection and all the sacrifices they have made during my hard times. They were my core inspiration to move forward and accomplish this long and difficult journey.

Last but not least, I would always be indebted to my best friend Dr Tamoghna Ghosh who stood by me during each and every second of my difficult times. I express a huge and warm thanks to him to show faith in me and my hard work. I appreciate the constant patience he has kept and walked with me without complaints in the distressing hours of my research duration. It would have been impossible for me to work hard without his instilled enthusiasm. His trust in me kept me motivated to complete this task.

(Apurva Chatrath)



CONTENTS

| | |
|---|------|
| ABSTRACT..... | i |
| ACKNOWLEDGEMENT | vii |
| CONTENTS..... | ix |
| LIST OF FIGURES | xiii |
| LIST OF TABLES | xvii |
| Chapter 1 | 1 |
| INTRODUCTION | 1 |
| Chapter 2 | 7 |
| REVIEW OF LITERATURE | 7 |
| 2.1 <i>Candida tropicalis</i> : a human pathogen | 8 |
| 2.1.1 Biofilm and its occurrence | 9 |
| 2.1.2 Factors affecting biofilm formation | 14 |
| 2.1.3 Biofilm virulence, pathogenesis and antifungal drug resistance..... | 15 |
| 2.2 Natural compounds and their antimicrobial activities..... | 21 |
| 2.2.1 Characteristics of essential oils and terpene molecules | 23 |
| 2.2.2 Antimicrobial activities of essential oils and terpenes..... | 24 |
| 2.2.3 Effect of essential oils against <i>Candida</i> species | 26 |
| 2.2.4 Mechanism of action of essential oils and terpenes | 28 |
| 2.3 Citral: an antimicrobial agent..... | 32 |
| 2.3.1 Biosynthesis of citral..... | 33 |
| 2.3.2 Combating antimicrobial resistance..... | 33 |
| Chapter 3..... | 37 |
| MATERIALS AND METHODS | 37 |
| 3.1 Materials..... | 37 |
| 3.1.1 Microorganisms, media and growth conditions | 37 |
| 3.1.2 Reagents | 37 |

| | | |
|--------|--|----|
| 3.2 | Methods..... | 40 |
| 3.2.1 | <i>In vitro</i> biofilm growth of <i>C. tropicalis</i> | 40 |
| 3.2.2 | <i>C. tropicalis</i> susceptibility towards selected terpenes | 40 |
| 3.2.3 | Antibiofilm activities of terpenes on <i>C. tropicalis</i> | 41 |
| 3.2.4 | Colourimetric XTT reduction assay..... | 42 |
| 3.2.5 | Quantification of ergosterol content | 42 |
| 3.2.6 | Cell surface hydrophobicity and auto-aggregation of <i>C. tropicalis</i> cells | 42 |
| 3.2.7 | <i>In vitro</i> time-kill kinetics of terpenes on <i>C. tropicalis</i> | 43 |
| 3.2.8 | Morphological changes in <i>C. tropicalis</i> matured biofilm cells during treatment . | 43 |
| 3.2.9 | Effect of citral and thymol on the cell membrane permeability | 44 |
| 3.2.10 | Field emission scanning electron microscope (FE-SEM) and confocal laser scanning microscope (CLSM) | 44 |
| 3.2.11 | Measurement of reactive oxygen species (ROS) levels..... | 45 |
| 3.2.12 | Catalase (CAT), peroxidase (POD) and superoxide dismutase (SOD) enzyme activities..... | 45 |
| 3.2.13 | Whole-cell lipid peroxidation determination | 46 |
| 3.2.14 | Alkaline Comet Assay | 47 |
| 3.2.15 | RNA isolation, cDNA synthesis, and real-time expression analysis | 47 |
| 3.2.16 | Protein sequence retrieval..... | 50 |
| 3.2.17 | Sequence alignment and secondary structure prediction | 50 |
| 3.2.18 | Homology modelling | 50 |
| 3.2.19 | Structure validation..... | 50 |
| 3.2.20 | Molecular docking | 51 |
| 3.2.21 | Protein extraction and quantification | 51 |
| 3.2.22 | One-Dimensional (1D) polyacrylamide gel electrophoresis..... | 52 |
| 3.2.23 | Two-dimensional (2D) polyacrylamide gel electrophoresis..... | 52 |
| 3.2.24 | Imaging of the gel and software analysis..... | 53 |
| 3.2.25 | In-gel trypsin digestion and peptides extraction | 53 |

| | | |
|-----------|--|----|
| 3.2.26 | Protein Identification and database search using mass spectrometry | 54 |
| 3.2.27 | 1D ¹ H-NMR Analysis of extracellular matrix | 54 |
| 3.2.28 | Statistical analysis | 55 |
| Chapter 4 | | 57 |
| RESULTS | | 57 |
| 4.1 | <i>In vitro</i> biofilm formation of <i>Candida tropicalis</i> and its inhibition by selective terpenes | 57 |
| 4.1.1 | Growth curve of <i>C. tropicalis</i> biofilm formation..... | 57 |
| 4.1.2 | Antifungal activities of terpenes against <i>C. albicans</i> and <i>C. tropicalis</i> | 59 |
| 4.1.3 | Inhibition of biofilm formation and eradication of preformed biofilm..... | 59 |
| 4.1.4 | Effect on cell surface hydrophobicity and auto-aggregation of <i>C. tropicalis</i> in the presence of terpenes | 61 |
| 4.1.5 | Time-kill kinetics of terpenes against <i>C. tropicalis</i> | 61 |
| 4.1.6 | Morphological changes in <i>C. tropicalis</i> biofilm on administration of terpenes ... | 62 |
| 4.2 | Deciphering the probable mode of action of citral and thymol against <i>C. tropicalis</i> biofilm..... | 63 |
| 4.2.1 | Citral and thymol indicated no direct binding to the cell membrane but thymol acts via cell wall..... | 64 |
| 4.2.2 | Ergosterol content was unaltered in the presence of citral and thymol | 66 |
| 4.2.3 | FE-SEM and CLSM analysis displayed damage to the biofilm in the presence of citral and thymol | 66 |
| 4.2.4 | Impairment of the plasma membrane integrity of <i>C. tropicalis</i> biofilm cells in the presence of citral and thymol..... | 69 |
| 4.2.5 | Citral and thymol generated reactive oxygen species (ROS) | 70 |
| 4.2.6 | Enzymatic activities of catalase (CAT), peroxidase (POD) and superoxide dismutase (SOD) during citral and thymol treatment | 70 |
| 4.2.7 | Occurrence of lipid peroxidation in the presence of citral and thymol..... | 72 |
| 4.2.8 | DNA damage in <i>C. tropicalis</i> biofilm cells on treating with citral and thymol.... | 72 |
| 4.2.9 | Citral upregulated <i>ERG11/ CYT450</i> genes whereas thymol upregulated <i>CNBI</i> and <i>SOD1</i> genes..... | 73 |

| | | |
|------------------------------------|--|-----|
| 4.3 | <i>In silico</i> molecular modelling and docking analysis of lanosterol-14- α -demethylase (Erg11p) from <i>C. tropicalis</i> with citral | 73 |
| 4.3.1 | Protein sequence was retrieved from NCBI database | 74 |
| 4.3.2 | Query and template sequence alignment and prediction of secondary structure.. | 74 |
| 4.3.3 | Homology modelling and structure validation of <i>CtErg11p</i> | 78 |
| 4.3.4 | Specification of the model selected for docking studies..... | 82 |
| 4.3.5 | Molecular docking studies of <i>CtErg11p</i> | 82 |
| 4.4 | Delineating the differentially expressed proteins and variations in extracellular matrix of <i>C. tropicalis</i> biofilm in response to citral | 84 |
| 4.4.1 | Citral induces variation in the proteome of <i>C. tropicalis</i> biofilm cells | 84 |
| 4.4.2 | Differential expression of the proteome during citral administration..... | 87 |
| 4.4.3 | Variations in metabolic profiling of extracellular matrix in the biofilm of <i>C. tropicalis</i> | 92 |
| Chapter 5 | | 95 |
| DISCUSSION | | 95 |
| CONCLUSION AND FUTURE PERSPECTIVES | | 109 |
| BIBLIOGRAPHY | | 111 |
| PUBLICATIONS | | 143 |
| CONFERENCES | | 145 |

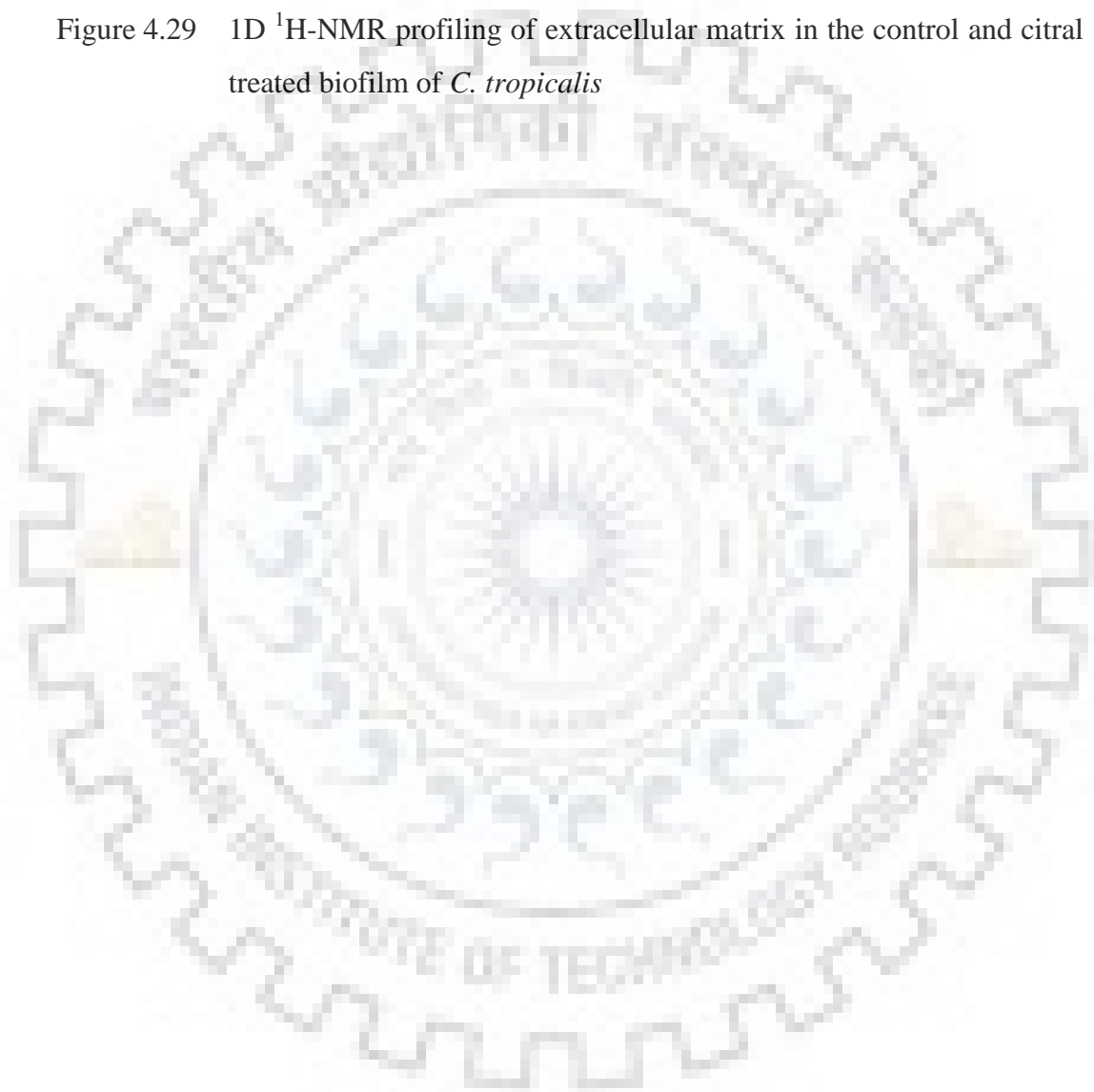
LIST OF FIGURES

| Figure No. | Figure Title | Page No. |
|-------------|---|----------|
| Figure 2.1 | Schematic representation of <i>C. tropicalis</i> lifestyle | 12 |
| Figure 2.2 | Fate of antifungal agents during <i>C. tropicalis</i> biofilm treatment | 19 |
| Figure 2.3 | Biosynthesis of citral | 33 |
| Figure 2.4 | Probable mode of action of citral on <i>C. tropicalis</i> | 36 |
| Figure 3.1 | Temperature profiling of RT-PCR reaction | 48 |
| Figure 4.1 | Biofilm formation of <i>C. tropicalis</i> on different substrates | 58 |
| Figure 4.2 | Bright-field microscopic and scanning electron microscopic (SEM) images of <i>C. tropicalis</i> biofilm | 58 |
| Figure 4.3 | Trends of biofilm inhibition and eradication effects of citral and thymol | 60 |
| Figure 4.4 | <i>In vitro</i> time-kill curves of <i>C. tropicalis</i> when treated with terpenes and amphotericin B | 62 |
| Figure 4.5 | Scanning electron microscopic (SEM) images showing damage to <i>C. tropicalis</i> biofilm | 63 |
| Figure 4.6 | Percentage of ergosterol content in <i>C. tropicalis</i> biofilm | 65 |
| Figure 4.7 | Images through field emission scanning electron microscopy (FE-SEM) | 67 |
| Figure 4.8 | Confocal laser scanning microscopic images (CLSM) of <i>C. tropicalis</i> biofilm; dual stained | 67 |
| Figure 4.9 | COMSTAT analysis of <i>C. tropicalis</i> biofilm | 68 |
| Figure 4.10 | Fungicidal effects of citral and thymol on <i>C. tropicalis</i> biofilm cells | 69 |

| | | |
|-------------|---|-------|
| Figure 4.11 | Graphical representation of the DCFDA fluorescence of <i>C. tropicalis</i> biofilm representing ROS production during treatment of amphotericin B, citral, and thymol | 70 |
| Figure 4.12 | Elevation in activities of antioxidant enzymes in response to citral and thymol | 71 |
| Figure 4.13 | Lipid peroxidation in the presence of citral and thymol | 72 |
| Figure 4.14 | DNA damage visualization through comet tailing | 72 |
| Figure 4.15 | Effect of citral and thymol on the relative expression of the selected genes in <i>C. tropicalis</i> | 73 |
| Figure 4.16 | FASTA sequence of the query <i>CtErg11p</i> retrieved from NCBI | 74 |
| Figure 4.17 | Multiple sequence alignment (MSA) of the deduced amino acid sequence of <i>C. tropicalis</i> <i>Erg11p</i> with 5V5Z and 5FSA | 75 |
| Figure 4.18 | Secondary structure of <i>CtErg11p</i> predicted using PDBsum | 76-77 |
| Figure 4.19 | Molecular model: A. Cartoon representation of the generated 3D model of <i>CtErg11p</i> and B. porphyrin ring of <i>CtErg11p</i> | 78 |
| Figure 4.20 | ProSA-web Z-scores of the predicted 3D model of <i>CtErg11p</i> | 79 |
| Figure 4.21 | ERRAT plot of <i>CtErg11p</i> showing the overall quality factor or ERRAT score of the model | 79 |
| Figure 4.22 | Ramachandran plot of the predicted 3D model of <i>CtErg11p</i> | 80 |
| Figure 4.23 | Modeled structures of citral isomers: A. geranial; B. neral; and C. itraconazole | 82 |
| Figure 4.24 | Docked poses of the <i>CtErg11p</i> | 84 |
| Figure 4.25 | <i>C. tropicalis</i> proteins resolved using one-dimensional (1D) gel electrophoresis | 85 |
| Figure 4.26 | Two-dimensional gel electrophoresis (2DE) reference map of citral- | 87 |

induced differentially expressed proteins of *C. tropicalis* biofilm cells

- Figure 4.27 Schematic representation of proposed multiple modes of actions of citral 91
- Figure 4.28 OPLS-DA model comparisons between control and citral-treated samples 92
- Figure 4.29 1D ^1H -NMR profiling of extracellular matrix in the control and citral treated biofilm of *C. tropicalis* 93





LIST OF TABLES

| Table No. | Table Title | Page No. |
|-----------|--|----------|
| Table 2.1 | Characteristics of <i>Candida</i> species biofilm | 10 |
| Table 2.2 | Selected terpenes with documented antimicrobial effects | 25-26 |
| Table 3.1 | Composition of phosphate-buffered saline (PBS) | 37 |
| Table 3.2 | Recipe of staining and destaining solutions | 39 |
| Table 3.3 | List of stock solutions | 39 |
| Table 3.4 | Components of RT-PCR reaction mixture | 48 |
| Table 3.5 | Primers used for real-time RT-PCR | 49 |
| Table 4.1 | Calculated Minimum Inhibitory Concentrations (MICs), Biofilm Inhibitory Concentrations (BICs) and Biofilm Eradicating Concentrations (BECs) of tested terpenes and fluconazole | 60 |
| Table 4.2 | Representing Hydrophobicity Index (HI) and auto-aggregation of <i>C. tropicalis</i> yeast cells | 61 |
| Table 4.3 | IC values ($\mu\text{g/mL}$) of drugs in the absence and presence of sorbitol (0.8 M) and ergosterol (400 $\mu\text{g/mL}$) against <i>C. tropicalis</i> | 65 |
| Table 4.4 | Amino acid residues present in the principal motif of the protein | 77 |
| Table 4.5 | Ramachandran plot statistics I | 80 |
| Table 4.6 | Ramachandran plot statistics II | 81 |
| Table 4.7 | Main chain parameters plot statistics | 81 |
| Table 4.8 | Binding parameters of citral in association with <i>CtErg11p</i> | 83 |
| Table 4.9 | Summary of the identified proteins using 1D bands with differential expression in response to citral | 86 |

Table 4.10 Summary of the identified proteins using 2D spots in differentially expressed proteome of *C. tropicalis* biofilm cells in the presence of citral 88-91



Chapter 1

INTRODUCTION

Candida species are widely associated yeasts with humans in commensalism but turn into opportunistic pathogens during the extensive use of broad-spectrum antibiotics and suppression of the host immune system (Krasner, 2002). *Candida* occurs on the skin and mucosal surfaces and in the genitourinary tract as well as the gastrointestinal tract (Sardi *et al.*, 2013). A majority of nosocomial infection is dedicated to *Candida* species worldwide with more severity in immunocompromised patients (Low and Rotstein, 2011). *Candida* species alone contributes to more than 70% of the hospital-acquired infections (Xess *et al.*, 2007; Negri *et al.*, 2012; Pandey *et al.*, 2012; Chander *et al.*, 2013). Among all, *Candida albicans* is the most common infection causing species in the genus *Candida*, however, non-*albicans Candida* species are also on boom especially *C. glabarata* and *C. tropicalis* (Deorukhkar, Saini and Mathew, 2014). *C. tropicalis* closely resembles *C. albicans* in taxonomy. Infections due to *C. tropicalis* have increased dramatically on a global scale thus, proclaiming this organism to be emerging pathogenic yeast with higher prevalence in the Asia-Pacific and Europe regions (Kothavade *et al.*, 2010; Sardi *et al.*, 2013). Also, *C. tropicalis* is the most prevalent non-*albicans Candida* species in tropical countries responsible for a high mortality rate due to candidiasis and also significantly accountable for candidal bloodstream infections (Kothavade *et al.*, 2010; Tan *et al.*, 2010; Chander *et al.*, 2013). It is majorly responsible for 67- 90% of the epidemiological nosocomial candidaemia among non-*albicans Candida* species in India (Negri *et al.*, 2012; Chander *et al.*, 2013). The prevalence of *C. tropicalis* has been increased drastically with a significant mortality rate as the host population is becoming immunocompromised worldwide (Chakrabarti *et al.*, 2015).

Most of the *Candida* infections are associated with the formation of biofilm on biotic and abiotic surfaces (Crump and Collignon, 2000). *C. tropicalis* is capable of proper biofilm formation resulting in frequent biofilm-producing species among non-*albicans Candida* species (Tan *et al.*, 2010; Tascini *et al.*, 2018). Biofilm lifestyle of yeast cells represents a unique phenotypic trait of the pathogenic species under stressful conditions. This life form is vastly established as more resistant towards the antifungal agents and evades immune responses of the host (Dominguez and Andes, 2017). Abiotic surfaces such as medical devices have also shown the formation of biofilm by the *Candida* species (Andes, 2017). The detection of biofilm-forming ability in *Candida* species is of utmost importance as these organisms not only

colonize medical devices but also lead to resistant healthcare-associated infections (Sardi *et al.*, 2013). Furthermore, *in vivo* studies of rat and rabbit also depicted the similar biofilm formation on central venous catheter models (Nett and Andes, 2015). Components of the immune system including neutrophils, macrophages, blood cells, and platelets were found embedded in *in vivo* biofilm. As a consequence, researchers have now realised the fact that it is important to study the biofilm communities rather than planktonic forms for the characterization of the infectious potential of fungal pathogens. The ability of biofilm formation by *C. tropicalis* is majorly responsible for its virulence, resistance and drug tolerance towards conventional antifungal agents. *C. tropicalis* exhibits an intrinsic ability to form the biofilm on the biotic as well as abiotic surfaces (Kothavade *et al.*, 2010). The infected devices isolated from the patients have revealed the formation of biofilm which seeds further recurrent infections (Lynch and Robertson, 2008).

C. tropicalis biofilm has shown elevated resistance towards conventional drugs, including fluconazole and amphotericin B as well as other antifungal agents (Harrison, Turner and Ceri, 2007; Bergamo *et al.*, 2015). *Candida* species have evolved numerous mechanisms; including alteration of targets, reduction in uptake and active extrusion, in order to combat the effects of standard antifungal drugs (Pfaller, 2012). The biofilm growth rate has also been widely linked to the resistance in *Candida* biofilm towards antifungal agents. Additionally, when the minimum inhibitory concentrations of conventional drugs including chlorohexidine, fluconazole, amphotericin B and nystatin were compared during the *Candida* biofilm development at early, intermediate and maturation phases, the progression of drug resistance was observed in parallel association with the increased metabolic activity of the biofilm (Cavalheiro and Teixeira, 2018). Therefore, the increased drug resistance is directly related to the maturation process of biofilm rather than lower metabolic rate of the cells during biofilm maturation. Interestingly, a subpopulation of cells with slower growth rate tends to confer antifungal resistance in biofilm which is consisting of a heterogeneous cell population with different growth rates (LaFleur, Kumamoto and Lewis, 2006). The morphological forms exhibited by *C. tropicalis* are similar to those shown by *C. albicans*, despite this, only a few studies have explored the importance of *C. tropicalis* morphology on virulence. Moreover, the matrix material surrounding biofilm of *C. albicans* and *C. tropicalis* varies as former contains carbohydrates, proteins, hexosamine, phosphorus, and uronic acid whereas later contains 27% of hexosamine, low carbohydrate and proteins (Al-Fattani and Douglas, 2006). Since the two species differ in genetic make-up, their proteome will differ and they must respond differently in the biofilm formation during pathogenesis and towards antifungal agents used for their

eradication. *C. tropicalis* holds higher antifungal traits due to the robust architecture of biofilm, presence of extracellular matrix, decrement in metabolic activity, proteome difference and presence of persister cells (Bizerra *et al.*, 2008). One of the major factors dealt with antifungal tolerance of *C. tropicalis* biofilm than its planktonic counterparts could be oxidative stress tolerance in accordance with previous studies (Acker, Dijck and Coenye, 2014).

These emerging threats caused by non-*albicans* *Candida* species through resistance towards conventional drugs have urged to identify new alternatives or modification of existing antifungal agents to defy the dominant tendency of infection. In the era of the growing resistance of fungal diseases especially *Candida* species, it is tempting to get new treatments to defy biofilm resistance. The use of natural products is common from the earliest civilizations and well known for their antiseptic and medicinal properties (Božović *et al.*, 2017). In recent decades, the development of new bioactive compounds based on modified natural products is suggestively considered to overcome the emerging resistance (Di Santo, 2010). One such natural alternative could be essential oils, rich in terpenes which are widely recognized for their antimicrobial properties including antifungal activity along with their explicit aroma (Nazzaro *et al.*, 2017). Various terpenes have demonstrated multiple modes of actions against planktonic cells in *Candida* species. However, their effects on the biofilm formation and its eradication are still in infancy. Numerous researches have documented the efficient antimicrobial activity of these essential oils and terpenes when administered alone or in combination with other drugs (Chouhan, Sharma and Guleria, 2017). Strong actions of citral and thymol have been defined in several studies with *C. albicans* and other non-*albicans* *Candida* species (Marchese *et al.*, 2016; Baser, Demirci and Bueno, 2017; da Silva *et al.*, 2017). Citral and thymol are generally regarded as safe (GRAS) by the Food and Drug Administration for human consumption and food additives (Food and Drug Administration 2015a; 2015b). Citral (3, 7-dimethyl-2, 6-octadienal), a major component of the essential oil of *Cymbopogon citratus* (~ 75%), has exhibited potent activity against *Candida* species (Taweekhaisupapong *et al.*, 2012; Leite *et al.*, 2015; da Silva *et al.*, 2017). Whereas, thymol (2-isopropyl-5-methyl phenol) is present majorly in thyme oil (*Thymus vulgaris*) possessing various pharmacological as well as antimicrobial properties.

Since antifungal resistance is inevitable, it is crucial to get powerful insights into the molecular mechanisms that govern the tolerance of drugs in order to hinder the resistance. An understanding of the specific targets involved in a particular agent is critical in developing novel and effective therapeutic strategies (Robbins, Caplan and Cowen, 2017). Recent reports

have shown well-defined activities of citral against a number of microorganisms and efforts are made to study its mode of action. Also, many synergistic studies have reported that citral is a potent inhibitor when used in combination with conventional drugs (Ortiz *et al.*, 2010; Zore *et al.*, 2011). A critical area for further detailed studies appears to be the evaluation of the possible molecular targets to develop alternative therapies against pathogenic infections. Moreover, the development of more efficient citral derivatives is required in order to enhance its bioactive potential. Only limited data is available on citral treated biofilm of *C. tropicalis* expressing the differences in proteome with respect to the healthy biofilm (Chatrath *et al.*, 2018). The exploration of molecular mechanisms involved in certain drug resistance is highly required to understand the differential regulation of specific proteins.

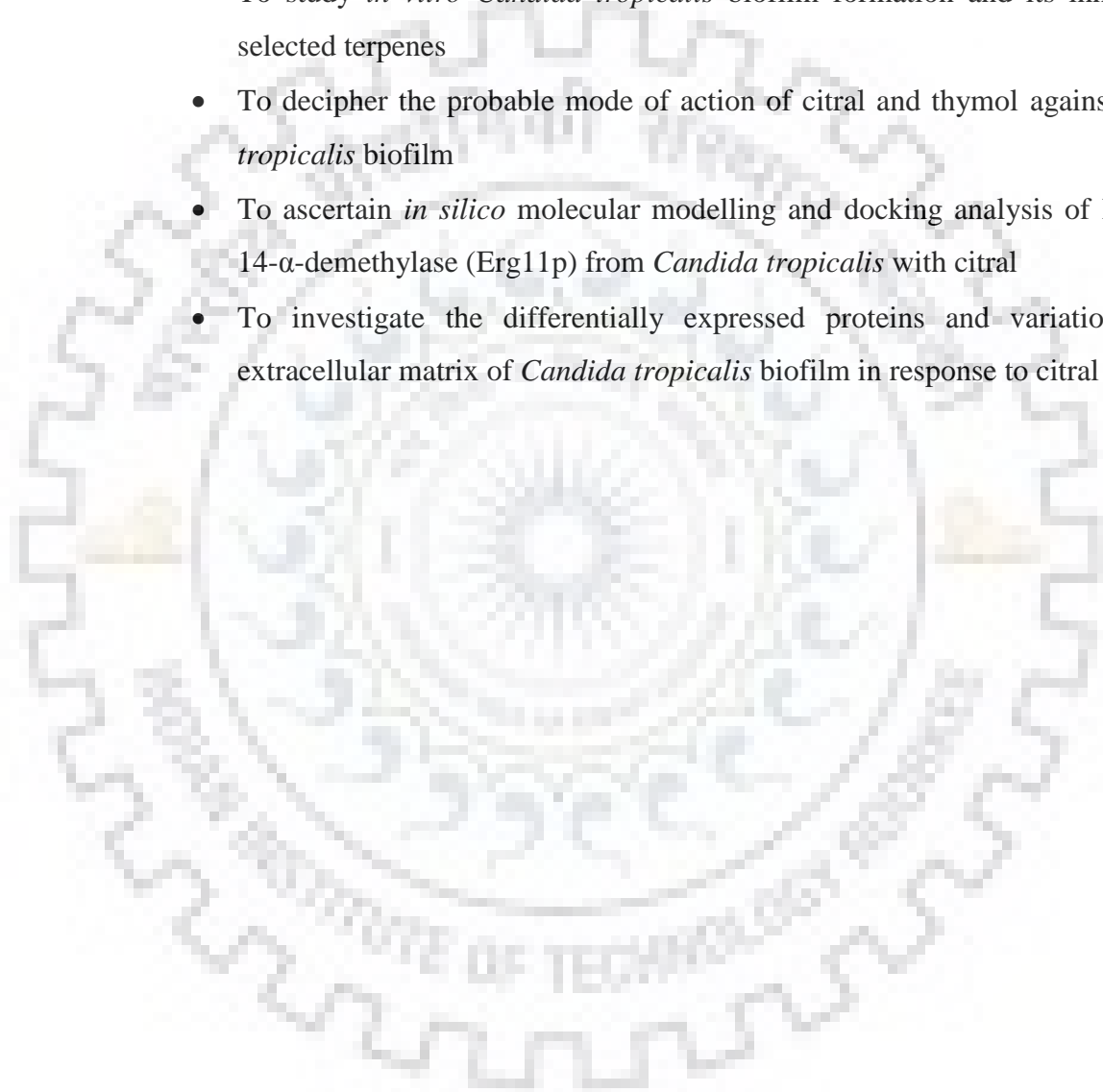
As discussed before, *C. albicans* is the predominant species; however, infections caused by non-*Candida albicans* species are frequently alarming (Pfaller *et al.*, 2011). These are of major concern because they have also acquired resistance to antifungal therapies similar to *C. albicans* (Cleveland *et al.*, 2012; Pfaller *et al.*, 2015). *C. tropicalis* is frequently observed to be azole resistance under clinical studies. Azoles are the most commonly used broad-spectrum drug against fungal infections (Pfaller *et al.*, 2010). The azoles inhibit fungal cytochrome P-450 lanosterol 14- α -demethylase (Erg11p) protein, a key enzyme of the ergosterol biosynthetic pathway, resulting in an altered fungal cell membrane. *C. tropicalis* isolates have shown azole drug-tolerance, which are attributed due to the point mutations in Erg11p. The outpacing of antifungal resistance compared to new drug development is pushing the human race towards natural remedies such as terpenes. A previous study has shown that the mechanism of action of citral does not involve the direct binding to the membrane ergosterol but it likely mediates through the inhibition of ergosterol biosynthesis (Sousa *et al.*, 2016).

“Hypothesis-free” system biology tools such as genomics, proteomics and bioinformatics can be utilized to investigate the molecular machinery of the antifungal resistance and drug development. The identification of the potential drug targets which are frequently involved in essential signaling pathways is required to explore the molecular mechanism of action which can be used for the development of the novel therapeutics and optimization of the existing agents. The molecular mechanisms that govern the pathophysiological phenomena could be understood by genomics and proteomics disciplines of essential sciences. Recent findings in these areas have outlined the concept of mechanisms followed by *Candida* biofilm. The studies on *Candida* biofilm at genomic levels have given powerful insights into the mechanisms of biofilm formation. Furthermore, the changes in proteome in association with the change in mutant virulence, drug response and serological

response to candidiasis have confined largely to the cell wall analysis (Thomas *et al.*, 2006; Pitarch *et al.*, 2007). The study of biofilm development, virulence, resistance and drug tolerance using proteomics approach is still in its infancy. In the present study, the effect of certain terpenes on the biofilm of *C. tropicalis* has been elaborated.

The overall thesis has been compiled with the following undertaken objectives:

- To study *in vitro* *Candida tropicalis* biofilm formation and its inhibition by selected terpenes
- To decipher the probable mode of action of citral and thymol against *Candida tropicalis* biofilm
- To ascertain *in silico* molecular modelling and docking analysis of lanosterol-14- α -demethylase (Erg11p) from *Candida tropicalis* with citral
- To investigate the differentially expressed proteins and variations in the extracellular matrix of *Candida tropicalis* biofilm in response to citral





Chapter 2

REVIEW OF LITERATURE

As early as Hippocrates, *Candida* has been perhaps well encountered as an archetypal opportunistic pathogen in human. Since very long, it has been isolated as harmless inhabitants of various human body niches such as an oral cavity, vagina, skin and gastrointestinal tract of healthy individuals (Suhr and Hallen-Adams, 2015). *Candida* mostly occurs on the skin and mucosal surfaces and in the genitourinary tract and gastrointestinal tract (Sardi *et al.*, 2013). However, during certain circumstances, the infection due to *Candida* prevails ranging from superficial skin or mucosal membrane to life-threatening deep-seated systemic infections (Tsui, Kong and Jabra-Rizk, 2016). A majority of nosocomial infection is dedicated to *Candida* species worldwide with more severity in immunocompromised patients (Low and Rotstein, 2011). The mortality rates due to candidiasis are arising and frequently reported to be as high as 40% to 60% in clinical settings (Pappas *et al.*, 2018). Among all, *Candida albicans* is the most common infection causing species in the genus *Candida*, however, non-*albicans Candida* species are also on boom especially *C. glabrata* and *C. tropicalis* (Deorukhkar, Saini and Mathew, 2014). The host's immune status plays a vital role in the transition of *Candida* to an opportunistic pathogen such as altercations with immunocompromised patients during transplants, chemotherapy and disorders like HIV/ AIDS (Gupta and Gupta, 2017). Furthermore, widespread infections of *Candida* have been observed in association with medical devices including catheters, shunts, implants, pacemakers and tubes (Lavery, Gorman and Gilmore, 2015). The high mortality rate has been observed among catheter-related vascular infections (Muhammed, Kourkoumpetis and Mylonakis, 2018).

The major contributors of virulence such as biofilm formation in *Candida* which results in its versatility to adapt in varying habitats are required to understand as a medical priority. The structured ecosystem of biofilm is profound in most microbes as natural habitat frequently contributing around 65% of most microbial infections (Douglas, 2003). Biofilm, phenotypic form, comprises microbial communities encapsulated inside extracellular matrix differing free-floating counterparts (Dominguez and Andes, 2017). The eradication of *Candida* biofilm is difficult due to its high resistance towards antifungal agents resulting in a must implant removal to combat the spreading of infection (Lewis, 2005). Frequent economic and clinical consequences associated with *Candida* biofilm instigate the recent research to focus on prevention and management of biofilm. The emerging threats caused by *C. albicans* and non-

albicans *Candida* species have started to show resistance which urges to identify new alternatives or modification of existing antifungal agents to defy the dominant tendency of infection.

2.1 *Candida tropicalis*: a human pathogen

In 1910, *C. tropicalis* was first isolated and named as *Oidium tropicale* from a patient suffering from fungal bronchitis (Castellani, 1912). The yeast belongs to Ascomycota and reproduces asexually by budding. Several yeasts of order Saccromycetals are of medical importance either in causing some disease or through drug production capabilities. The appearance of *C. tropicalis* colonies is pale white to cream on Sabouraud's dextrose agar with a smooth texture and slightly wrinkled edges on prolonged growth. *C. tropicalis* has the capabilities of assimilating as well as fermenting sugars such as sucrose, maltose, galactose and trehalose using oxidative pathway (Kurtzman, Fell and Boekhout, 2011). Moreover, the yeast cells of *C. tropicalis* have the ability to form biofilm which are determined to be virulent and resistant towards various broad-spectrum drugs like azoles (Fanning and Mitchell, 2012). Biofilms are formed by microorganisms which can adhere to the solid surfaces through various internal machinery outcomes. Biofilms are structured 3D lifestyle which is comprised of three fundamental steps for development: 1) attachment of the cells to the substratum facilitated by cell wall proteins; 2) intermediate phase involves multiplication of the cells, and 3) maturation of the cells and extracellular matrix production required for nutrients distribution and limited diffusion of antifungals. The matured biofilm, which is a reservoir of cells surrounding matrix is also considered having persister cells which remain dormant beneath the biofilm but are capable of continuing infection if exposed (Douglas, 2003). The extracellular matrices vary from species to species in genus *Candida*. The composition of *C. tropicalis* extracellular matrix is distinct from that of other *Candida* species as it is comprised of fewer carbohydrates, proteins and lipids but more hexosamine (Al-Fattani and Douglas, 2006).

These biofilms play an important role in microorganism survival which includes protection from the external environment, drug resistance, metabolic cooperation, nutrient distribution, genetic modification, persister cells to expand infection, and cell signaling (Ramage *et al.*, 2012). Microbial community formation results in alteration of gene expressions and molecular mechanisms to overcome stress efficiently (Robbins, Caplan and Cowen, 2017). *Candida* cells can also signal to each other in response to the external stimuli (Alonso-Monge *et al.*, 2009). This main mechanism of cellular communication is called quorum sensing and mediates cell survival during adverse conditions (Albuquerque and Casadevall, 2012). The

biofilm formation is a multistep process which depends on the cellular adhesion to form a basal layer (Chandra *et al.*, 2001). The growth of the biofilm is regulated by a number of genes such as unscheduled meiotic gene expression (*UME6*), lanosterol 14- α -demethylase (*ERG11*), biofilm and cell wall regulator 1 (*BCR1*), multidrug resistance (*MDR1*) etc. (Srivastava, Singla and Dubey, 2018). Moreover, certain physiological alteration like phenotypic switching and morphogenesis are also observed in strains of *C. tropicalis* (Moralez *et al.*, 2016). Once the biofilm milieu is established in *C. tropicalis*, it can evade a number of external stress, environmental stimuli and drugs. The biofilm once matured contains persister cells to retain its infection, individual cells are dispersed to expand the infection and extracellular matrix is maintained for regular nourishment and environmental tolerance. Evidence has shown the blood-stream dissemination of infection through biofilm formation is a frequent cause of candidemia (Tumbarello *et al.*, 2012). Also, the thick extracellular matrix of *C. tropicalis* impairs oxygen and nutrient supply to the host cells resulting in lower metabolic activity and certain cell death (Alnuaimi *et al.*, 2013). Various episodes of biofilm production by *C. tropicalis* have been reported in clinical investigations in recent years (Paiva *et al.*, 2012; Pannanusorn *et al.*, 2013; Udayalaxmi and D'Souza, 2014). These high incidences of *C. tropicalis* infections have attracted many researchers to combat antifungal resistance and increase the survival of the patients.

2.1.1 Biofilm and its occurrence

The ability of biofilm formation also varies with differences in *Candida* species as listed in Table 2.1. Generally, overall morphology, antifungal resistance and extracellular matrix composition can differ in biofilm with species variation. Some researchers have documented that *C. albicans*, *C. krusei* and *C. dubliniensis* biofilm shows confluences in comparison to the other *Candida* species (Samaranayake *et al.*, 2005; Parahitiyawa *et al.*, 2006; Ramage *et al.*, 2009). Also, different strains belonging to the same species of *Candida* differ dramatically in their biofilm-forming ability (Hawser and Douglas, 1994) indicating variations in the strong or weak biofilm-forming ability of strains within same *Candida* species (Jin *et al.*, 2003; Thein, Samaranayake and Samaranayake, 2007). Wild-type strains of *Candida* are able to form more healthy and confluent biofilm than reference strains of the laboratory.

Table 2.1 Characteristics of *Candida* species biofilm

| <i>Candida</i> species | Growth of Biofilm | Characteristics of Biofilm | Extracellular Matrix | Drug Resistance | References |
|-------------------------------|--------------------------|---|-----------------------------|------------------------|---|
| <i>C. albicans</i> | Very Good | Basal blastospores; a mixture of yeast, pseudo hyphae and hyphae; multi-layered; thick extracellular matrix rich in polysaccharides | Thick | High | (Hawser and Douglas, 1994; Kuhn <i>et al.</i> , 2002; Samaranayake <i>et al.</i> , 2005; Parahitiyawa <i>et al.</i> , 2006; Uppuluri <i>et al.</i> , 2010; Tumbarello <i>et al.</i> , 2012) |
| <i>C. tropicalis</i> | Good | Cellular chains of blastospores; thick extracellular matrix with low amounts of proteins and carbohydrates | Thick | High | (Heffner and Franklin, 1978; Kuhn <i>et al.</i> , 2002; Al-Fattani and Douglas, 2006; Parahitiyawa <i>et al.</i> , 2006; Tumbarello <i>et al.</i> , 2012) |
| <i>C. krusei</i> | Good | Large blastospores; few pseudohyphae; thick polymeric extracellular matrix | Thick | Very high | (Hawser and Douglas, 1994; Samaranayake <i>et al.</i> , 2005; Parahitiyawa <i>et al.</i> , 2006; Pannanusorn, Fernandez and Römling, 2013) |
| <i>C. parapsilosis</i> | Average/ Good | Aggregated blastospores in lesser amount with variations in strains; thin extracellular matrix with high carbohydrates and proteins | Thin | High | (Hawser and Douglas, 1994; Kuhn <i>et al.</i> , 2002; Samaranayake <i>et al.</i> , 2005; Uppuluri <i>et al.</i> , 2010; Taff, Nett and Andes, 2012; Tumbarello <i>et al.</i> , 2012) |
| <i>C. glabrata</i> | Average | Only scant blastospores; thin biofilm with a high content of carbohydrates and proteins | Thin | ND | (Hawser and Douglas, 1994; Kuhn <i>et al.</i> , 2002; Parahitiyawa <i>et al.</i> , 2006; Tumbarello <i>et al.</i> , 2012) |
| <i>C. dubliniensis</i> | Average | Chains of cells and filamentous form with variations in strains; multi-layered; thin extracellular matrix | Thick | High | (Hawser and Douglas, 1994; Ramage, VandeWalle, <i>et al.</i> , 2001; Kuhn <i>et al.</i> , 2002; Taff, Nett and Andes, 2012) |

Previously, a similar phenomenon was reported among the strains of *C. albicans* (Jin *et al.*, 2003). Differential abilities of biofilm formation have been also observed among *C. parapsilosis* strains (Hawser and Douglas, 1994). Some recent researches have shown remarkable biofilm activities of non-*albicans Candida* species when compared to *C. albicans* species (Shin *et al.*, 2002; Girish Kumar and Menon, 2006). Further, imminent research warns to study emerging pathogens such as *Candida* species due to their rigorous biofilm-forming ability. Various microscopic techniques including fluorescence microscopy, scanning electron microscopy (SEM) and confocal laser scanning microscopy (CLSM) based observation of *Candida* biofilm formation and structure have given an understanding of its microstructure. The biofilm development is typically comprised of four consecutive steps: microorganism adhesion to the surface; discrete microcolony formation; secretion of extracellular matrix and maturation of three-dimensional structure; and dispersal of progeny biofilm cells (Figure 2.1). Firstly, the adherence of free-floating *Candida* cells to the substratum takes place for 0.5 to 2 h (Samaranayake and MacFarlane, 1981, 1990; Samaranayake *et al.*, 1995). The adhesion of the cells is primarily governed by non-specific interactions like hydrophobic and electrostatic forces between the substratum and the free-floating cells (Samaranayake and MacFarlane, 1990; Donlan and Costerton, 2002). Furthermore, the release of specific adhesion molecules such as agglutinin-like glycoproteins from cells facilitates stronger adhesion to the substratum (Zhao *et al.*, 2006). As soon as blastospores have adhered, a spatially complex sequenced division is formed which leads to the aggregation of cells in a well-organized manner. The nascent community cells undergo morphogenesis depending on certain factors including carbon sources, species and substratum. For instance, *Candida* biofilm formation on catheter surfaces have been extensively studied and described well with the above mentioned sequential steps involving early phase characterizing adherence of blastospores and their development into distinct microcolonies; intermediate phase contributing in bilayer structure formation of yeast, pseudo-hyphae and hyphae along with secretion of extracellular matrix; and maturation phase corresponding to the dense network of biofilm cells embedded within thick biofilm matrix layer (Chandra and Mukherjee, 2015). *Candida* biofilms, *in vivo*, the formation also seem to follow a similar sequence (Andes, 2017). Although, the thickness appears to be greater (up to 100 μm) and faster maturation is depicted in these biofilms in comparison to the biofilm grown *in vitro* ranging from 25 μm to 450 μm (Chandra *et al.*, 2001; Ramage, Vandewalle, *et al.*, 2001; Andes *et al.*, 2004). The biofilm of *Candida* species is typically formed on flat, hydrophobic surfaces distributing biphasic components i.e. a layer of blastospores adhered to the surface and covering made up of sparse layer formed of hyphal elements embedded inside extracellular matrix (Baillie and Douglas, 1999; Chandra *et al.*, 2001). The multilayered structure of matured

biofilm facilitates the diffusion of nutrients and waste disposal by specialized water channels between yeast/ hyphal cells from the environment to the beneath layers (Ramage, Vandewalle, *et al.*, 2001).

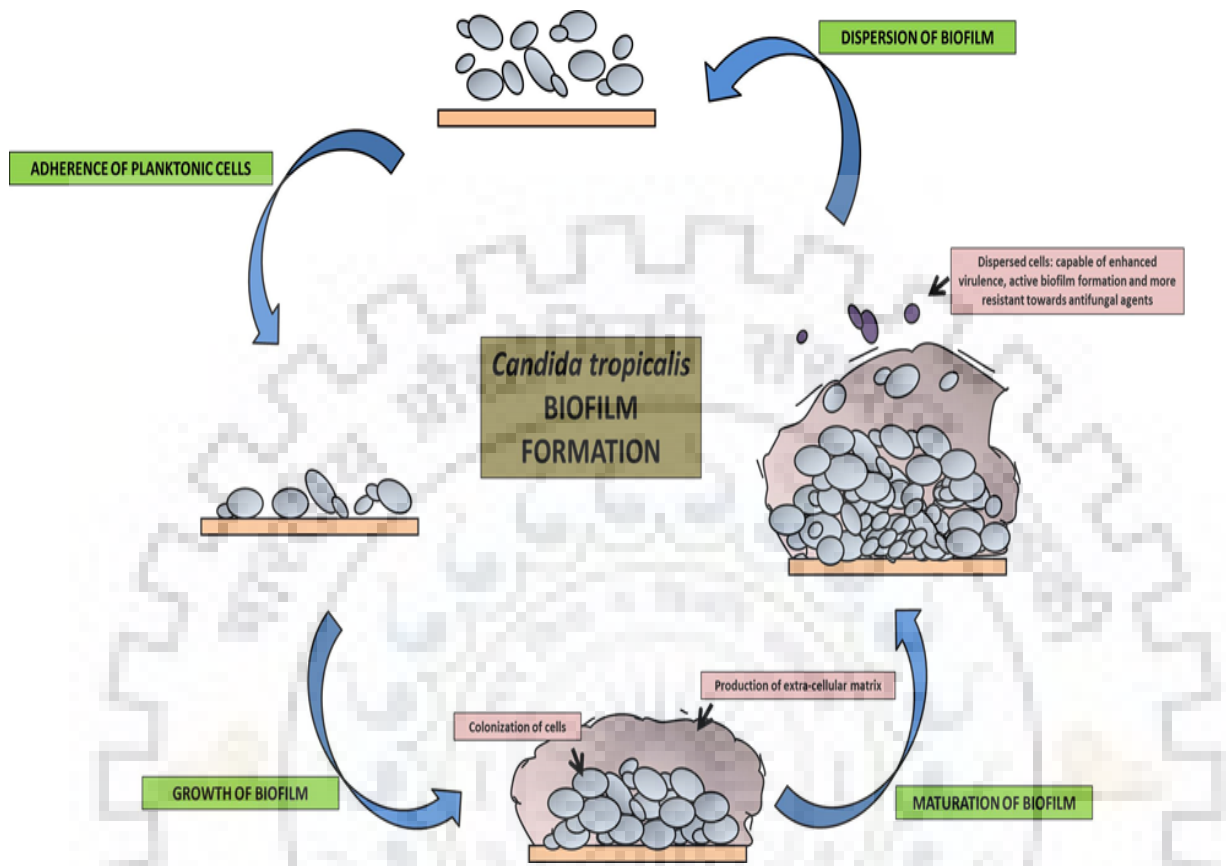


Figure 2.1 Schematic representation of *C. tropicalis* lifestyle

The SEM analysis of *C. albicans* biofilm has shown the formation of biofilm in heterogeneous nature with a mixture of blastopores, hyphae and pseudo-hyphae embedding inside an extra impervious extracellular matrix. The secretion of extracellular matrix by the biofilm is a unique feature of its growth. Microorganisms are immobilized inside a three-dimensional, highly hydrated, gel-like and locally charged environment formed by extracellular matrix produced substances. *Candida* cell adhesion and biofilm formation are supposed to be pivotally controlled by the biofilm extracellular matrix. Also, several special functions are potentially served by this during biofilm growth including maintenance of biofilm integrity through scaffold, phagocytic cell defence, limitation to active drug diffusion and/ or in a combination of all of the above. In bacterial biofilms, primary matrix polymers are exopolysaccharides. Likewise, nearly 40% carbohydrate forms the extracellular matrix of *Candida* biofilm contributing as a major component with varying species (Hawser, Baillie and Douglas, 1998; Al-Fattani and Douglas, 2006). For instance, *C. albicans* biofilm contains 39.6% of total carbohydrate content whereas, *C. tropicalis* biofilm is consist of only 3.3% of

carbohydrates, however, the major component of its extracellular matrix was glucose (32.2%) followed by hexosamine (27.4%). Furthermore, the protein composition was 5% and 3.3% in *C. albicans* and *C. tropicalis*, respectively. Moreover, small amounts of other components such as uronic acid, hexosamine and phosphorus are also found (Al-Fattani and Douglas, 2006). In recent evidence, studies have suggested that even planktonic cell cultures grown under laboratory conditions are also capable of secreting the biofilm extracellular matrix components.

Biofilm is composed of species-specific yeast blastospores, pseudohyphae, hyphae and extracellular matrix however; the formation of hyphae does not show a uniform feature of biofilm (Cavalheiro and Teixeira, 2018). The general steps of biofilm formation include: 1) adhesion of the cells or spores or sporangia on to the surface of the substrate; 2) secretion of adhesins proteins such as (agglutinin-like sequence (Als), hyphal wall protein 1 (Hwp1p), activator of CUP1 Expression (Ace2p), biofilm and cell wall regulator 1 (Bcr1p)) and hyphal structures; 3) microcolonies formation and secretion of extracellular matrix forming a monolayered structure; 4) formation of compact three-dimensional structure of the microcolonies surrounding extracellular matrix and development of nutrient and water channels; 5) maturation of the biofilm capable of cell spore formation and other survivor structures; and 6) dispersal of yeast cells in the form of conidia or hyphal fragments to initiate new infections. Filamentous fungi also secrete small proteins like hydrophobins usually involved with the hyphal adhesion on the hydrophobic surfaces during the formation of biofilm (Wösten, 2001).

In vitro planktonic cultures shared a high degree of similarity between the protein profiles of liquid supernatant and extracellular matrix of *Candida* (Thomas, Bachmann and Lopez-Ribot, 2006). The *Candida* biofilm extracellular matrix production varies with the factors including carbon source, species/ strains and the medium flow rate. Generally, within favourable conditions, the copious extracellular matrix is produced by *C. albicans* in comparison to *C. glabrata* which produces lesser matrix (Parahitiyawa *et al.*, 2006). A large amount of extracellular matrix is also formed by *C. tropicalis* biofilm (Al-Fattani and Douglas, 2006). Various studies on extracellular matrix production in the presence of different carbon sources have provided mixed results. For example, some studies have shown a similar amount of extracellular matrix production when *Candida* biofilm was grown in glucose or galactose as carbon sources (Hawser, Baillie and Douglas, 1998), however, some have shown contrasting results (Jin *et al.*, 2004). Furthermore, *C. albicans* biofilm extracellular matrix production is also affected by nutrients flow rate as extracellular matrix synthesis can be markedly increased

with medium flow rate when compared to the static conditions (Hawser, Baillie and Douglas, 1998). However, extensive matrix formation was favoured by a higher flow rate (Al-Fattani and Douglas, 2006).

2.1.2 Factors affecting biofilm formation

The biofilm formation in *Candida* is affected by many factors such as nutrients, availability of oxygen, substratum, extracellular matrix, and presence of saliva and species variations. Several abiotic surfaces used as model systems *in vitro* including catheter disks made of silicone elastomer, polymethylmethacrylate, acrylic, glass, acrylic and plastic have been employed to develop the biofilm of various *Candida* species (Hawser and Douglas, 1994; Nikawa *et al.*, 1996; Baillie and Douglas, 1999; Chandra *et al.*, 2001; Jin *et al.*, 2004). Furthermore, biotic surfaces model such as engineered human oral mucosa has also been considered as substrate (Mukherjee *et al.*, 2014). The subsequent biofilm formation and cell adhesion could be influenced by the physicochemical properties of the substrate. For example, acrylic surfaces provide lesser adhesion to the *Candida* than the denture's soft lining materials (Radford, Challacombe and Walter, 1998). Similarly, *Candida* biofilms are also developed in varying amounts on different materials of the catheters such as latex urinary catheters form the most extensive biofilm followed by polyvinylchloride (PVC) than polyurethane (Hawser and Douglas, 1994). Contrastingly, 100% pure silicone elastomer are significantly less capable of biofilm formation, however, rough surface topology favours biofilm formation which is minimized with the smoothest surface. The ability of *C. albicans* to form biofilm could be changed by modifying the surface properties of biomaterials including surface contact angle (Chandra *et al.*, 2005). Also, the studies with different nutrients such as carbon sources and their effects have produced conflicting results. Nikawa *et al.*, (1997) have shown that a higher degree of biofilm is formed by *C. albicans* in 50 mM glucose than 500 mM galactose, in contrast, to reverse observation by Hawser and Douglas (1994) (Hawser and Douglas, 1994; Nikawa *et al.*, 1997). Moreover, other researchers have shown that the *C. albicans* biofilm formation is favoured by glucose, lactose and fructose in comparison to that of maltose and sucrose (Parahitiyawa *et al.*, 2006). Also, the presence of surrounding body fluids including serum and saliva in the body has shown a significant enhancement of biofilm formation by *Candida* (Nikawa *et al.*, 1997). On the other hand, one group has noticed that the biofilm formation was not affected in the presence of salivary coating regardless of supplementation of dietary sugar (Jin *et al.*, 2004). The above two contrasting observations may occur due to the difference in the quality of the saliva collected from the individuals, sample collection method

or way of saliva applications as stressed previously in other comparative studies (Samaranayake, Hughes and MacFarlane, 1984). However, it is conceivable that the serum and saliva presence along with varying carbon sources in the environment acts in a complex manner which modulated the biofilm formation by *Candida*.

Oxygen availability is also a major cause in biofilm formation which enables it to get formed either anaerobically or aerobically. However, only limited studies have been found focusing specifically on the biofilm formation by *Candida* under anaerobic conditions (Biswas and Chaffin, 2005; Thein, Samaranayake and Samaranayake, 2007). A previous study has demonstrated the formation of biofilm in anaerobic condition by *Candida* species (Thein, Samaranayake and Samaranayake, 2007). In contrast to a previous study, where *C. albicans* (SC-5314) has suggested inability of the biofilm formation in multi-layered structure within strict anaerobic conditions when formed on plastic, denture material and poly-L-lysine coated glass the study by Thein *et al.*, (2007) have successfully formed biofilm in anaerobic conditions using multiple *Candida* strains and species. Interestingly, non-*albicans Candida* species can also form biofilms under anaerobic condition; however, in *Candida*, the rigorous anaerobic conditions during sub-culturing step can preclude the ability of biofilm formation by the cells (Biswas and Chaffin, 2005; Thein, Samaranayake and Samaranayake, 2007). Furthermore, *Candida* growth within periodontal pockets and root canal systems leading to the polymicrobial infections have shown to occur in anaerobic milieu (Reynaud *et al.*, 2001; Siqueira Jr and Sen, 2004).

2.1.3 Biofilm virulence, pathogenesis and antifungal drug resistance

The biofilm formation by most of the fungal and bacterial species is often reported in natural environments which are formed when the planktonic cell is transformed into sessile variates (Donlan and Costerton, 2002). It is consist of sessile cells attached to the substratum communicating well among them in the protection of the extracellular matrix (Chandki, Banthia and Banthia, 2011). This biofilm was well studied majorly in bacteria and among some of the fungi usually pathogenic such as *Candida sp.*, *Cryptococcus sp.* and *Aspergillus sp.* (Fanning and Mitchell, 2012). The gene expression profiling of *C. albicans* and *A. fumigatus*, when compared in yeast and biofilm form, revealed the biofilm formation as a highly regulated process implementing increased resistance and persistence of infections under the external environment. In the medical field, the biofilm formation has particular importance because of its capability to get adhered to the medical devices like catheters as well as on the mucosal and skin surfaces. The acquired infection through the biofilm is usually recurrent and dispersal of

cells could get access to the blood circulation where it can reach to the internal organs causing deep-seated pathogenesis leading to a high mortality rate (Rabin *et al.*, 2015). The biofilm structure complexity, the presence of extracellular matrix, metabolic heterogeneity and upregulation of specific efflux pumps contributes to the increased resistance in these communities (Ramage *et al.*, 2012). Additionally, other contributing factors include surface contact, quorum-sensing molecules and nutrients. Various factors have been held responsible for the increased antifungal resistance in *Candida* biofilm. These include the presence of persister cells, secretion of the extracellular matrix, altered growth/ metabolic rate of biofilm cells and increased expressions of resistant genes. The biofilm drug resistance is associated with the binding of the drug to the extracellular matrix and persister cells production representing about a fraction of the total cell population upholding metabolic heterogeneity (Lewis, 2010).

Both planktonic cells and biofilm are phenotypic as well as genotypic variants. For instance, more than 3000 differentially regulated genes of various pathways were observed in these two forms (Cromie *et al.*, 2017). These genes were either associated with antifungal resistance or upregulated secondary metabolic pathways (Calvo *et al.*, 2002). The studies on the biofilm formation of both non-mating, *a/a*, and mating cells, *a/α* and *α/α*, have revealed a pheromone related signaling pathway in *C. albicans* responsible for nosocomial infections in human. Morphologically similar biofilm of *C. albicans* appears in alternative forms exhibiting significantly different characteristics depending upon the configuration of the mating-type locus (*a/a* versus *a/α* or *α/α*) which regulates distinct signal transduction pathways. The biofilm made of *a/α* cells is impermeable to the molecules of size range 300Da to 140kDa depicting resistance to the antifungal agents. In contrast, the *a/a* or *α/α* cells forming biofilm are permeable to the molecules of above-mentioned range and therefore showing sensitivity to the antifungals and also penetrated by host defence cells. *C. albicans* cells must go through a transition from white cell to the opaque cell type in order to mate. *α/α* opaque cells induce a mating response pheromone released upon switching. The release of pheromone also induces mating-incompetent *a/a* white cells to develop adhesive phenotype which leads to the biofilm formation and mating (Daniels *et al.*, 2006). Therefore, *Candida* is of major concern due to its capability to adapt phenotypically inside biofilm reforming the status of drug development in order to combat the infection caused keeping in view the undesirable effects of these molecules in human (Silva *et al.*, 2017).

2.1.3.1 *Biofilm resistance towards conventional drugs*

Hawser and Douglas (1995) have first demonstrated the increased antifungal resistance in *Candida* biofilm mode of growth. *Candida* biofilm is more resistant (up to 30 to 2000 times) than the planktonic counterparts against antifungal agents such as fluconazole, ketoconazole, itraconazole and amphotericin B (Hawser and Douglas, 1995). Subsequently, more researchers have confirmed the aforementioned observations (Chandra *et al.*, 2001; Ramage, Wickes and Lopez-Ribot, 2001; Kuhn *et al.*, 2002; Serefko, Chudzik and Malm, 2006; Jain *et al.*, 2007). The study on resistance against fluconazole is of particular interest as it is frequently used for the patients suffering from HIV/ AIDS. *In vitro*, *Candida* biofilm resistance against fluconazole ranges from 250 to 400 times more in comparison to that of planktonic cells (Chandra *et al.*, 2001; Ramage, Wickes and Lopez-Ribot, 2001). Fluconazole resistance has also been observed during *in vivo* *Candida* biofilm formation, where the minimum inhibitory concentration was found to be increased as high as 128 times to that of planktonic cells (Chandra *et al.*, 2001; Andes *et al.*, 2004). To overcome the clinical burden of biofilm resistance, newer antifungal agents including the liposomal formulation of amphotericin B and echinocandins have been developed and emerged as possible hope. However, more studies are required to define the particular effectiveness of these alternatives against *Candida* biofilm (Bachmann *et al.*, 2002; Kuhn *et al.*, 2002).

The major targets of abovementioned antifungal agents are cell wall or cell membrane. Azole targets the enzyme cytochrome dependent lanosterol-14- α -demethylase (Erg11p) which is involved in the ergosterol biosynthetic pathway. Ergosterol is found in the cell membrane and majorly responsible for the fluidity and integrity of the membrane as well as nutrient transport and chitin synthesis (Lupetti *et al.*, 2002). The resistance to azoles is attained through various factors such as efflux pumps or multidrug transporters and amino acid substitution on Erg11 protein (Sanglard, Coste and Ferrari, 2009). Despite all these resistance, azoles are the third most commonly used drug in therapeutics (Sanglard, 2016). The impairment of ergosterol biosynthetic pathway results in porous plasma membranes which results in osmotic imbalance and rapid collapse of the cell (Georgopapadakou and Walsh, 1994).

Amphotericin resistance is also seen in *C. tropicalis* isolates with altered ergosterol binding on the cell membrane. The mutant product of ergosterol inhibits the binding of amphotericin B to the ergosterol. Generation of oxygen species is also evident part of the fungicidal mechanism of action of some antifungals including amphotericin B (Mesa-Arango *et al.*, 2014). Moreover, the frequent use of amphotericin B in patients has also resulted in

immunosuppression (Ullmann *et al.*, 2006). Multi-drug resistance between azoles and amphotericin B is acquired due to concomitant mutations in the encoding sterol 14 α -demethylase (*ERG11*) and encoding C22 desaturase (*ERG5*) genes (Martel *et al.*, 2010).

Another class of antifungals echinocandins is increasingly used during invasive *Candida* infections targeting fungal cell wall through locking β -1, 3-D-glucan synthase and has proved effective drug against *C. tropicalis* with the lowest number of resistant strains (Perlin, 2011). However, the dosage required in these cases was limiting the use and thus, making it of lesser practice. Echinocandins target glucan synthetase which includes biosynthesis of β -1, 3-D-glucan (Onishi *et al.*, 2000). *C. tropicalis* were found less susceptible to echinocandin due to mutant 1, 3-beta-glucan synthase (*FKS*) genes and adaptation towards the stress. Moreover, the cell wall of the fungus is a dynamic structure and adapts compensatory mechanism over inhibited components by producing alternatives. Chen *et al.*, (2011) have also established the role of calcineurin, a phosphatase which combats the stress of the cell wall through chitin synthesis (Chen *et al.*, 2011). The thickening of the chitin layer of the fungal cell wall in *C. tropicalis* is a response of calcineurin during micafungin stress.

2.1.3.2 Resistance due to extracellular matrix

The extracellular matrix, as a physical barrier, contributes to enhanced drug resistance in the biofilm community by preventing antimicrobial access to the embedding cells. The physicochemical properties of drug as well as the nature and amount of extracellular matrix are largely responsible for the hindrance of antimicrobial to reach the biofilm cells. Moreover, the enzymes present within the extracellular matrix of bacterial biofilm can also digest the drugs. The role of *Candida* biofilm extracellular matrix in drug resistance is still unclear. For instance, the *C. albicans* biofilm showed increased resistance to amphotericin B as the matrix synthesis was stimulated to enhance when grown under constant liquid flow (Al-Fattani and Douglas, 2006). Also, the survival rate of *Candida* biofilm cells was reduced to 20% on extracellular matrix removal in the presence of amphotericin B (Baillie and Douglas, 1999).

Once the antifungal agents have been administered to the *C. tropicalis* biofilm for treatment, it could have few fates (Figure 2.2). Firstly, the drug could not penetrate the extracellular matrix and remains ineffective at a very early stage. The drugs with larger molecular weight could tend to suffer no penetration at all. However, the agent with moderate size could get inside the extracellular matrix but gets trapped inside the polymeric components. This could also be the fate of more reactive molecules which may get consumed with the components of the extracellular matrix therefore, gets deficit for treatment. Further, if the

antifungal agent has reached the cell it could encounter with the resistant nature of the biofilm cell due to the altered nature of the cell wall and cell membrane of cells. Lastly, the ability of a cell to survive certain dosage of antifungal drugs comes into play. The alterations of biofilm cell proteome results in a significant rise in drug tolerance which leads to the higher dosage requirements and therapeutic failures.

On the contrary, Al-Fattani and Douglas (2004) have reported that the poor penetration of drugs within the extracellular matrix does not seem to solely contribute to antifungal drug resistance (Al-Fattani and Douglas, 2004). Similarly, other researchers have shown that static biofilm development exhibits the same level of antifungal drug resistance against fluconazole, amphotericin B and flucytosine as that of cells grown with a larger amount of extracellular matrix in the shaker (Baillie and Douglas, 2000). This field of research certainly gives a promising future for clinical implications of extracellular matrix and its components as potential drug targets.

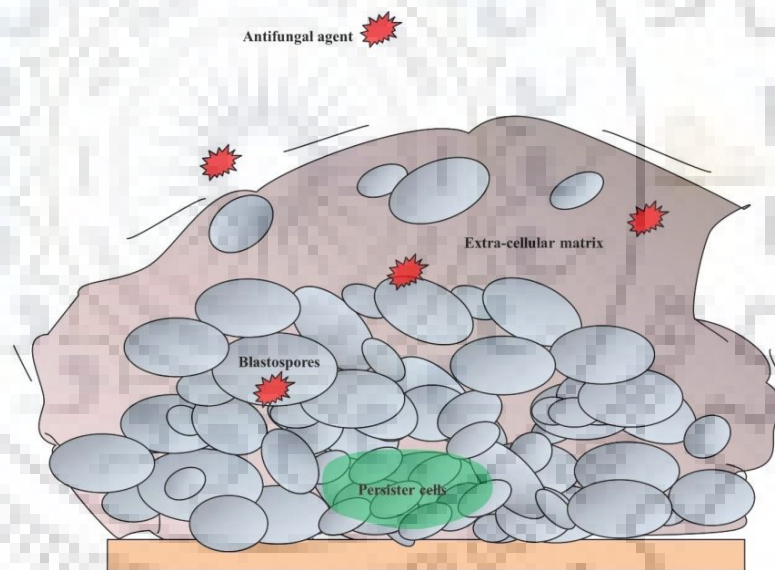


Figure 2.2 Fate of antifungal agents during *C. tropicalis* biofilm treatment

2.1.3.3 Drug resistance of biofilm at the cellular level

The molecular mechanisms of antifungal resistance in the biofilm of *Candida* have not been fully decoded. Some studies have described the involvement of major drug efflux pumps and ATP-binding cassette in increased azole drug resistance. However, the efflux pumps contribute only during the early phase of *Candida* biofilm development, whereas, membrane sterol contributes during intermediate and latter stages to the azole resistance (Mukherjee *et al.*, 2003). The upregulation of candida drug resistance 1 (*CDR1*), candida drug resistance 2 (*CDR2*) and multidrug resistance 1 (*MDR1*) genes seem to be responsible for azole drug

resistance during *Candida* biofilm development. Remarkably, the deletion of these three genes does not affect the high-level drug resistance of the matured biofilm of *Candida* (Mukherjee *et al.*, 2003). Garcia-Sanchez *et al.* (2004), by employing microarray analysis, have demonstrated that the expression of *CDR* and *MDR* genes is early phase-specific while contributing to the azole resistance, whereas, sterol composition change is involved in azole resistance during maturation phase (García-Sánchez *et al.*, 2004). Conversely, research involving *in vivo* biofilm model have demonstrated the results differently, such as the significant upregulation of *CDR1* and *CDR2* during biofilm development than planktonic counterparts, whereas, the expression of *MDR1* and *ERG11* genes were found similar in both the planktonic and biofilm cells (Andes *et al.*, 2004). Furthermore, both *in vivo* and *in vitro* genome-wide expression analysis are required to explore sophisticatedly the specific roles of genes involved in antifungal resistance of *Candida* biofilm.

2.1.3.4 Role of persister cells in biofilm resistance

The persister cells which are not the mutants but the phenotypic variants of wild type cells can survive the antibiotics at higher concentrations of minimum inhibitory concentration (MIC) (Keren, Kaldalu, *et al.*, 2004). The dormant persister cells of *Escherichia coli*, *Pseudomonas aeruginosa* and *Staphylococcus aureus* accounting only 1% of the total population in a bacterial biofilm are observed to be responsible for multidrug tolerance (Keren, Kaldalu, *et al.*, 2004; Keren, Shah, *et al.*, 2004). Similarly, in *Candida* biofilm, a subpopulation of cells has been observed to be highly tolerant against antifungal agents who are not seen in planktonic counterparts (LaFleur, Kumamoto and Lewis, 2006). *Candida* biofilm also exhibits a biphasic killing pattern where susceptible subpopulation was died in the presence of antifungals, however, surviving persister cells showed multidrug resistance. Further, reinoculating those surviving cells was able to produce viable biofilm with a newer subpopulation of persister cells which confirmed them to be the heritable wildtype variants of genotypes. More research is required to study this intriguing phenomenon in biofilm biology.

2.1.3.5 Effect of metal ions on biofilm

Interestingly, the search for the role of these metal ions on biofilm modulation in *Candida* species could give essential insights on biofilm formation (Harrison *et al.*, 2006; Harrison, Turner and Ceri, 2007). For instance, *C. tropicalis* biofilm was reported to be 65 times more resistant than their planktonic counterparts when treated with metal ions (Harrison *et al.*, 2006). Among most heavy metals with tested toxicity, metal ions such as Hg^{2+} , Cu^{2+} or CrO_4^{2+} at very higher concentrations could only kill *Candida* cells that are adhered to the

surface. Harrison *et al.* (2007) have also extended their studies on the examination of the metal ions role over its resistance, drug and cell type interconversion in *Candida* biofilm grown on microtiter plates with metal ions gradient arrays (Harrison, Turner and Ceri, 2007). Certain metal ions such as (Co^{2+} , Zn^{2+} , Cu^{2+} , Hg^{2+} , CrO_4^{2+} , Ag^+ , Cd^{2+} , AsO_4^{3-} , SeO_3^{2-} and Pb^{2+}) have identified to block or trigger the transition between yeast and hyphal cell types at many sub-inhibitory concentrations. Therefore, on the exposure of metal ions to the *Candida* biofilm, the structure of biofilm tends to vary as a layer cake, domed, mycelial or flat as described by the authors. Hence, these studies highlight the metal ions function to modulate the spatial structure and morphogenesis of the *Candida* biofilm. The authors have postulated that the drug resistance which develops parallel with the biofilm maturation due to multiple cellular morphogenesis could alter the susceptibility against antifungal defences in the presence of metal ions. However, detailed research is again needed in this field.

2.2 Natural compounds and their antimicrobial activities

The production of a significant number of compounds from plants mainly comprises of essential oils. Essential oils are usually the plant-derived complex mixture of both polar and non-polar natural compounds. These are used commonly ever since from the earliest civilization in various parts of the world and has given circumstantial insights to defend oneself from threats in the environment. The potentials of compounds obtained from natural sources are known to possess antimicrobial properties against a wide range of foodborne pathogens (Gyawali and Ibrahim, 2014). The current outpacing drug resistance from the standard antibiotics has given the alarm to recondition the remedies from the past that could save our future. Therefore, the recent development of essential oils for their holistic as well as an alternative use for antimicrobial purposes has led the investigators to elucidate their precise mechanism of action. These compounds alone or in combination may vary in potency and spectrum of antimicrobial activity. During synergy, the essential oils combat a wide range of microbes through multiple targets. Other artificially designed antimicrobial cationic peptides have also shown fungicidal effect against *C. albicans* through multiple targets including cell wall structure disruption and compromised cell membrane permeability which leads to high ROS accumulation, eased entry into the cells and apoptosis induction (Maurya *et al.*, 2013).

Furthermore, the use of essential oils in many cultures is profound all around the world. The essential oil was the term given by a Swiss medicine reformer, Paracelsus von Hohenheim, in the 16th century. Previously, called as aromatic oils their uses have been cultural as well as religious for healing purposes. Although the exact notable existence of essential oils is hard to

recognize, however, the cave paintings found in Lascaux located near Dordogne in France has suggested uses of plants for healing purposes in everyday life. This earliest evidence of human knowledge has been carbon-dated far back to 18,000 BC. Ayurveda derived from “*Ayur*” meaning life and “*Veda*” meaning knowledge, is the best known traditional Indian medicine which incorporates the use of essential oils as remedial potions with a history of approx. 3000 years. The Vedic literature has listed various compounds such as sandalwood, ginger, turmeric, etc. documenting a total of more than 700 herbs as good healing materials with usage in perfumery and other therapeutic purposes.

Several researchers are involved to identify and isolate compounds of natural origin which are safe and less toxic with potent antifungal activity against pathogenic fungi (Liu *et al.*, 2017). Various plant parts including leaves, stems, roots and seeds are explored to find biologically active components with emphasis on the antifungal action for fighting infections alone or in synergy with other drugs (Wagner, 2011). Essential oils of plant origin are of wide-spectrum use with eminent qualities of multifunctional applications including antimicrobial properties in traditional medicine and aromatherapy. Essential oils constitute monoterpenes that give characteristic aromas and flavours extensively used in food, cosmetics, fragrance and pharmaceuticals. Since ancient times, various plants are employed in treating infections without certain knowledge of microorganisms. Although medicinal plants are still in use and have wide applications in remote areas with effective antimicrobial activity, extensive investigation on the components of these plant extracts and their components are on the boom to dig for effective medications from natural resources.

A number of researchers are dedicated towards isolation and characterizations of these essential oils and their administration through modern means. Extensive studies are employed to check the *in vitro* effects of pure essential oils against microorganisms and clinical studies to find out undesirable side effects like allergies. Also, the extraction, purification and storage of these volatile compounds are extremely necessary. Volatile properties of these components can be exploited in clinical studies to administer these oils as drugs and combat emerging resistance of microbes against conventional drugs. Essential oils are found effective many times against the drug-resistant strains of various bacteria and fungus. However, not much of essential oils are recommended or studied for clinical administration. Therefore, it is of the utmost need to elaborate on the administration of such oils in diseased conditions.

2.2.1 Characteristics of essential oils and terpene molecules

Essential oils are highly lipophilic in nature and have a low molecular weight which may correspond to its antifungal properties making it capable to disrupt the cell membrane resulting in cell death or inhibiting germination and sporulation of fungi. Additionally, only partial success is attained upon small molecules acting as effective antifungals due to the chemical reaction of these with the extracellular biofilm matrix restricting their penetration. For instance, in bacteria, the increase in the resistant properties towards antimicrobial agents due to biofilm formation and production of extracellular matrices implemented a search of new naturally plant-derived therapeutic alternatives including essential oils.

Essential oils synthesizing aromatic plants have to protect themselves from secreting terpenes that could damage the architecture of living biological cellular membrane. The evolution has made such aromatic plants to survive in the presence of these terpenes by following certain mechanisms. For instance, only the epidermal cells, or to be precise the epidermal oil glandular cells are the primary site for the biosynthesis of monoterpenes in *Majorana hortensis* Moench (Croteau, 1977). Furthermore, the glycoside bound monoterpenes are reported to exist, in several, Lamiaceae members (Merks and Svendsen, 1989). The careful examination of the glycosides of terpenes could report in different behaviour with respect to the cellular toxicity. Also, free terpene molecules have shown a toxic effect on the cell membranes of the bacteria, and the plant chloroplasts (Knobloch, Weis and Weigand, 1986; Knobloch *et al.*, 1989; Di Pasqua *et al.*, 2007). Not surprisingly, the terpenes have established toxicity to the plant cell cultures (Brown, Hegarty and Charlwood, 1987).

The survival and development of aromatic plants are evolutionarily permitted by the arrangement of essential oil glands which were isolated from the surrounding living plant parenchyma as depicted by various historical anatomical drawings similar to the morphological essential oil glands details over the plant leaf surface. The exposed oil glands are able to damage the surrounding plants through evaporation of terpenoid molecules, a phenomenon termed as “Allelopathy” (Rice, 1987). In conifers, the pollutants from the atmosphere may cause leakage of the well-separated endogenous terpenes from needles which can further damage the cellular organelles (Vollbrecht *et al.*, 1987). Some heterotrophic bacterial strains have been isolated with the ability of growth in limonene using it as the only carbon source (Kokkini and Papageorgiou, 1987). Furthermore, it was assumed that such microorganisms could decay these terpenes into lesser or non-toxic smaller components which can be used as building blocks of carbon by using extracellular enzymes.

2.2.2 Antimicrobial activities of essential oils and terpenes

Essential oils temper the growth of microorganisms and biofilm development similar to other phytochemicals employing specific mechanisms of actions (Hyldgaard, Mygind and Meyer, 2012). Although, microorganism grow to a certain threshold value causing pathogenesis, however, several mechanisms of action also trigger cell signaling, biofilm and other pathogenic parameter development and production of specific molecules. Food and Drugs Administration (FDA) have classified essential oils as generally recognized as safe (GRAS) due to their plant origin and are considered less harmful than synthetic products to the consumers (Smith *et al.*, 2005). The three groups namely, alcohol, aldehyde and phenol comprising effective terpenes with documented antimicrobial activities against bacteria and some fungal species were selected on the basis of the literature survey to elaborate their effects against *C. tropicalis* biofilm. The terpenes used in the present studies have been enlisted in Table 2.2.

The research which includes the discovery of new and effective natural products is devoted to obtaining good antimicrobial activity with low toxicity. The examination of these essential oils against biofilm is encouraged as the use of naturally occurring small molecules are less likely to develop any resistant phenotype due to multifactorial targets and are greatly supported being safer alternatives (Chung and Toh, 2014). Tea tree oil has also shown a significant effect as antifungal and antimicrobial agents (Hammer, Carson and Riley, 2004). Also, the natural bioactive precursor analogues such as carvacrol derived were designed and represented significant biofilm inhibition of *S. pneumoniae* and *E. coli* biofilm (Aneja *et al.*, 2018). Essential oils by far have shown great effects during treatment of mixed biofilm including both bacteria and fungi usually encountered on the occurrence of chronic infections (Pekmezovic *et al.*, 2016).

Essential oils and their components such as terpenes which could not be administered orally have an important issue of safety. However, the topical use of carvacrol (a component of *Origanum* oil) and eugenol (a component of *Syzygium* oil) have demonstrated safety in *in vivo* treatment of oral and vaginal candidiasis in rats (Chami *et al.*, 2004, 2005). The toxicity of essential oils is distinctly reliable on the concentration and form of their application (Hammer *et al.*, 2006). A very low irritant capacity has been reported in tested 5% and 25% concentration of tea tree oil ointment, cream and gel formulations, when tested with a patch of 10% tea tree oil in patients (Aspres and Freeman, 2003; Veien, Rosner and Skovgaard, 2004). Moreover, the contact allergy reactions and irritation could be avoided by using lower concentrations of the

agent, thus, the use of essential oils at 100% concentrations are not recommended (Hammer *et al.*, 2006).

Table 2.2 Selected terpenes with documented antimicrobial effects

| S.No. | Components | Origin | Activities | References |
|-----------------|----------------|-------------------|---|---|
| ALCOHOL | | | | |
| 1. | Geraniol | <i>Rosa</i> | Synergistic/ antagonistic | (Lee <i>et al.</i> , 2008) |
| 2. | Menthol | <i>Mentha</i> | Cell membrane/ wall damage Efflux pump inhibition Biofilm inhibition Anti-quorum sensing Mycotoxin production | (Ramage <i>et al.</i> , 2002; Chen <i>et al.</i> , 2013; Husain <i>et al.</i> , 2015; Friedman, Henika and Mandrell, 2016; Bound, Murthy and Srinivas, 2016) |
| ALDEHYDE | | | | |
| 3. | Citral | <i>Cymbopogon</i> | Antifungal effect Cell membrane/ wall damage Synergistic/ antagonistic Biofilm inhibition Mycotoxin production | (Chang, Chen and Chang, 2001; Ramage <i>et al.</i> , 2002; Usta <i>et al.</i> , 2003; LaFleur, Kumamoto and Lewis, 2006; Sharma and Tripathi, 2008; Vieira <i>et al.</i> , 2009; Friedman, Henika and Mandrell, 2016) |
| 4. | Cinnamaldehyde | <i>Cinnamomum</i> | Cell membrane/ wall damage Efflux pump inhibition Action on mitochondria Mycotoxin production | (Ramage <i>et al.</i> , 2002; Pina-Vaz <i>et al.</i> , 2004; LaFleur, Kumamoto and Lewis, 2006; Ahmad <i>et al.</i> 2011; Belenky and Collins 2011; Kavooosi and da Silva, 2012; Chen <i>et al.</i> , 2013; Cotoras <i>et al.</i> , 2013; Freires <i>et al.</i> , 2014) |
| PHENOL | | | | |
| 5. | Carvacrol | <i>Origanum</i> | Antifungal effect Cell membrane/ wall damage Change in cell growth and morphology Efflux pump inhibition Action on mitochondria Mycotoxin production Synergistic/ antagonistic Anti-quorum sensing | (Dorman and Deans, 2000; Pina-Vaz <i>et al.</i> , 2004; Hammer <i>et al.</i> , 2006; LaFleur, Kumamoto and Lewis, 2006; Kohanski <i>et al.</i> , 2007; Wu <i>et al.</i> , 2008; Lee <i>et al.</i> , 2008; Gusarov <i>et al.</i> , 2009; Rammanee and |

| | | | |
|----|---------|-----------------|--|
| | | | Hongpattarakere, 2011; Kong <i>et al.</i> , 2012; Chen <i>et al.</i> , 2013; Nazzaro <i>et al.</i> , 2013; Rajput and Karuppayil, 2013; Burt <i>et al.</i> , 2014; Noberga <i>et al.</i> , 2016; Haque <i>et al.</i> , 2016; Ghalem, 2017; Requena, Vargas and Chiralt, 2019) |
| 6. | Eugenol | <i>Syzygium</i> | Antifungal effect Cell membrane/ wall damage Synergistic/ antagonistic Biofilm inhibition Mycotoxin production (Hammer, Carson and Riley, 2004; Vieira <i>et al.</i> , 2009; Shreaz <i>et al.</i> , 2010; Belenky and Collins 2011; Friedman, Henika and Mandrell, 2016) |
| 7. | Thymol | <i>Thymus</i> | Antifungal effect Cell membrane/ wall damage Change in cell growth and morphology Efflux pump inhibition ROS production Synergistic/ antagonistic Mycotoxin production (Dorman and Deans, 2000; Ramage <i>et al.</i> , 2002; Hammer, Carson and Riley, 2004; Wu <i>et al.</i> , 2008; Lee <i>et al.</i> , 2008; Vieira <i>et al.</i> , 2009; Kong <i>et al.</i> , 2012; Chen <i>et al.</i> , 2013; Rajput and Karuppayil, 2013; Tolba <i>et al.</i> , 2015; Noberga <i>et al.</i> , 2016; Nazzaro <i>et al.</i> , 2017) |

2.2.3 Effect of essential oils against *Candida* species

Essential oils extracted from *Ocimum americanum* have shown good antibiofilm activity against *C. albicans* (Thaweboon and Thaweboon, 2009). Eugenol demonstrated higher antibiofilm activity against the sessile cells of *C. albicans* with MIC₅₀ to be 500mg/mL which is two folds higher in comparison to the 48h grown yeast cells (He *et al.*, 2007). Furthermore, the ultrastructure of the biofilm when observed through Scanning Electronic Micrograph (SEM) imaging illustrated the damage to the constituents of the biofilm with the bare diffusion of the eucalyptus and peppermint oil exerting a metabolic interference (Hossain *et al.*, 2016).

The antibiofilm activity is assigned to some of the active components of these essential oils such as linalool, geranial, menthol, eugenol, 1,8-cineole, limonene etc. which reduces the development of biofilm. A study on the antifungal activities of eucalyptus, clove, peppermint and ginger grass has demonstrated potent inhibition of *C. albicans* and its biofilm. Also, eucalyptus oil exhibited potentially higher activity compared to fluconazole (Agarwal, Lal and Pruthi, 2010). Likewise, the essential oils of *Rosmarinus officinalis* on the coating with nanoparticles strongly inhibit the adherence and development of biofilm on the catheter by *C. albicans* and *C. tropicalis* (Chifiriuc *et al.*, 2012). Certainly, the effective concentrations of essential oils overlap the toxicity range to the mammalian cells, therefore, essential oils are considered low at the level of environment and health. The development of essential oils as free or with the coating is of great interest in biomedicine especially in the area of human pathogenesis such as candidiasis due to frequent emergence of antifungal resistance opening new directions in drug designing with effective antifungal as well as antibiofilm properties. Essential oils of *Cymbopogon citratus* and *Syzygium aromaticum* are reported with efficient antibiofilm activity against some drug-resistant strains of *C. albicans* (Khan and Ahmad, 2012). The microscopic studies on the 3D biofilm structure by using light and scanning electron microscope has confirmed the deformities on the surface topology in the presence of sub-MICs indicating damage to the cell membrane. Few studies have employed the atomic force microscopy (AFM) to visualize the biofilm morphology on solid surfaces including both hydrated and dehydrated states. These researchers have demonstrated the effectiveness of the antifungal agents causing morphological changes in the structure of the biofilm in comparison to the yeast counterparts.

Laurus nobilis essential oil demonstrated antifungal properties by inhibiting biofilm adhesion and formation in *Candida* species (Peixoto *et al.*, 2017). The increase in MIC value in the presence of sorbitol, an osmotic protector, suggested its mode of inhibition at the level of the cell wall. The affinity of essential oil towards ergosterol confirmed its involvement in alteration of the cell membrane and ion permeability showing similarity with conventional polyenes such as nystatin. Additionally, the adherence inhibition of essential oil was also observed at a concentration of 1000mg/mL targeting the earlier disruption of biofilm formation which results in an early cure of infection due to *Candida* species (Trindade *et al.*, 2015).

Myrtus communis essential oil has inhibited the adherence and formation of biofilm among clinically isolated species of *Candida* including *C. albicans*, *C. parasilosis* and *C. tropicalis* (Cannas *et al.*, 2014). Therefore, the search for new compounds is necessary to overcome the adverse effects of increased resistance against available antifungal therapies.

However, the boost in research improving antimicrobial therapies is an utmost requirement to generate new and cheap drugs against candidiasis.

A study has documented the action of formyl-phloroglucinol meroterpenoids such as eucarobustol E against *Candida* biofilm cells by blocking the transition of yeast cells into hypha and reduction in cell surface hydrophobicity which hinders ultimate adhesion of the cells on the abiotic surface (Liu *et al.*, 2017). Moreover, the expression of genes regulating hyphal growth including *EFG1*, *UME6*, *TEC1*, *CPHI*, *HGCI*, and *EEDI* was downregulated, however, genes related to ergosterol biosynthesis as well as farnesol synthesis were upregulated.

2.2.4 Mechanism of action of essential oils and terpenes

Fungal infections are difficult to combat in comparison to the bacterial infections as the causal organism are itself eukaryotic organisms making it difficult for therapeutic treatment. One interesting feature to consider is the unique chitinous cell wall of fungus which may be exploited as the specific primary target of toxic agents due to its absence in human cells. The development of intrinsically resistant strain and species could develop effective large-scale chemical treatments. The major concern of fungal pathogens includes its onset and severity which depends on the inoculum, resistance and immunological condition of the host. Essential oils and its components are considered as the most promising fungal inhibitor of natural origin (Kalemba and Kunicka, 2003). Various essential oils obtained from a number of plants and herbs possess intense antifungal properties (Lang, Buchbauer and Journal, 2012).

A number of studies have suggested that the essential oils and its components could act in synergistic as well as antagonistic manner (Stević *et al.*, 2014). The increase in fungistatic activity when used in combination has more advantages as pathogens are not capable to acquire resistance against multiple essential oils that easy. Phenolic terpenes act as antifungal agents due to the presence of functional hydroxyl group in them. Thymol and carvacrol interact with ergosterol, a major component of the cell membrane and alters the integrity of the membrane subsequently damaging the cell. Carvacrol has shown strong antifungal activities when tested alone. The antifungal activity of carvacrol plausibly corresponds to its binding to the sterol of the cell membrane thus damaging the integrity of the membrane which is lethal (Chavan and Tupe, 2014). Structurally similar thymol also interacts with the sterol components of the cell membrane through binding even with different location of the hydroxyl group unlike eugenol (Ultee, Bennik and Moezelaar, 2002). Thymol also affects the morphology of mycelium by changing the localization of chitin in the hyphae. Similarly, linalool also interferes with the

stability of the fungus along with the formation of the biofilm. Essential oils can inhibit more than one parameter of cell survival acting synergistically. The sesquiterpene hydrocarbons and its oxygenated derivatives exhibit high efficiency with low drug resistance in the fungus in comparison to the whole essential oils (Hyldgaard, Mygind and Meyer, 2012). Certain deoxyglucosides of citronellal, borneol, carvacrol, fenchol, menthol, thymol and S-(-)-perillyl alcohol does exhibit remarkable antifungal properties against *Aspergillus flavus*, *A. ochraceus* and *Fusarium oxysporum* (Bound, Murthy and Srinivas, 2016). Citronellal deteriorates the cell membrane of the spore releasing cellular contents due to high extracellular conductivity in *Penicillium digitatum* when studied *in vivo* (Wu, OuYang and Tao, 2016).

2.2.4.1 Effect on the cell wall and cell membrane

The growth and viability of fungi rely on the cell wall which consists of three major structural elements including chitin, glucan, and mannan, usually considered as drug targets. Chitin is synthesized by chitin synthase forming a long linear homopolymer of β -1, 4 linked N-acetylglucosamine (GlcNAc). It is required for the construction of the cell wall which is essential for fungal survival. The chitin polymerization inhibition damages cell growth and division affecting cell wall maturation, bud ring formation and septum formation (Lesage and Bussey, 2006). Various compounds of natural origin demonstrate a similar activity against the cell wall of the fungus. Anethole inhibits chitin synthase (CHS) activity in a dose-dependent manner. Trans-anethole ascertains morphological changes in hyphae such as swallowing the hyphal tips as studied against the *Mucor mucedo* IFO 7684, filamentous fungus (Yutani *et al.*, 2011). Therefore, the disruption of the cell wall caused by thinning of the hyphal wall, distorting and final transformation in hollow and flattened hyphal tips due to essential oil which leads to its bifurcation into bud-like structures (Oussalah, Caillet and Lacroix, 2006). Thymoquinone, present majorly in the essential oil of black cumin seed extensively damages the fungal cell wall and membrane (İşcan, İşcan and Demirci, 2016).

Fungal cells essentially require the plasma membrane for its survival, therefore, any alteration in the structure and function involving its synthesis or maintenance causes damage to the cell and ultimate death. The mode of action and blockage of toxin production by essential oils depicts structure-based varying potency levels. Citronellal inhibits the growth of *C. albicans* by distorting the membrane integrity and cell cycle arrest (Singh, Fatima and Hameed, 2016). Cinnamaldehyde acts actively against bacteria, yeasts, and filamentous fungi through inhibition of the activities of ATPases, alterations in the cell membrane integrity and structure and cell wall biosynthesis. Therefore, cinnamaldehyde and its derivatives are considered as potent antifungal agents against various fungal isolates (Shreaz *et al.*, 2010). Essential oils

could accumulate in the hydrophobic molecules inside the lipid bilayer structured cell membrane which allow the easy transfer of these components into the cell. Furthermore, the lipophilic, as well as water-soluble properties of different essential oils, perform varying antifungal activities. The inhibitory process of essential oils is affected due to the interference of a specific functional group with the membrane-associated enzymes (Xie, Fang and Xu, 2004).

The essential oil of tea tree oil and its components are found to alter the cell membrane fluidity and thus permeability due to compromise in the membrane-associated functions in *C. albicans* (Hammer, Carson and Riley, 2004). Certain essential oils can act at singular or multiple levels. Essential oils of *Litsea cubeba* and its major component citral are reported to inhibit *Aspergillus niger*, *Alternaria alternate*, *Fusarium solani* and *F. moniliforme* by damaging their cell wall, distortion in the cell membrane through inhibiting ergosterol biosynthesis in *C. albicans* causing cytoplasmic leakage and inhibiting peptidoglycan, DNA, RNA and protein synthesis. The disruption of regular sterol biosynthetic pathway leads to the lesser production of ergosterol similar to that of cholesterol by essential oil and its major components of *Coriandrum sativum* (Freires *et al.*, 2014). The reduction in the ergosterol content of the cell membrane corresponds to metabolic and osmotic instability which further negotiates the cellular ability to reproduce and infect (Rajput and Karuppayil, 2013).

2.2.4.2 Effect on mitochondria

Mitochondrial dehydrogenases such as lactate, malate, and succinate dehydrogenases are inhibited by some essential oils reducing the ATP biosynthesis, therefore, mitochondrial efficiency. In *C. albicans*, the citric acid cycle and ATP synthesis in mitochondria are inhibited by the antifungal action of the essential oil of *Anethum graveolens* (Chen *et al.*, 2013). A report on terpenes has suggested that the levels of reactive oxygen species (ROS) and ATP generation are altered due to diminishing mitochondrial content (Haque *et al.*, 2016). Fungi can synthesize nitric oxide (NO) endogenously in response to chemical stresses ultimately causing cell death (Vieira *et al.*, 2009). NO also protects the edible fungi mycelia from oxidative damage induced through heat stress (Kong *et al.*, 2012). ROS production during antibiotic administration is lethal to bacteria and fungi causing cell death (Kohanski *et al.*, 2007). Essential oils demonstrated a potential to treat oxidative damage by reducing the levels of H₂O₂, NO and NO synthase (Kavoosi and da Silva, 2012). Thymol exhibits effective fungicidal activity against *Aspergillus flavus* through scavenging ROS and is frequently used on crops infected with *A. flavus* (Shen *et al.*, 2016).

2.2.4.3 Effect of the efflux pump

H⁺-ATPase in the plasma membrane of the fungal cell is responsible for the physiology of the cell through nutrient uptake which is supported by a transmembrane electrochemical proton gradient. Furthermore, the H⁺-ATPase is also involved in the regulation of intracellular pH, pathogenicity, cellular growth, dimorphism and medium acidification (Perlin, Seto-Young and Monk, 1997). According to a study of certain essential oil active components on *C. albicans*, thymol and eugenol are involved in the inhibition of H⁺-ATPase resulting in excellent fungicidal drugs even on azole-resistant bacteria. Furthermore, carvacrol and thymol demonstrated a synergistic effect with azole incorporating inhibition of the efflux-pump genes such as *CDR1* and *MDR1*.

2.2.4.4 Quorum sensing

The microorganisms in response to external stress activate the cell to cell communication better known as cell signaling to make microcolonies. The released molecules accumulate cells and increase cell density which protects them against outside harsh conditions. The occurrence of quorum sensing is well reported in various microorganisms including fungi (Nazzaro *et al.*, 2013). E-farnesol is a well-studied such sensing molecule which is present in *C. albicans* and is also capable of inhibiting the formation of hyphae and cell adherence to the surface (Ramage *et al.*, 2002). Alcohol derived from tyrosine known as tyrosol is reported to stimulate hyphal formation showing an opposite effect to farnesol (Alem *et al.*, 2006). The addition of exogenous tyrosol does not show any change to the biofilm whereas, it can partially overcome the effect of farnesol. However, the inhibition of hyphal formation is dominated in the presence of exogenous farnesol as well as tyrosol.

2.2.4.5 Release of mycotoxins

The expression of some key enzymes required during catabolism and mycotoxins are reduced in the presence of essential oils. Mycotoxicosis is one of the top ten hazardous concerns in human health affecting billions of people in developing countries (Williams *et al.*, 2004). Since the over usage of synthetic antifungal agents can subsequently increase the risk of drug resistance among human pathogen leading to less therapeutic capability, therefore, the fungal groupings are enhanced (Brul and Coote, 1999). The toxic fungal contamination arises an economic loss caused by hazardous health issues. Mycotoxins are referred to as naturally occurring compounds secreted from fungi which are toxic to humans and are usually carcinogenic, classified by International Agency for Research on Cancer (Bennett and Klich, 2003). Certain deoxyglucosides of borneol, carvacrol, citronellol, fenchol, menthol, thymol,

and S-(-)- perillyl alcohol are generally reported with an inhibitory effect on the production of mycotoxins like aflatoxin (Bruns *et al.*, 2010). Essential oils of *Curcuma longa* have reportedly inhibited the expression of aflatoxin-related genes in *A. flavus* through two regulating genes, *AFLR* and *ALFS* and five structural genes, *AFLD*, *AFLM*, *AFLO*, *AFLP* and *AFLQ* resulting in low transcriptional level and consequently less production of mycotoxin (Hu *et al.*, 2017). In some cases, the mycotoxin production is linked to biofilm formation under increased environmental factors and their interactions including pH, temperature and water activity as observed in *A. parasiticus* (*AFL* genes), *Fusarium culmorum* (*TRI* genes) and *Penicillium verrucosum* (*OTA* genes). Moreover, eugenol is depicted as an active compound which blocks aflatoxin B1 (*AFB1*) production representing the anti-toxinogenic effect of essential oils. Eugenol acts through down-regulation of the cluster genes expressing aflatoxin out of which 19 genes were turned off whereas 8 genes were expressing at 10 to 20 folds reduced levels (Jahanshiri *et al.*, 2015). Furthermore, the essential oils of clove, cinnamon, lemongrass, palmarosa and oregano showed anti-deoxynivalenol (DON) activity by inhibiting DON accumulation in grains affected with *Fusarium* species (Velluti *et al.*, 2004). Also, the essential oils of *Satureja hortensis*, *Zataria multiflora*, carvacrol, and thymol decreased the production of DON in *F. graminearum* (Kalagatur *et al.*, 2015).

2.3 Citral: an antimicrobial agent

Cymbopogon citratus (Lemongrass) of family Poaceae exhibited potent antifungal activity against *Candida* species. Citral is one of the major components of *Cymbopogon* spp. oil analyzed using GC analysis and is the vital member of monoterpenes. It is a monoterpene aldehyde which consists of two isomers: neral (cis-citral) and geranial (trans-citral). Monoterpenes have proven the bioactive potential to develop alternative antimicrobial agents. *C. citratus* and *C. flexuosus* can yield up to 80% of the citral among total monoterpenes. Citral possesses a characteristic lemon-like smell which attracts a wide application in the soap, flavours and fragrance industries. It also has potential bioactivity in medicine and pharmaceuticals. Recent reports have established the role of citral as an analgesic, antispasmodic, anti-inflammatory, sedative, diuretic and antipyretic (Nishijima *et al.*, 2014). A number of neural applications of citral have been tested by various researchers and found its potential in treating neural disorders including Alzheimers diseases. Citral has gained immense interest in research because of its potential in treating a number of diseases as well as artificially synthesizing essential products such as Vitamin A.

2.3.1 Biosynthesis of citral

All the monoterpenes are synthesized from deoxy-xylulose-5-phosphate (DOXP) or methylerythritol-4-phosphate (MEP) pathways. The radiolabeled studies of the substrates in lemongrass have revealed the biosynthesis of citral through geraniol oxidation. The steps involve pyrophosphate (PP_i) removal from geranyl diphosphate (GPP); acetylation of geraniol forming geranyl acetate (GA); GA gets slowly hydrolyzed to geraniol by geranyl acetate esterase (GAE); and finally, geraniol is oxidized to citral by geraniol dehydrogenase, an NADP-dependent enzyme (Figure 2.3).

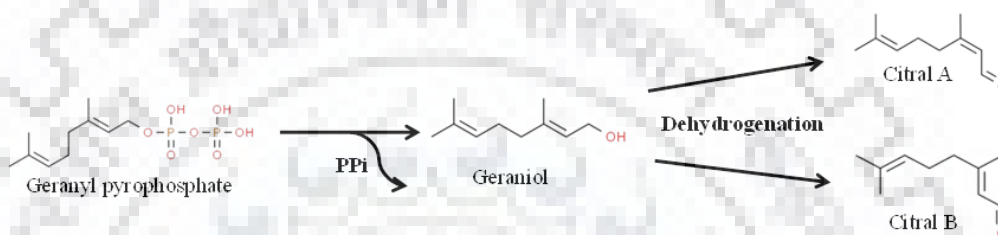


Figure 2.3 Biosynthesis of citral

2.3.2 Combating antimicrobial resistance

Presently, the rapid evolution microbial resistance against fewer available antibiotics and acclaimed drugs has stressed the clinical practices. Moreover, the presence of only a limited number of antimicrobials with high-cost production and low specificity has also worsened the situation. Addressing these well-known antimicrobial resistances attained through evolving current novel strategies are of utmost importance. One effective remedy could be the development of the alternative and efficient natural compounds preferably from a plant source to lower the toxicity. To overcome this state of drug limitation, monoterpenes a well-known group of naturally occurring class of isoprenoids can prove potentially important in developing alternative antibiotics. Isoprenoids consist of a monoterpene class (C_{10}) with thousands of colourless, volatile and lipophilic metabolites.

Recent reports have shown well-defined activities of citral against a number of microorganisms and efforts are made to study its mode of action. Citral can act potentially in the chemotherapy as well as synergistically along with employed drugs such as azoles against fungal diseases. Numerous recently published reports have demonstrated the more focused antimicrobial properties of citral and its derivatives in order to decipher the mode of their action in preventing diseases. The growth inhibition of *Penicillium italicum* and *Rhizopus stolonifera* has marked strong antifungal potential of citral and its derivatives (Saddiq and

Khayyat, 2010). These reports lead citral to be a potent source for the treatment of a number of diseases including bacterial and fungal infections. Oxidative derivatives such as epoxides are, however, recognized as strong inhibitory agents towards the growth of fungi and *Staphylococcus aureus*, a methicillin-resistant bacterium in comparison to the native citral (Singh *et al.*, 2017). Interestingly, the epoxides are more proficient against bacteria when compared to the standard antibiotics including ampicillin, nalidixic acid, and nitrofurantoin. The bioactivities of citral against fungal diseases have also been explored and found effective when used as epoxides.

A recent report has suggested the antimicrobial properties of various conjugated acid derivatives of citral which were more potent in comparison to nystatin and chloramphenicol. The essential oil of lemongrass and its major component citral showed significant antibacterial activities against bacterial pathogens including *Escherichia coli*, *Bacillus cereus*, *Streptococcus aureus* and *Streptococcus agalactiae* isolated from bovine (Aiemsaard *et al.*, 2011). The mild heat treatment at 55 °C for 15 mins of bacteria in the presence of citral, β -pinene, and linalool has revealed powerful antimicrobial activity when administered in combination with each other (Belletti *et al.*, 2010). The chemotherapy of fungal diseases incorporating citral has also displayed promising bioactivities.

The combinatorial administration of citral with fluconazole has displayed strong synergistic action against bacteria and fungi. A study of six terpenoids including citral has reported significant synergistic effect with fluconazole against various isolates of fluconazole-resistant *Candida albicans* (Zore *et al.*, 2011). The tested terpenoids had potent inhibitory effects against the cellular growth of *C. albicans* through hindrance at diverse phases of the cell cycle. Citral and citronellal are thought to have initiated apoptosis through intervention during the S- phase of the cell cycle. Also, these terpenoids exhibited astonishing activity towards yeast as well as hyphal growth at concentrations which are non-toxic to the HeLa cells. Essential oils of Lemongrass and citral are significantly active against *C. albicans* and other non-*albicans* *Candida* species including *C. parapsilosis*, *C. krusei*, *C. tropicalis* and *C. glabrata* (Silva *et al.*, 2008). Monoterpenes such as nerolidol, eugenol, alpha-terpineol, and citral can affect the ultra-structural changes in *Trichophyton mentagrophytes* (Park *et al.*, 2009). It was found that citral at a dose > 0.1mg/mL acts effectively against the hyphal growth of *T. mentagrophytes* whereas dose > 0.2mg/mL irreversibly damages the cellular organelles and cell membrane. Moreover, citral and citronellol derived amides including 5, 9-dimethyl-deca-2, 4, 8-trienoic acid and 9-formyl-5-methyl-deca-2, 4, 8-trienoic acid acts against *S. aureus* as NorA efflux pump inhibitors (Thota *et al.*, 2008). Furthermore, citral induces sub-

lethal injury to outer as well as cytoplasmic membrane inactivating wild strain BJ4 of *E. coli* (Espina *et al.*, 2013).

Dalleau *et al.*, (2008) have extensively studied several molecules which are prevalent in essential oils and compared their antibiofilm activity (Dalleau *et al.*, 2008). *Candida* biofilm shows a significant reduction in their growth when treated with components including citral, linalool, geraniol, thymol, menthol, carvacrol, etc. and exhibited up to 75% inhibition on higher concentrations. *Candida* biofilm, when treated with the essential oils of *C. citratus*, was observed by using SEM and AFM differentiating the structural damages on liquid and vapour phase application (Tyagi and Malik, 2010). The untreated cells appeared healthy as intact clustered cells whereas, during treatment of essential oils to the cells were deformed with the lost original shape and shrunk. The cells were relatively flattened instead of any significant effect on its dimensions with respect to its length and breadth. The vapour phase treatment clearly demonstrated a higher impact on the cellular surface by altering the cell dimensions and therefore, overall morphology. The antibiofilm activity of *C. nardus* has shown the inhibition of transition of yeast to hyphal forms when used against *C. albicans* (De Toledo *et al.*, 2016). The microscopic illustrations have shown an absence of any filamentous structure in the presence of essential oil concentrations ranging from 15mg/mL to 1000 mg/mL. Essential oils of *C. nardus* successfully inhibit the growth and formation of a biofilm of *C. albicans* in MIC range of 250mg/mL to 1000mg/mL whereas; the hyphal formation is inhibited from 15.8mg/mL to 1000mg/mL depending on the stage of maturity. Citrus essential oils can significantly eradicate mixed polymicrobial infections commonly found in chronic infections in which bacteria and fungi together contribute a healthcare burden (Pekmezovic *et al.*, 2016). The study revealed that citrus affects the cell membrane of *C. albicans* by increasing permeability in fungal counterparts and alters cell signaling sensing in *Pseudomonas aeruginosa*.

Hence, by far citral has demonstrated the potential of an active molecule against various microorganisms. Numerous bacteria and fungi have shown sensitivity towards citral and its derivatives. The mechanism of action of citral is multifaceted and acts at diverse cellular machinery of bacteria as well as fungi. Here, the activity of citral against *C. tropicalis* biofilm has been elaborated in detail. Citral can potentially act at multiple cellular levels of *C. tropicalis* as predicted in Figure 2.4.

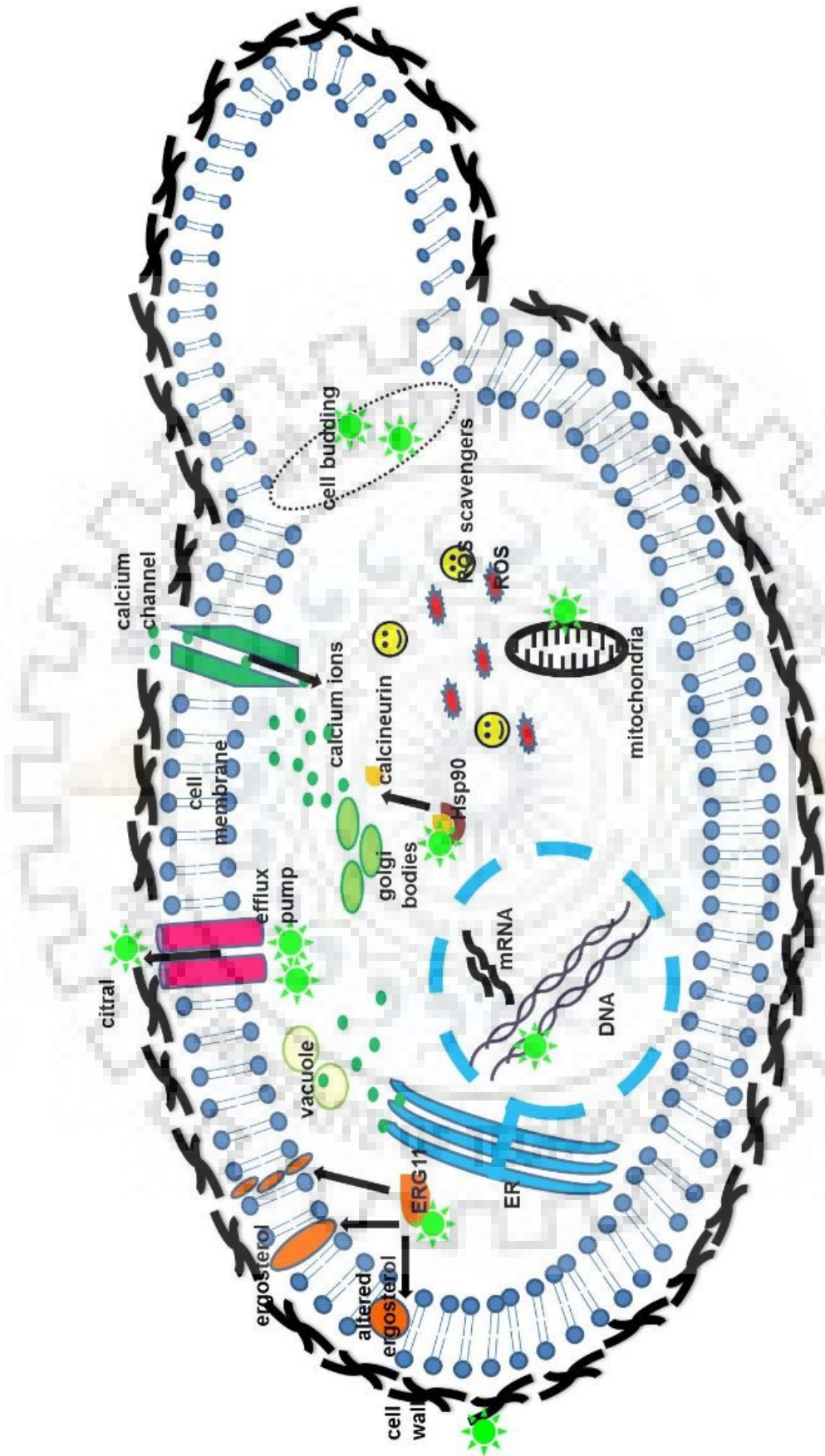


Figure 2.4 Probable mode of action of citral on *C. tropicalis*

3.1 Materials

3.1.1 Microorganisms, media and growth conditions

Candida albicans (NCIM-3102) and *Candida tropicalis* (NCIM-3118) strains were procured from National Chemical Laboratory (NCL), Pune, India. Studies were performed using preserved glycerol stock, regularly revived on Sabouraud's dextrose agar medium (HiMedia, India) at 30°C. The cells were cultured in Sabouraud's dextrose broth (HiMedia, India) for 24h at 30°C with 200rpm, agitation. For biofilm formation, Roswell Park Memorial Institute (RPMI-1640) medium with L-glutamine without sodium bicarbonate, buffered with 0.165M morpholinepropanesulfonic acid (HiMedia, India), set to a pH of 7, was used. Stock solutions of conventional drugs; fluconazole and amphotericin B, alcoholic terpenes; geraniol and menthol, aldehydic terpenes; citral and cinnamaldehyde and phenolic terpenes; carvacrol, eugenol, and thymol ordered from Sigma Aldrich, Germany, were made in dimethyl sulfoxide (DMSO) (CDH, India) as 100× concentrations of working solutions and were freshly used.

3.1.2 Reagents

3.1.2.1 Phosphate buffered saline (0.1M, pH 7.4)

The 10× stock concentration of phosphate-buffered saline (PBS) was prepared and diluted up to a concentration of 1× was used as a final working solution.

Table 3.1 Composition of phosphate-buffered saline (PBS)

| S.No. | Chemicals | Stock (10×) | Working (1×) |
|-------|----------------------------------|-------------|--------------|
| 1. | NaCl | 1.37M | 137mM |
| 2. | KCl | 27mM | 2.7mM |
| 3. | Na ₂ HPO ₄ | 100mM | 10mM |
| 4. | KH ₂ PO ₄ | 18mM | 1.8mM |

3.1.2.2 Antifungal agent

The stock concentrations of standard drugs i.e. fluconazole and amphotericin B; and terpenes i.e. geraniol, menthol, citral, cinnamaldehyde, carvacrol, eugenol, and thymol were prepared at a concentration of 205.6mg/mL each in DMSO.

3.1.2.3 2, 3-bis (2- methoxy- 4- nitro- 5- sulfophenyl)- 2H- tetrazolium- 5-carboxanilide sodium salt (XTT) solution

The stock solution of XTT salt was prepared at a concentration of 5mg/mL in 1× PBS.

3.1.2.4 Menadione solution

1mM stock concentration of menadione was prepared in isopropanol.

3.1.2.5 Ergosterol and sorbitol solutions

The stock solutions of ergosterol and sorbitol were prepared at the concentrations of 4mg/mL and 2M, respectively.

3.1.2.6 Propidium Iodide (PI)

The stock solution of PI was prepared at a concentration of 1mg/mL using 1×PBS.

3.1.2.7 FUN-1 and concanavalin-Alexa Fluor 488 conjugate solutions

The stock concentrations of FUN-1 and concanavalin-Alexa Fluor 488 conjugate were prepared at the concentrations of 10mM and 5mg/mL, respectively.

3.1.2.8 Chloromethyl- dicholodihydrofluorescein diacetate (CM-H2DCFDA) solution

A stock solution of 1mM was made in 1×PBS.

3.1.2.9 Protease inhibitor mix

7× stock concentration of cOmplete mini EDTA free protease inhibitor cocktail (Roche, Germany) was freshly prepared by dissolving one complete tablet in 1.5mL 1×PBS.

3.1.2.10 Tris-Glycine running buffer

10× Tris-Glycine was prepared by dissolving 30g of Tris-base, 144g of glycine and 10g of SDS making a final volume of 1L to serve as a stock solution.

3.1.2.11 Ethidium bromide (EtBr)

The 10mg/mL stock solution of EtBr was prepared.

3.1.2.12 Staining and destaining solutions

The detailed composition of both solutions was as follows:

Table 3.2 Recipe of staining and destaining solutions

| Solutions | Components |
|------------------|---|
| Staining | 0.5% (w/v) coomassie brilliant blue R-250 50% methanol 10% glacial acetic acid 40% distilled water |
| Destaining I | 50% methanol 10% glacial acetic acid 40% distilled water |
| Destaining II | 10% glacial acetic acid 90% distilled water |

3.1.2.13 Miscellaneous

The stock solutions of frequently used components have been listed below:

Table 3.3 List of stock solutions

| S. No. | Chemicals | Concentrations |
|---------------|--|-----------------------|
| 1. | NaCl | 3M |
| 2. | EDTA | 0.5M |
| 3. | Tris-Cl | 1.5M |
| 4. | SDS | 10% |
| 5. | KH ₂ PO ₄ (pH 6.5) | 1M |

3.2 Methods

3.2.1 *In vitro* biofilm growth of *C. tropicalis*

The biofilm was formed on the surface of sterile 96-well flat bottomed culture plates and with silicone elastomer discs in RPMI-1640 incubated statically at 37°C up to 72h. The growth kinetics of biofilm formation was studied using colourimetric assay at different timings. Biofilm was formed in three different phases: adhesion phase (6h), intermediate phase (24h), and mature phase (48h). The XTT reduction assay was done to quantify the biofilm formation in terms of metabolically active cells where the absorbance at 2h, 4h, 6h, 24h, 48h, 60h, 72h, respectively, were read at an optical density (OD_{492 nm}) using 96-well plate reader (Spectramax, Molecular Devices, USA).

3.2.2 *C. tropicalis* susceptibility towards selected terpenes

Activities of geraniol, menthol, citral, cinnamaldehyde, carvacrol, eugenol, and thymol against planktonic cells were tested by broth microdilution method using CLSI (M27-A3) (Clinical and Laboratory Standards Institute) guidelines (CLSI, 2017). Briefly, planktonic cells were grown in Sabouraud's dextrose broth for 24h at 30°C with 200rpm shaking. The harvested cells were washed using sterile phosphate-buffered saline (1×PBS, 0.1M, pH 7.4) and resuspended at 2×10³ cells/mL concentration in the Sabouraud's dextrose broth medium. Serially double diluted concentrations from 0µg/mL to 1024µg/mL of each terpene was prepared in Sabouraud's dextrose broth and the cell suspension of 100µL was added to each well of 96-well microtiter plates so that the final working volume contains 1×10³ cells/mL with the final DMSO concentration not exceeding more than 5% in any assay. Pre-sterile 96-well polystyrene microtiter plates (Tarsons, India) were set with 100µL of each dilution as treatment and control well contained 5% DMSO dispensed in Sabouraud's dextrose broth. 100µL of cell suspension was added in each well of 96-well microtiter plates to mix with terpenes at their respective working concentrations. Thereafter, the plates were incubated at 30°C for 24h, and final growth was measured by 96-well plate reader (Spectramax, Molecular Devices, USA) at an optical density (OD_{600 nm}) (Ramage, VandeWalle, *et al.*, 2001). The minimum inhibitory concentration (MIC) of each component was determined by employing the following formulae:

$$\text{Percentage of yeast cells} = [1 - (\text{OD}_{600} \text{ sample} / \text{OD}_{600} \text{ control})] \times 100\%.$$

3.2.3 Antibiofilm activities of terpenes on *C. tropicalis*

The biofilm formation assay was performed in 96-well polystyrene microtiter plates as described earlier (Pierce *et al.*, 2008; Nett *et al.*, 2011). Briefly, the cells at a concentration of 2×10^6 cells/mL were suspended in a 100 μ L volume in each well in RPMI-1640. Serial double dilutions of each terpene were made in RPMI-1640 and added to each well as treatment while acquiring a final concentration of cells as 1×10^6 cells/mL and concentrations of each terpene ranging from 0 μ g/mL to 1024 μ g/mL. Control wells were prepared with 5% DMSO in RPMI-1640. Plates were incubated at 37°C for 48h. For preformed biofilm, the cells were suspended at a concentration of 1×10^6 cells/mL, taking 100 μ L of suspension in each well of 96-well polystyrene plates. The plates were then, incubated at 37°C for 24h. After incubation, non-adherent cells were removed through aspiration of media and the wells were washed thrice using 1 \times PBS. Residual PBS was removed by inverting the plates over blotting sheets. A volume of 100 μ L of serially double diluted concentration (0 μ g/mL to 1024 μ g/mL) of each terpene, not exceeding DMSO by 5%, was added to each well with treatment, whereas, control wells were made using 5% DMSO in RPMI-1640. The plates were incubated at 37°C for another 24h. The metabolic activity of biofilm was quantitatively determined by colourimetric XTT [2, 3-bis (2- methoxy- 4- nitro- 5- sulfophenyl)- 2H- tetrazolium- 5-carboxanilide sodium salt] reduction assay. The biofilm inhibitory concentration (BIC) and biofilm eradicating concentration (BEC) were calculated by computing the percentage of metabolic activity displayed by biofilm cells when treated with each terpene was calculated using the formulae:

$$\text{Metabolic activity (\%)} = [1 - (\text{OD}_{492} \text{ sample} / \text{OD}_{492} \text{ control})] \times 100\%$$

Fluconazole, a standard drug, was taken as a positive control.

Furthermore, the effect of each terpene on cell membrane/ cell wall was determined by ergosterol and sorbitol assays. The MIC₅₀, BIC₅₀ and BEC₅₀ (minimum inhibitory concentration of planktonic cells, biofilm inhibitory concentration and biofilm eradicating concentration, respectively at which the cell growth was reduced to 50% to that of the healthy cells) for *C. tropicalis* were determined using microdilution method (as described above) in the treated/ untreated wells from 0 μ g/mL to 1024 μ g/mL supplemented with 400 μ g/mL of ergosterol and 0.8M sorbitol as an osmotic supporter, obtained from Sigma-Aldrich, USA to study the ergosterol binding and sorbitol effect, respectively (Escalante *et al.*, 2008). Amphotericin B (1 μ g/mL, 4 μ g/mL and 8 μ g/mL) was taken as the control drug for the ergosterol assay.

3.2.4 Colourimetric XTT reduction assay

After appropriate incubations of microtiter plates, media was aspirated and biofilm was washed using 1×PBS (sterile). Colourimetric XTT reduction assay was performed as reported earlier (Pierce *et al.*, 2008). 5mg/mL stock solution of XTT tetrazolium salt (Sigma, Germany) in 10mL of 1×PBS was mixed to get 0.5mg/mL working solution. 1µM final concentration of menadione (Sigma, Germany) was added to XTT. 100µL of working XTT-menadione solution was dispensed into each well containing prewashed biofilm. A blank without cells was set for background subtraction. All the plates were incubated at 37°C in the dark for 1h and absorbance was taken at 492nm. The amount of colour change due to the formation of formazan was directly correlated to the metabolic activity of the cells.

3.2.5 Quantification of ergosterol content

The total amount of intracellular ergosterol was quantified at the respective BIC₅₀ and BEC₅₀ of citral and thymol. The biofilm was formed as mentioned above and was introduced with citral (BIC₅₀ (64µg/mL) and BEC₅₀ (128µg/mL)) and thymol (BIC₅₀ (32µg/mL) and BEC₅₀ (128µg/mL)) along with a positive (Amphotericin B (BIC₅₀ (4µg/mL) and BEC₅₀ (8µg/mL)) and negative control (0µg/mL). The ergosterol quantification was performed as described a previous study (Khan, Iqbal and Singh, 2013). The obtained content of ergosterol was calculated by the following equation: The ergosterol content was estimated as a percentage of the wet weight of the cell pellet (100mg) by the following equations:

$$\text{Ergosterol Content (\%)} = \frac{\left[\left\{ \frac{A_{281.5}}{E_1} \right\} \times F \right]}{\text{cell pellet (wt.)}} - \frac{\left[\left\{ \frac{A_{230}}{E_2} \right\} \times F \right]}{\text{pellet (wt.)}} \times 100$$

Considering, F as ethanol dilution factor and E₁ and E₂ values to be 290 and 518 as the determined ergosterol content in terms of percentage per cm for crystalline ergosterol and 24(28) DHE (dehydroergosterol), respectively (Singh, Fatima and Hameed, 2016).

3.2.6 Cell surface hydrophobicity and auto-aggregation of *C. tropicalis* cells

C. tropicalis cell adhesion to the solvents was employed to determine the cell surface hydrophobicity. The adhesion of cells to xylene (non-polar solvent) determines the hydrophobic characteristic of cells. Briefly, the cells with 10⁸cells/mL were suspended in 1×PBS (0.1M, pH 7.4). 3mL of cell suspension was added with 1mL of xylene in an acid-washed glass tube. The obtained mixture was kept at 37°C for 10mins and vortexed up to 1min.

The vortexed mixture was incubated at 37°C for 45mins, after that the absorbance of the aqueous phase was read at 520nm. The hydrophobicity was estimated as hydrophobicity index (HI) using the following equation:

$$HI (\%) = (A_1 - A_2 / A_2) \times 100$$

(Where, A₁: inoculum absorbance and A₂: aqueous phase absorbance)

The specific adherence of cells was estimated using the auto-aggregation assay. The biofilm cells were harvested at 5000g for 10mins at 4°C and washed in 1×PBS (0.1M, pH 7.4). The cells were set at 10⁸cells/mL in the suspension using 1×PBS. 3mL of cell suspension was vortexed for 10s and incubated at 37°C for 2h. After incubation, the absorbance was read at OD_{600 nm}. The calculation of auto-aggregation followed:

$$Auto - aggregation (\%) = (1 - A_{2h} / A_{0h}) \times 100.$$

3.2.7 *In vitro* time-kill kinetics of terpenes on *C. tropicalis*

The fungicidal activity of the terpenes and amphotericin B against *C. tropicalis* yeast cells was measured by time-kill analysis as described previously (Credito, Lin and Appelbaum, 2007). Yeast cells (10³cells/mL) with the MIC₅₀ of each terpene and amphotericin B were incubated at 37°C and shaking at 250rpm. Aliquots were taken from each tube at 0, 30, 60, 90 and 120mins after addition of the antifungal agents at MIC₅₀, and the samples were diluted and spread on Sabouraud's dextrose agar plates in triplicates. The plates were incubated at 37°C for 24h, and the colonies were counted.

3.2.8 Morphological changes in *C. tropicalis* matured biofilm cells during treatment

Qualitative analysis of the effect of terpenes on the biofilm was analyzed by employing a scanning electron microscope (SEM) (Carl Zeiss, Germany). Briefly, the biofilm was formed on silicone elastomer in 12-well cell culture plates (Tarsons, India). Catheters were disinfected and treated with sterile fetal bovine serum (FBS) (Gibco, Thermo Fisher Scientific, USA) as described earlier (Pierce *et al.*, 2008). Briefly, FBS treated catheters were dispersed with yeast cells with a concentration of 1×10⁶cells/mL, incubating at 37°C for 24h and the biofilm were allowed to form in the presence of BEC₅₀ concentrations of terpenes and fluconazole for another 24h. Control biofilm was prepared with 5% DMSO. At the end of the biofilm formation, for SEM analysis biofilm was dried and processed as described by Chandra *et al.* (2006) with slight modifications (Chandra, Mukherjee and Ghannoum, 2008). Briefly, biofilm was washed using 1×PBS and subsequently fixed with (2% v/v) glutaraldehyde (HiMedia,

India), followed by dehydration in a series (25%, 50%, 75%, and 100%) of ethanol solutions. Finally, gold sputtering was performed over the samples and images were acquired using SEM.

3.2.9 Effect of citral and thymol on the cell membrane permeability

The propidium iodide (PI) staining of *C. tropicalis* was done in order to study the fungicidal effect of citral and thymol. The cells were suspended at a concentration of 1×10^4 cells/mL after treatment with amphotericin B (4 µg/mL), citral (16 µg/mL), thymol (8 µg/mL), and cells without treatment were taken as the control. The cells were collected by centrifugation at 6000 rpm for 10 mins at 4°C. The cell pellet was washed twice in 1×PBS. Both the treated and untreated samples were stained with 1 µL of PI (1 mg/mL) (Thermo Scientific, USA). A control was also taken with untreated and unstained cells. The instrument was calibrated using Sphero rainbow calibration particles (GE Healthcare, USA). The samples were analyzed using flow cytometer (BD FACSVerser flow cytometer, BD Biosciences, USA) with PI-stained (excitation at 485 nm and emission at 630 nm) for dead cells. Briefly, 10,000 cells were sorted for each sample. The forward scatter (FSC), side scatters (SSC), and phycoerythrin (PE) was recorded for analysis.

3.2.10 Field emission scanning electron microscope (FE-SEM) and confocal laser scanning microscope (CLSM)

Qualitative analysis of the effect of citral and thymol on biofilm was evaluated by field emission scanning electron microscope (FE-SEM) (Carl Zeiss AG, EVO 40, Germany) and confocal laser scanning microscope (CLSM), LSM -700 (Carl Zeiss, Germany) as described in the earlier study (Chandra, Mukherjee and Ghannoum, 2008), with slight modifications. Biofilm was formed in 12-well cell culture plates using disinfected silicone elastomers coated with sterile FBS, as described above. Briefly, FBS treated silicone elastomer discs were dispersed with a cell concentration of 1×10^6 cells/mL in RPMI-1640 and were incubated at 37°C for 24h. The biofilm formed on the elastomer surfaces was washed using 1×PBS and incubated for another 24h in the presence of amphotericin B (4 µg/mL) BEC₅₀ concentration i.e. 128 µg/mL of both components. Control biofilm was formed in the presence of 5% DMSO in RPMI-1640. For FE-SEM, biofilm was dried and processed further. Briefly, biofilm was washed using 1×PBS and was subsequently fixed in 2% (v/v) glutaraldehyde (HiMedia, India), followed by dehydration in a series of 25%, 50%, 75% and 100% of the ethanol (Merck, USA). Finally, the elastomer discs were glued on stubs and sputter-coated with gold for 30s. The biofilm was then examined using FE-SEM.

For CLSM, biofilm was formed on silicone elastomer in the presence of the BEC₅₀ (128µg/mL) concentration of citral and thymol; and control biofilm was formed in RPMI-1640 with 5% DMSO. The biofilm was then, stained with fluorescent stains FUN-1 (Molecular Probes, Invitrogen, USA) at a working concentration of 1mM and Concanavalin-Alexa Fluor 488 conjugate (Invitrogen, USA) at a working concentration of 0.5mg/mL following incubation for 30mins at 37°C in dark, the biofilm was then observed using ZEN imaging software and analyzed using Image J software. The images were obtained in series to get the three-dimensional view, each positioned at the intervals of 1µm in the z-axis.

The three-dimensional biofilm structures were quantified using COMSTAT software (Heydorn *et al.*, 2000). The stacks of images which were obtained using CLSM were further analyzed by exporting these z-series images to COMSTAT plugin of Image J software. Biomasses, average thickness, the surface to bio-volume ratio and substratum coverage were considered parameters to be analyzed.

3.2.11 Measurement of reactive oxygen species (ROS) levels

The intracellular ROS levels in *C. tropicalis* biofilm were assessed using the fluorescent dye chloromethyl- dicholodihydrofluorescein diacetate (CM-H2DCFDA) from Sigma-Aldrich, USA in the presence of both at BIC₅₀ (64µg/mL for citral and 32µg/mL for thymol) and BEC₅₀ (128µg/mL of each) (Cho and Lee, 2011). Amphotericin B (BIC₅₀: 4µg/mL and BEC₅₀: 8µg/mL) was taken as control drug. Briefly, the biofilm cells with and without treatment were added with 20µM CM-H2DCFDA and incubated at 37°C for 1h. The fluorescence intensity was measured with excitation (485nm) and emission (535nm) using fluorescent microplate reader (Synergy H1 Micro mode Reader, USA).

3.2.12 Catalase (CAT), peroxidase (POD) and superoxide dismutase (SOD) enzyme activities

The protein extracts of *C. tropicalis* biofilm with treatment of citral and thymol at their respective BIC₅₀ and BEC₅₀ and control without treatment were prepared and the antioxidant enzymatic activities were monitored in accordance with the previously prescribed protocol with little modifications (Khan *et al.*, 2011). Briefly, the biofilm cells were lysed and re-suspended in 1mL grinding buffer (250mM sucrose, 10mM Tris-Cl (pH 7.5), 1mM PMSF). The resulting homogenate was centrifuged at 15000rpm for 45mins at 4°C. The supernatant containing soluble protein was estimated using BCA assay while using BSA as a standard. Enzymatic activities were measured using a UV-Vis spectrophotometer (Varian Cary 100, USA).

To determine the activity of the CAT, 10 μ L of each protein sample was added to 1.99mL of 1 \times PBS and 1mL of H₂O₂ (1.9mM) making a final volume up to 3mL as the reaction mixture. The decrease in absorbance due to H₂O₂ disappearance was recorded for 30s intervals up to 3mins at 25°C in a quartz cuvette (path length = 1cm) at 240nm. The resulting catalase activity was assessed in terms of μ mol H₂O₂ consumption/min/mg protein taking a molar extinction coefficient of 43.6M⁻¹cm⁻¹.

The POD activity was calculated using 100 μ L of the protein sample added in 25mM HEPES buffer (pH 6.8) (HiMedia, India) comprising 4mM guaiacol (HiMedia, India) and 10mM H₂O₂ incubated for 15min at 25°C. The change in absorbance during tetraguaiacol formation was monitored every 30s at 470nm (path length = 1cm) for 3mins at 25°C. The activity of peroxidase was represented in μ mol/min/mg protein as calculated using a molar extinction coefficient of 26.61M⁻¹cm⁻¹.

To measure the activity of SOD, 100 μ L of protein samples were mixed with pyrogallol-Tris buffer (100 μ L) and pyrogallol inhibition was measured every 30s for 3mins at an optical density of 420nm. The superoxide dismutase units were calculated in the form of pyrogallol autoxidation using the following formulae:

$$\frac{\text{Units of SOD}}{\text{mL}} = \left[\frac{(A - B)}{A} \times 50 \times 100 \right] \times 0.6 (df)$$

Considering, *A* as the difference in control absorbance per 1min and *B* as the difference in treated sample absorbance per 1min and *df* as the dilution factor. The obtained results were expressed in U/mg protein.

3.2.13 Whole-cell lipid peroxidation determination

In order to determine the lipid peroxidation in the whole cell, the level of malondialdehyde (MDA) reacting with thiobarbituric acid reactive substances (TBARS) was measured (Ohkawa, Ohishi and Yagi, 1979). After administration of citral (BIC₅₀, BEC₅₀) and thymol (BIC₅₀, BEC₅₀) for 6h, the cell suspension of *C. tropicalis* was centrifuged at 12000rpm for 5mins. The collected pellets were washed in 1 \times PBS twice and again re-suspended in the lysis buffer (100mM NaCl, 10mM Tris-Cl, 1mM EDTA (pH 8.0), 1% SDS and 2% Triton-X 100) and sonicated at an amplitude of 50% for 5mins on ice. The cells were again centrifuged at 12000rpm for 2mins and thiobarbituric acid (TBA, 0.5% w/v) solution prepared in trichloroacetic acid (TCA, 5%) (1:1) was added to the supernatant. The mixture was heated for 60mins at 95°C and cooled down to 4°C. After incubation, the cells were centrifuged at

10000rpm for 10mins at 4°C. The resulting supernatant fraction was read for absorbance at the wavelengths of 532nm and 600nm. Three replicates were considered to minimize the error.

$$\text{Concentration of MDA } (\mu\text{M}) = (\text{Abs}532 \text{ nm} - \text{Abs}600\text{nm}) \times 1000/155$$

(Considering MDA-TBA adduct extinction coefficient at 532nm is $155\text{mM}^{-1}\text{cm}^{-1}$).

3.2.14 Alkaline Comet Assay

Yeast alkaline comet assay was performed as discussed previously (Miloshev, Mihaylov and Anachkova, 2002). 0.5% supportive agarose gel was spread on the glass slide and dried in air. Briefly, *C. tropicalis* cells were collected in a micro-centrifuge tube by centrifugation at 4000rpm for 5mins at 4°C. The obtained cell pellets were washed twice with sterile 1×PBS and resuspended in buffer S (1M sorbitol and 25mM KH_2PO_4 , pH 6.5). Approximately 5×10^4 cells were mixed with 2mg/mL Zymolyase 20T (USBio, USA) in 0.7% low melting agarose and spread over the supportive agarose slide. The coverslips were placed over the gel and incubated at 37°C for 20mins. The following procedures were performed at 10°C in order to minimize the enzyme activity at the endogenous cellular level. Further, the coverslips of the slides were removed and the slides were incubated in lysis buffer (1M NaCl, 30mM NaOH, 50mM EDTA (pH 8), and 0.1% lauryl sarcosine) for 1h to lyse the spheroplasts. Afterwards, the slides were rinsed thrice in 30mM NaOH and 10mM EDTA (pH 12.4) for 20mins each to unwind the DNA. The slides were then subjected to the electrophoresis in the same buffer at 0.5V/cm for 20mins. Following electrophoresis, the slides were submerged in 10mM Tris-Cl (pH 7.5) for 10mins in order to neutralize the gel. The fixation was done by subsequent dipping of the slides in 76% and 96% ethanol, respectively. At last, the slides were air-dried followed by staining in 1mg/mL of ethidium bromide and visualization was performed using fluorescence microscopy (Axio Vert.A1, Carl Zeiss, USA). All the above steps were done in the dark for minimizing DNA damage.

3.2.15 RNA isolation, cDNA synthesis, and real-time expression analysis

The RNA was isolated from the control and treated biofilm cells at BEC_{50} concentrations of citral and thymol i.e. 128 $\mu\text{g}/\text{mL}$ of each which were grown for 48h using RNA-XPress reagent (HiMedia, India) according to the manufacturer's protocol. Briefly, ~ 200mg of the cells with and without treatment were crushed in liquid nitrogen and treated with the reagent. The obtained gel-like pellet was finally dissolved in RNase-free water and was quantified using NanoDrop 1c (Thermo Scientific, USA). Genomic DNA contamination was removed by

RNase-free–DNase set (Qiagen, Germany). Reverse transcription was performed in a total volume of 20µL using 2µg of RNA by first-strand cDNA synthesis kit (Thermo Scientific, USA), following prescribed protocol.

The normalization was done using glyceraldehyde-3-phosphate dehydrogenase (*GAPDH*). RT-PCR was carried out using SYBR Green PCR-Master Mix (Roche, Germany) in replicates with three sets of experiments. PCR mix as listed in Table 3.4 was used for each gene. The RT-PCR was performed (Step 1: 95°C for 3mins, Step 2: 95°C for 15s, 51.5°C for 45s, and 72°C for 30s for 40 cycles) using Eppendorf Realplex Master Cycler (Figure 3.1). The data was analyzed to determine the fold change in the expression of the gene by calculating ratio = $2^{-\delta\delta C_t}$, using C_t values (Pfaffl, 2001). To evaluate the gene expression levels of key genes responsible for antifungal resistance at the transcriptomic level, real-time RT-PCR was performed. The primers (GCC Biotech, India) used for this study are listed in Table 3.5.

Table 3.4 Components of RT-PCR reaction mixture

| dH ₂ O | SYBR Green Mix | Forward Primer | Reverse Primer | Template |
|-------------------|----------------|----------------|----------------|----------|
| 6.75µL | 10µL | 1µL | 1µL | 1.25µL |

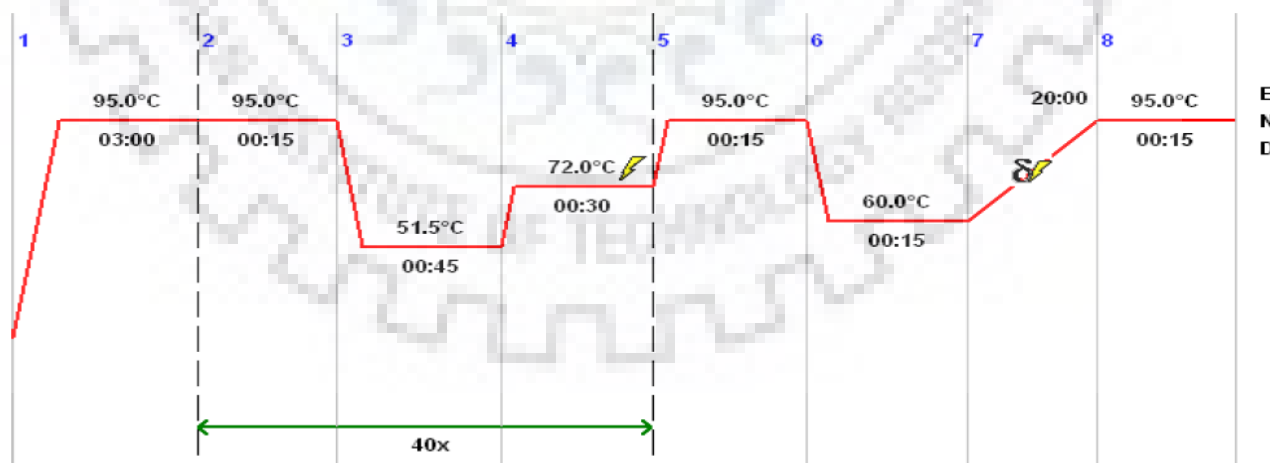


Figure 3.1 Temperature profiling of RT-PCR reaction

Table 3.5 Primers used for real-time RT-PCR

| Gene | Gene ID | Primer | Amplicon length (bp) | T_m (°C) | Sequence 5' to 3' |
|--|----------------|---------------|-----------------------------|---------------------------|----------------------------|
| enolase | <i>ENO1</i> | Fwd | 176 | 50.2 | TATTGCCATGGATGTT GCTT |
| enolase | <i>ENO1</i> | Rev | | | CTTCAGCGAATGGAT CTTCA |
| aldehyde dehydrogenase | <i>ALD5</i> | Fwd | 196 | 51.8 | TTGTTACCGGTGGTG CTAGA |
| aldehyde dehydrogenase | <i>ALD5</i> | Rev | | | GAGTGAATACCAGCA GCCAA |
| sterol 14-demethylase | <i>ERG11</i> | Fwd | 120 | 50.5 | ACTCATGGGGTTGCC AATGT |
| sterol 14-demethylase | <i>ERG11</i> | Rev | | | AGTTGAGCAAATGAA CGGTC |
| Cytochrome P450 52A1 | <i>CYT450</i> | Fwd | 169 | 54.0 | GTTCTGCTGTGTTTCC AGCC |
| Cytochrome P450 52A1 | <i>CYT450</i> | Rev | | | AGACCCAGAGAATGT CAAGGC |
| 2-oxoglutarate dehydrogenase complex | <i>KGD2</i> | Fwd | 135 | 55.0 | GGTGCATTCTCCAAG GCTGT |
| 2-oxoglutarate dehydrogenase complex | <i>KGD2</i> | Rev | | | CAAACCCTTTGGTGT GGCAA |
| superoxide dismutase | <i>SOD1</i> | Fwd | 140 | 54.0 | TTCAAGGTTCTGGTTG GGCT |
| superoxide dismutase | <i>SOD1</i> | Rev | | | AGCATGTTCCCAAGC ATCAA |
| calcineurin subunit B | <i>CNB1</i> | Fwd | 112 | 55.0 | AGATGGGTCAGGGGA AATTGAC |
| calcineurin subunit B | <i>CNB1</i> | Rev | | | ACGACCATCACCATC TGTGTC |
| glyceraldehyde-3-phosphate dehydrogenase | <i>GAPDH</i> | Fwd | 153 | 54.0 | GTCAACGATCCATTC ATTGC |
| glyceraldehyde-3-phosphate dehydrogenase | <i>GAPDH</i> | Rev | | | AGCTGGGTCTCTTTCT TGGA |

3.2.16 Protein sequence retrieval

The sequence of *CtErg11p* (Accession Number: AMR44151.1) was retrieved in FASTA format from the National Centre for Biotechnology Information (NCBI) database (<http://www.ncbi.nlm.nih.gov/>). Similar sequences were searched for the query sequence using the **Basic Local Alignment Search Tool** (Altschul *et al.*, 1990) against Protein Data Bank (PDB) for the selection of a template. An appropriate template based on the percentage sequence coverage and percentage sequence identity was identified.

3.2.17 Sequence alignment and secondary structure prediction

The multiple sequence alignment was performed using ClustalW (<http://www.ebi.ac.uk/Tools/msa/clustalw2/>). The alignment was done between FASTA sequences of *CtErg11p* along *CaErg11p* (PDB ID: 5V5Z) and *CaErg11p* (PDB ID: 5FSA). The secondary structure was analysed using Easy Sequencing in PostScript (ESPrict) (<http://esprict.ibcp.fr/ESPrict/ESPrict/>) allowing rapid visualization of the aligned sequence (Gouet *et al.*, 1999). The secondary structure was evaluated using PDBsum (<http://www.ebi.ac.uk/thornton-srv/databases/cgi-bin/pdbsum/GetPage.pl?pdbcode=index.html>) (Laskowski *et al.*, 1997).

3.2.18 Homology modelling

The theoretical three dimensional (3D) structure of *CtErg11p* was generated through homology modelling in comparison to the template 5V5Z crystal structure using Modeller 9.10 (Eswar *et al.*, 2008). The input of the sequence was an alignment file of the *CtErg11p* with the structure of the template, atomic coordinates and a simple script file. A total of four 3D protein structures were generated and processed for further validation. The GMQE and QMEAN4 Z-score were compared and the model with values 0.84 and -1.57, respectively, was selected for further analysis.

3.2.19 Structure validation

The models of *CtErg11p* were analysed and the best model was selected on the basis of SAVES server (<http://nihserver.mbi.ucla.edu/SAVES/>), ProSA (<https://prosa.services.came.sbg.ac.at/prosa.php>) and RAMPAGE (<http://mordred.bioc.cam.ac.uk/~rapper/rampage.php>) evaluating various parameters using ProSA plot, ERRAT plot and VERIFY-3D. ProSA plot determines the structure irregularities by calculating Z-score for the overall model quality as the deviation of the volumes from the

standard. ERRAT plot calculates the average overall quality with confidence to reject regions. The VERIFY-3D assigned the structural class based on the location of 1D amino acid sequence location and environment to compare the compatibility of the 3D atomic model. RAMPAGE plotted the Ramachandran plot assessing various parameters including planarity and geometry of the atoms as a function of atomic resolution.

3.2.20 Molecular docking

Docking studies of two ligands namely neral and geranial (isomers of citral) and a standard drug, itraconazole with *CtErg11p* were performed using AutoDock 4.2.6. (Morris *et al.*, 2009). *CtErg11p* was employed with hydrogens atoms and Kollman charges using AutoDock MGL Tools 1.5.6. The charged receptor was saved in .pdbqt format. The ligands were retrieved from PubChem (<https://pubchem.ncbi.nlm.nih.gov/>) in .sdf format and converted in a .pdbqt format using Open Babel (O'Boyle *et al.*, 2011). The prepared model was added with hydrogen atoms and Gasteiger charges for neral and geranial which was saved in .pdbqt formats. The torsional degrees of freedom in the ligand molecule specified the ligand flexibility. The grid was optimized to allow ligand binding at heme domain. The grid was set using following parameters; spacing: 0.2 Å, centre point coordinates: X = -34.662, Y = -20.759 and Z = 29.814, dimension of grid box: 50 Å × 50 Å × 50 Å using AutoGrid 4.2.6. Further, the Lamarckian genetic algorithm method was implemented for docking. A total of 100 GA was run with other default parameters. The final docking was done using AutoDock Vina. The obtained docked molecules were analysed and the molecule with the lowest binding energy was selected for visual analysis using *Dassault Systèmes BIOVIA, Discovery Studio*.

3.2.21 Protein extraction and quantification

The protein was extracted following the earlier described method with brief modifications (Simpson, 2011). The biofilm was grown with/ without citral (16µg/mL) treatment as described in previous Section 3.2.3. The biofilm cells were scraped off the silicone elastomer and collected in a microcentrifuge tube using a centrifuge. The cells were washed twice with sterile 1×PBS. The cell pellets thus collected were further introduced with RIPA buffer (150mM NaCl, 1% Triton X-100, 0.5% sodium desoxycholate, 0.1% sodium dodecyl sulphate (SDS), 50mM Tris-Cl (pH 7.2)) and placed on ice for 30mins. The protease inhibitor cocktail was used to minimize protein degradation. After incubation, the cells were lysed using glass beads with the cycle of vortexing for 30s followed by resting on ice, for 30mins. The lysed cells were subjected to the centrifugation at 13000rpm for 20mins at 4°C. The supernatant

obtained was collected in fresh micro-centrifuge tubes and subjected to protein quantification. Bicinchoninic acid (BCA) assay kit (GE Healthcare, USA) was used to quantify the protein sample in the supernatant by taking bovine serum albumin (BSA) as a standard.

3.2.22 One-Dimensional (1D) polyacrylamide gel electrophoresis

The whole-cell protein lysates (75 μ g each) of treated/ untreated biofilm cells were prepared in 6 \times Laemmli buffer (375mM Tris-Cl (pH 6.8), 9% (w/v) SDS, 50% (v/v) glycerol, 9% (v/v) β - mercaptoethanol and 0.03% (w/v) bromophenol blue) and separated using a 5% stacking (0.063M Tris-Cl (pH 6.8), 5% (w/v) acrylamide, 0.1% (w/v) SDS, 0.12% (w/v) ammonium per sulphate and 0.17% TEMED), 12% resolving (0.38M Tris-Cl (pH 8.8), 12% (w/v) acrylamide, 0.1% (w/v) SDS, 0.12% (w/v) ammonium persulphate and 0.17% TEMED) 1D sodium dodecyl sulfate-polyacrylamide gels (SDS-PAGE) at a constant 90V. After separation, the gel was fixed, stained with comassie brilliant blue R-250, destained and imaged using a Gel Doc XR+ system (Bio-Rad) and differentially expressed proteins were selected for further identification. Protein bands of interest were excised and in-gel digested with trypsin (Promega, Madison, WI, USA) as described previously (Shevchenko *et al.*, 2006).

3.2.23 Two-dimensional (2D) polyacrylamide gel electrophoresis

For 2D polyacrylamide gel electrophoresis (2D-PAGE), the manual of BioRad Laboratories was followed. The protein samples were cleaned up using 2D clean-up kit (BioRad, USA). After clean up the proteins were quantified using the RC/ DC kit (BioRad, USA) and proceeded for isoelectric focusing (IEF). 50 μ g of each sample was dissolved in 200 μ L of Rehydration buffer II (BioRad, USA) containing 7M Urea, 2M thiourea, 4% CHAPS, 50mM dithiothreitol (DTT), 0.1% (v/v) ampholytes and 0.001% (w/v) bromophenol blue (BPB). The complete dilution of the samples in rehydration buffer was ensured before loading it on 7cm immobilized pH gradient (IPG) strips. The samples were then loaded on IPG strips and allowed to passively rehydrate for 16h at 20 $^{\circ}$ C. After 16h, the IPG strips were subjected to IEF in Protean IEF cell (BioRad, USA) at 20 $^{\circ}$ C. The focusing program was set at 250V, linearly for 30mins, followed by 500V, linear for 2h, then a rapid increase at 8000V to a maximum of 15000V/ h and lastly held at 4 $^{\circ}$ C for 10h. Following IEF, the IPG strips were equilibrated in prescribed equilibration buffer I and II, respectively, for 20mins each. Equilibration buffer I consist of 1.5M Tris-Cl (pH 8.8), 7M Urea, 2% (w/v) SDS, 20% (v/v) glycerol and 1% (w/v) DTT was used for reduction of IPG strips. Equilibration Buffer II whereas consisted of 4% iodoacetamide (IAA) in places of 1% DTT of Equilibration Buffer I

for alkylation of the reduced IPG strips. After equilibration, the IPG strips were introduced to the second-dimensional separation of proteins. The IPG strips were rinsed in running buffer by dipping it twice in 1×Tris-Glycine buffer using a forceps. The strip was carefully placed over the 12% polyacrylamide gel and over-layered with 0.5% agarose gel containing BPB to track the movement of protein samples. The gel was run for 1.5h at a constant 125V in Mini-protean gel apparatus (BioRad, USA). After the second dimension electrophoresis, the gel was stained using the silver stain using mass spectrometry compatible silver stain (Stochaj, Berkelman and Laird, 2007).

3.2.24 Imaging of the gel and software analysis

The 2-D gels were imaged using a GS-800 gel scanner (BioRad, USA). The image was selected for silver stain and exported with a resolution of 600dpi. The comparison of gels was performed using PDQuest analysis software for spot measurements. The gels were run in replicates and a master gel was selected. Proteins spots between the group gels were analysed by using default parameters of the software. After background removal, the spot detection and matching parameters were set by selecting large, faint and small spots with a sensitivity of 21 and scale size of 5. The Gaussian model was used during the test to find the spot centres. The individual spot volume was normalized for each resolved protein spot against total spot volume and area in the gel. The protein spots which were differentially expressed by at least 1.5-fold in the mean normalized spot volume were excised for identification. Student's t-test was performed for statistical analysis.

3.2.25 In-gel trypsin digestion and peptides extraction

The in-gel trypsin digestion was performed using a previously described protocol (Shevchenko *et al.*, 2007). The spots excised from the gel were destained in the solution with a 1:1 ratio of potassium ferrocyanide (30mM) and sodium thiosulphate (100mM). The spots were washed using mass spectrometric (MS)-grade water and were incubated in ammonium bicarbonate (ABC) (25mM) and acetonitrile (ACN) for 10mins at room temperature and 40% (v/v) ACN for 5mins followed by 100% (v/v) ACN. The spots were further reduced with 10mM DTT at 45°C for 20mins in ABC (25mM) and 20% (v/v) ACN followed by incubation of gel in 100% (v/v) ACN. The alkylation of the spot was done using 40mM IAA in 25mM ABC and 20% (v/v) ACN in dark at room temperature. The spots were further incubated in 100% (v/v) ACN, 25mM ABC and 20% (v/v) ACN and 100% (v/v) ACN, respectively. The spots were then kept on ice for 10mins. Afterwards, 25µg/mL trypsin in 30mM ABC was

added to the spots and kept at 4°C for 1h to facilitate gel absorption without enzyme activity. After incubation, the excess enzyme was removed and the gel spots were covered with 30mM ABC and kept at 37°C for 12h. After 12h, 0.1% (v/v) formic acid was added to the spot and supernatant was collected in a fresh micro-centrifuge tube. 100% ACN was added to the spot gel and supernatant was recovered after 10mins of incubation. 0.1% (v/v) formic acid was added again to the gel and supernatant was collected. The collected supernatant was dried out using Concentrator plus, Eppendorf, Germany. The protein samples were further used for protein identification.

3.2.26 Protein Identification and database search using mass spectrometry

For mass spectrometer analysis, the samples were prepared by reconstituting the dried peptides into TA 40 (40% ACN and 60% of 0.01% trifluoroacetic acid (TFA)). The samples were mixed in a 1:1 ratio with HCCA (alpha-cyano-4-hydroxy-cinnamic acid) matrix for ionization and spotted on a ground steel plate. The identification of proteins was carried out by ultrafleXtreme matrix-assisted laser desorption ionization reflecting (time of flight) (MALDI-TOF/TOF) mass spectrometer (Bruker Daltonics, Germany) equipped with 60-Hz nitrogen laser in the positive mode (Lewis, Wei and Siuzdak, 2006). The reflector method was selected with a mass range of m/z 700 to 3500Da. External calibrations was performed using peptide standard provided by Bruker Daltonics, Germany and saved in the method. After calibration, mass spectra for each sample were recorded using FlexControl software (version 2.0). The obtained spectra were analysed using FlexAnalysis software (version 2.0). The background noises, keratin contamination and peptide from trypsin autolysis were cleared from the mass list. Further, the protein identification was performed using the generated peak list of trypsin-digested peptides. The peak list files were subjected to the Mascot Server 2.4 (<http://www.matrixscience.com>) for NCBI database search. The search parameters were set as follows: 1) only 1 missed cleavage allowed, 2) fixed modification of carbamidomethyl cysteine, 3) methionine modification as a variable, 4) peptide charge to be +1, 5) 200ppm of peptide tolerance, and 6) 0.7Da of MS/ MS tolerance. The identified peptides and proteins were evaluated using probabilistic MASCOT scoring and $p < 0.05$ was considered significant.

3.2.27 1D ¹H-NMR Analysis of extracellular matrix

The silicon elastomer infected with *C. tropicalis* biofilm with/ without citral (16µg/mL) treatment were collected in 10mL of deionized water and subjected to the water bath sonication for 5mins followed by vortexing for 1min and the resultant supernatant was collected in a

micro-centrifuged tube. The supernatant was centrifuged at 4000rpm to pellet down the cells and extracellular matrix (in the supernatant) was collected in a fresh microcentrifuge tube. The obtained extracellular matrix of both control and citral-treated samples were lyophilized using Freeze Dryer (BioBase, China). For NMR analysis, the samples were prepared by adding 500 μ L of D₂O to the lyophilized cell extracts to avoid water peaks in NMR spectra. Standard DSS (4, 4-dimethyl-4-silapentane-1-sulfonic acid) was added to the treated sample as a chemical shift indicator to set the reference at 0ppm for 1D ¹H NMR spectra.

To study the changes in the extracellular matrix, Carr-Purcell-Meilboom-Gill (CPMG) 1D experiment was employed to see the variation in the metabolites (Lindon *et al.*, 2000). The spectra were recorded at 25°C on a Bruker AVANCE 500 MHz NMR spectrometer, Germany, equipped with a triple resonance (¹H, ¹³C, ¹⁵N) probe having a Z-axis shielded gradient. ¹H CPMG NMR spectra were recorded with 1024 scans and 65536 data points for both the control and citral-treated NMR samples. The phasing and baseline correction of thus obtained ¹H-CPMG-NMR spectra was done by TopSpin 3.5 software. The obtained mass list was checked with Biological Magnetic Resonance Data Bank (BMRB), online available software, in order to identify the metabolites. The peaks on the spectra were annotated using TopSpin 3.5 software. All the experiments were done in seven technical replicates and analysed using Metaboanalyst (v3.0) software. Orthogonal PLS-DA was performed to compare the metabolite variations. Statistical significance was further tested using student's *t*-test.

3.2.28 Statistical analysis

All of the experiments were performed in triplicates and were expressed as mean values with the corresponding standard deviations (SD). Statistical significance between treated and control groups was analyzed by one-way analysis of variance (ANOVA) with a p-value of $p \leq 0.05$ using SigmaPlot 14.0 software.



4.1 *In vitro* biofilm formation of *Candida tropicalis* and its inhibition by selective terpenes

Candida biofilm has shown more resistance to the antifungals agents than their planktonic counterparts. This resistance of biofilm against synthetic antifungal agents makes it crucial to find out more from the arsenal of natural products such as terpenes. In several studies, these terpenes have been ascertained with strong antifungal actions against *Aspergillus* species, *Saccharomyces cerevisiae* and *Candida* species. However, their antibiofilm activities against *Candida* species have not been completely investigated. So far, this is the first study to demonstrate *in vitro* antibiofilm activities of selective terpenes i.e. geraniol, menthol, citral, cinnamaldehyde, carvacrol, eugenol, and thymol against *C. tropicalis* were monitored.

4.1.1 Growth curve of *C. tropicalis* biofilm formation

The growth of *C. tropicalis* biofilm formed on polystyrene as well as silicone elastomer was quantified and observed to be matured at 48h. The standard *in vitro* procedures were followed to study the growth pattern of *C. tropicalis* biofilm on two different substrates. The growth has appeared as a sigmoidal curve with lag phase (6h), log phase (24h) and plateau phase (48h) after which the growth became stagnant as shown in Figure 4.1. The formation of biofilm consists of three distinguished phases, namely adherence phase (up to 4h) followed by intermediate phase (24h) and matured phase (48h) as observed using bright-field microscopy. Adherence of the cells takes place in the first 4h and can be seen as cells get attached to the substratum. As the biofilm proliferates, cells start forming micro-colonies by aggregating themselves. Further, the cells initiate secretion of extracellular matrix to intensify the virulence and development of resistance against antifungal agents in later stages. Since, both the substrates were showing similar growth kinetics, the polystyrene plates were used as substrates for biochemical assays whereas, silicone elastomers were considered for further morphological analysis using previously optimized protocols for *in vitro* biofilm studies. The three stages of biofilm formation are depicted in Figure 4.2 A-C. The matured form of biofilm possesses high confluency of cells which are tactfully structured in order to provide better nourishment and survival of the cells. In Figure 4.2 D, E, the *in vitro* matured biofilm were visualized and considered for the screening of the selected terpenes.

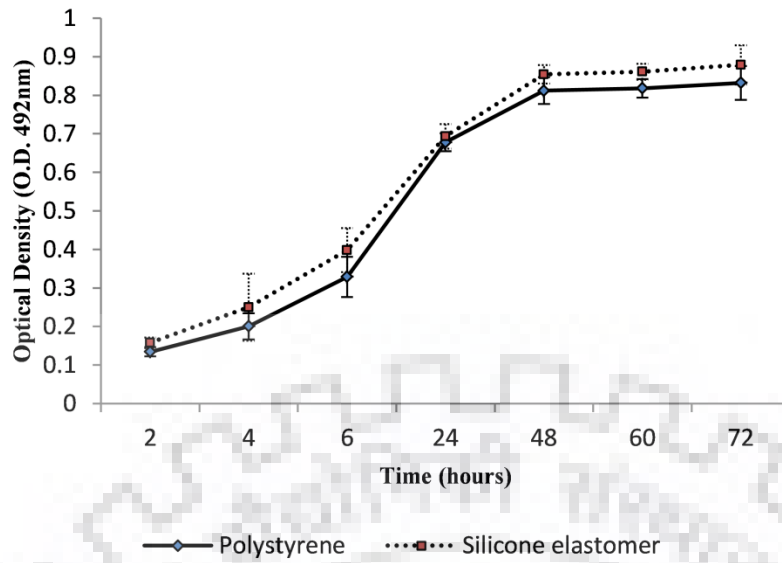


Figure 4.1 Biofilm formations of *C. tropicalis* on different substrates

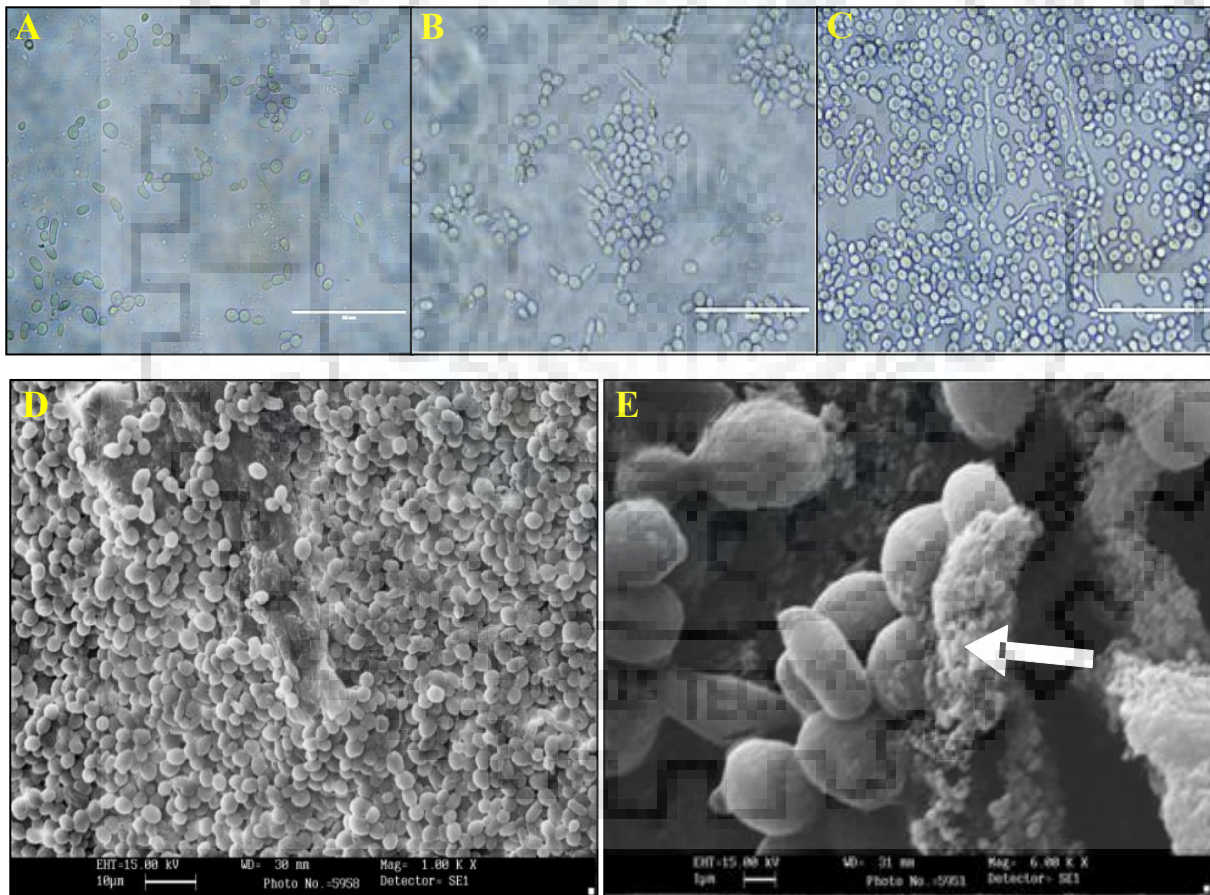


Figure 4.2 Bright-field microscopic images of *C. tropicalis* biofilm: A. Adhesion phase 6h (60 ×); B. Intermediate phase, 24h (60×); and C. Mature phase, 48h (60×). Scale: 50µm. Scanning electron microscopic (SEM) images of *C. tropicalis* biofilm grown on substrate reveals the surface topology: D. cell confluence on the substrate; and E. presence of extracellular matrix as indicated by the white arrow

4.1.2 Antifungal activities of terpenes against *C. albicans* and *C. tropicalis*

The activities of seven terpenes namely geraniol, menthol, citral, cinnamaldehyde, carvacrol, eugenol, and thymol were tested. The MIC values were determined for all the terpenes. The planktonic cells were grown in Sabouraud's dextrose broth following standard CLSI method. *C. tropicalis* and *C. albicans* cells were grown in serially double diluted concentrations of each terpene (0- 1024 μ g/mL) in the flat bottom 96-well plates. The MIC₅₀ is defined as the concentration with 50% cell growth, in contrast, to the control or untreated sample. MIC₅₀ values for different terpenes are represented in Table 4.1, calculated with acceptable standard deviations. Citral and thymol were found to have the lowest MIC₅₀ values as 32 μ g/mL and 16 μ g/mL, respectively, and were more effective against *C. tropicalis* in comparison to *C. albicans*. Even higher concentrations were required to completely inhibit cell growth. All experiments were done in triplicates to minimize the errors.

4.1.3 Inhibition of biofilm formation and eradication of preformed biofilm

The *in vitro* antibiofilm activities of terpenes against *C. tropicalis* were examined as represented in Table 4.1. The terpenes were used in serially doubled diluted concentrations (0- 1024 μ g/mL) and their inhibitory concentrations were evaluated. To know the inhibitory effect of terpenes on the formation of biofilm of *C. tropicalis*, the terpenes were added at the initial stage of biofilm formation. However, the effect of respective terpenes on preformed (matured) biofilm was checked when the biofilm was formed up to 24h i.e. inter-mediate phase and treated with serial double dilutions (0-1024 μ g/mL) of terpenes. BIC₅₀ and BEC₅₀ were defined as the concentration at which 50% of the cells are metabolically active. Interestingly, among all, citral and thymol were observed to be more effective against *C. tropicalis* rather than *C. albicans*. The calculated BIC₅₀ was 64 μ g/mL when treated with citral and 32 μ g/mL in the presence of thymol. Moreover, the effective BEC₅₀ was calculated to be 128 μ g/mL for both citral and thymol against *C. tropicalis* biofilm. On comparing the BIC₅₀ and BEC₅₀ values, it was observed that citral required two-fold whereas thymol needed a four-fold higher concentration for the eradication of the biofilm (Figure 4.3). Therefore, thymol is more effective in inhibiting the biofilm formation and became less competent on preformed biofilm. The robust habitat of matured biofilm is responsible for its survival ultimately leading to resistance against antifungal drugs.

Table 4.1 Calculated Minimum Inhibitory Concentrations (MICs), Biofilm Inhibitory Concentrations (BICs) and Biofilm Eradicating Concentrations (BECs) of tested terpenes and fluconazole. #Values represent the arithmetic means ($p \leq 0.05$) of the effective concentration against planktonic cells and biofilm

| # MICs, BICs and BECs ($\mu\text{g/mL}$) | | | | | | | | |
|---|--------------------|---------|--------------------|----------------|-------------------|---------|------------|-------------|
| Microorganisms | Alcoholic terpenes | | Aldehydic terpenes | | Phenolic terpenes | | | Azole |
| <i>Candida</i> spp. | Geraniol | Menthol | Citral | Cinnamaldehyde | Carvacrol | Eugenol | Thymol | Fluconazole |
| Minimum Inhibitory Concentration (MIC₅₀) | | | | | | | | |
| <i>C. albicans</i> | 32 | 64 | 64 | 128 | 64 | 64 | 32 | 16 |
| <i>C. tropicalis</i> | 64 | 128 | 32 | 256 | 128 | 128 | 16 | 32 |
| Biofilm Inhibitory Concentration (BIC₅₀) | | | | | | | | |
| <i>C. albicans</i> | 128 | 128 | 128 | 128 | 128 | 128 | 128 | 64 |
| <i>C. tropicalis</i> | 128 | 256 | 64 | 512 | 256 | 256 | 32 | 128 |
| Biofilm Eradicating Concentration (BEC₅₀) | | | | | | | | |
| <i>C. albicans</i> | 512 | 256 | 256 | 256 | 256 | 256 | 256 | 128 |
| <i>C. tropicalis</i> | 256 | 512 | 128 | >1024 | 512 | 512 | 128 | 256 |

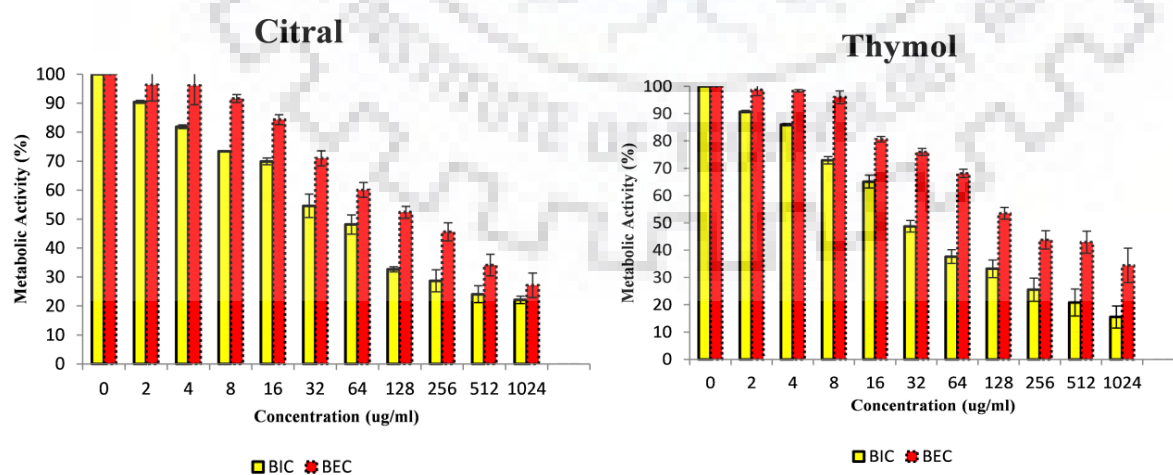


Figure 4.3 Trends of biofilm inhibition and eradication effects of citral and thymol

4.1.4 Effect on cell surface hydrophobicity and auto-aggregation of *C. tropicalis* in the presence of terpenes

The values of the hydrophobicity index of all the terpenes generated by fractionation in xylene (hydrophobic) and aqueous (hydrophilic) phases are shown in Table 4.2. A reduction in cell surface hydrophobicity was recorded for planktonic cells of *C. tropicalis* when briefly exposed to a sub-MIC₅₀ concentration of these terpenes. Here, the results demonstrated a decrease in cell surface hydrophobicity of *C. tropicalis* that would allow lesser biofilm formation indicating the possible application of these terpenes as antifungal agents in clinical settings. The decrement in auto-aggregation of cells also depicts the limiting biofilm formation in the presence of these terpenes. The behaviour of *C. tropicalis* cellular adhesion and reduction in hydrophobic properties is, in fact, an outcome of the reduction in surface hydrophobicity. Therefore, the use of selected essential oils seemingly represents as promising antifungal agents with reduced biofilm production by *C. tropicalis*.

Table 4.2 Representing Hydrophobicity Index (HI) and auto-aggregation of *C. tropicalis* yeast cells

| Terpenes | | HI (%) | Auto-aggregation (%) |
|-------------------|----------------------------|-------------|----------------------|
| Control (0 µg/mL) | | 97.19± 3.38 | 95.45± 2.41 |
| Alcohol | Geraniol (32 µg/mL) | 55.38± 2.57 | 53.78± 1.09 |
| | Menthol (64 µg/mL) | 53.26± 1.25 | 50.19± 2.42 |
| Aldehyde | Citral (16 µg/mL) | 58.59± 2.63 | 54.69± 2.16 |
| | Cinnamaldehyde (128 µg/mL) | 50.30± 3.60 | 47.74± 3.52 |
| Phenol | Carvacrol (64 µg/mL) | 56.41± 2.49 | 51.38± 2.35 |
| | Eugenol (64 µg/mL) | 52.93± 1.34 | 49.7± 1.51 |
| | Thymol (8 µg/mL) | 54.98± 3.31 | 51.44± 2.37 |

4.1.5 Time-kill kinetics of terpenes against *C. tropicalis*

The antifungal potencies of terpenes were studied by kill kinetics against yeast cells of *C. tropicalis*. The growth kinetics of *C. tropicalis* was carried out at MIC₅₀ concentrations of geraniol, menthol, citral, cinnamaldehyde, carvacrol, eugenol and thymol, respectively. The kill kinetics profiles as shown in Figure 4.4, depicts the fungicidal effects of these terpenes towards *C. tropicalis*. The reduction of cell viability was calculated to be ≥ 2.5 logs after 2h exposure. However, in the presence of terpenes *C. tropicalis* showed ≥ 1.5 logs reduction in viable cell count relative to the initial inoculum after 1 h whereas, on treating with amphotericin B, the

reduction of viable cell count was ≥ 2.5 log after 1h and ≥ 3.5 logs after 2h of exposure, in comparison to the control.

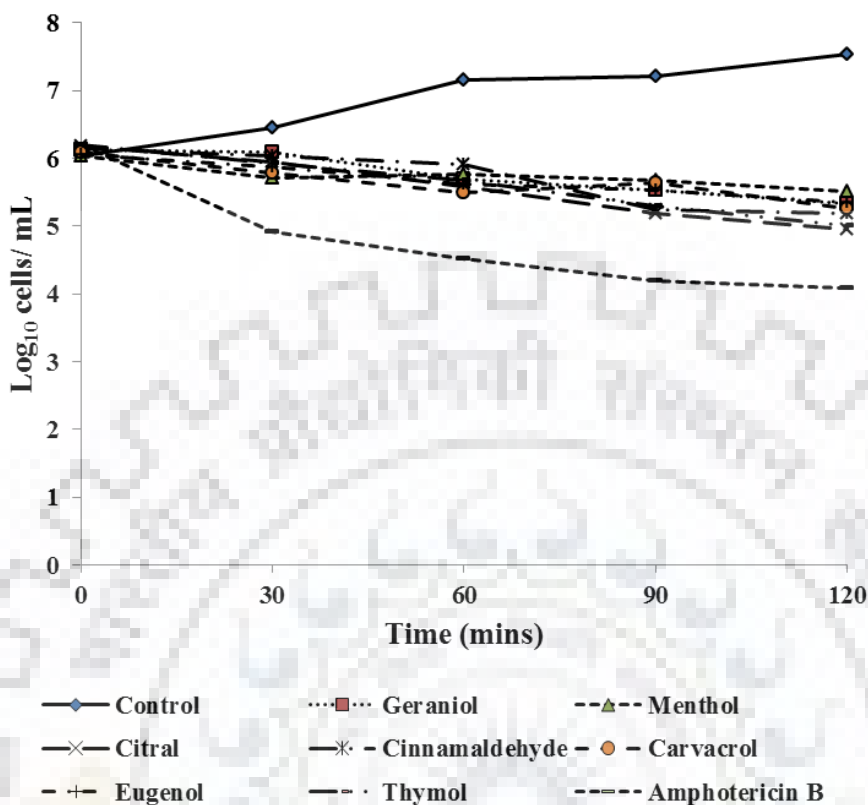


Figure 4.4 *In vitro* time-kill curves of *C. tropicalis* when treated with terpenes and amphotericin B. Reduction of ≥ 2.5 -3.5 log cells has been observed in yeast cells when treated with MIC₅₀ of these terpenes

4.1.6 Morphological changes in *C. tropicalis* biofilm on administration of terpenes

The changes in *C. tropicalis* biofilm and their cellular surfaces were visualized using SEM imaging. Control (0 μ g/mL) biofilm image showed a complex biofilm structure with clustered cells surrounded by extracellular matrix as given in Figure 4.5A. On treatment with BEC₅₀ of these terpenes, the biofilm cells were damaged which could possibly lead to the rupture of outer membrane creating a deformed morphology as represented in Figure 4.5 B-I. These morphological alterations of the cells could be associated with loss of cell membrane integrity resulting in cell death.

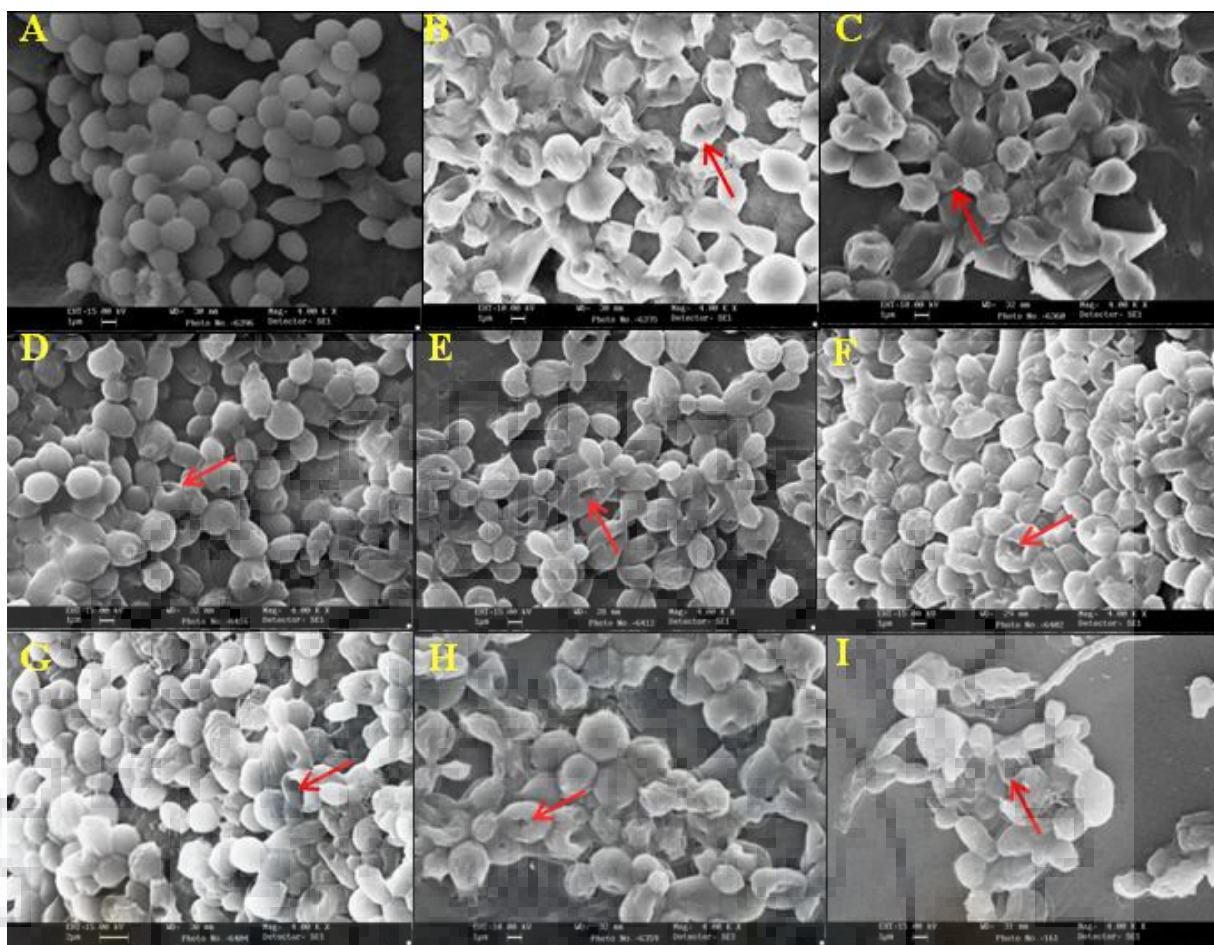


Figure 4.5 Scanning electron microscopic (SEM) images showing damage to *C. tropicalis* biofilm: A. control biofilm (0 μ g/mL); B. amphotericin B (4 μ g/mL); C. geraniol (256 μ g/mL); D. menthol (512 μ g/mL); E. citral (128 μ g/mL); F. cinnamaldehyde (1024 μ g/mL); G. carvacrol (512 μ g/mL); H. eugenol (512 μ g/mL); and I. thymol (128 μ g/mL). #Red arrows indicate cellular deformities

4.2 Deciphering the probable mode of action of citral and thymol against *C. tropicalis* biofilm

Based on the results obtained from the above-mentioned study, the comparative potentials of citral and thymol against *C. tropicalis* were examined. The antibiofilm effect of citral and thymol was recognized through biochemical assays and scanning microscopies to enlighten the cellular alterations. There are established key genes such as *ERG11*, *SOD1*, *ENO1*, and *CNB1* etc. which were documented to be in association with drug resistance in order to reduce the effect of well-known drugs involvement in major pathways followed by *C. tropicalis*. The relative expression of these key genes was also investigated to get the insights into the plausible mechanism for its survival during treatment by these two components.

4.2.1 Citral and thymol indicated no direct binding to the cell membrane but thymol acts via cell wall

The antibiofilm activity of citral and thymol against *C. tropicalis* was tested *in vitro* and their effects were studied through XTT reduction method. To calculate the inhibitory effect on the biofilm formation of *C. tropicalis*, both citral and thymol were added at the initial stage of biofilm formation. The *C. tropicalis* planktonic cells and its biofilm were grown in serially double diluted concentrations (0-1024 μ g/mL) of the citral and thymol and the minimum inhibitory concentration values (MICs) were determined as shown in Table 4.3. It was observed that citral (MIC₅₀ = 32 μ g/mL) and thymol (MIC₅₀ = 16 μ g/mL) were significantly effective against planktonic cells of *C. tropicalis*.

For preformed biofilm, the components were added after 24h (log phase) of biofilm formation. The BIC₅₀ value for citral was determined to be 64 μ g/mL while thymol inhibited biofilm formation at a lower concentration of 32 μ g/mL. The BEC₅₀ for both citral and thymol were observed to be 128 μ g/mL as the effective concentrations to eradicate matured *C. tropicalis* biofilm. Since citral and thymol have shown a good effect against planktonic cells and biofilm forms of *C. tropicalis*, further, the morphological changes in the biofilm form were examined.

Furthermore, the binding of citral and thymol to the fungal membrane sterol was ensured through the change in inhibitory concentration values (ICs) of both agents for *C. tropicalis* in the presence and absence of ergosterol. The exogenous ergosterol would prevent the binding to the fungal membrane's ergosterol if the activity of citral or thymol was instigated by binding to ergosterol. The ICs enhancement when substituted with the exogenous ergosterol with respect to the control assay was witnessed with no altercations in MIC₅₀, BIC₅₀ and BEC₅₀ as shown in Table 4.3.

An osmotic stabilizer such as sorbitol in the media could reverse the antifungal effect of the agents which targets the fungal cell wall. When the *C. tropicalis* was treated with both citral and thymol in the media supplemented with sorbitol, the IC values were not affected in the presence of citral. However, in the case of thymol, the shift of MIC₅₀ from 16 μ g/mL to 32 μ g/mL and BIC₅₀ from 32 μ g/mL to 64 μ g/mL suggested that thymol would act as an inhibitor of the cell wall synthesis or assembly.

Table 4.3 IC values ($\mu\text{g/mL}$) of agents in the absence and presence of sorbitol (0.8M) and ergosterol (400 $\mu\text{g/mL}$) against *C. tropicalis*. Values represent the arithmetic means ($p \leq 0.05$) of the effective concentration against planktonic cells and biofilm. Amphotericin B (positive control); NA: not tested in the sorbitol assay, +: the presence of the fungal growth in medium plus sorbitol and no drug

| Agents | Sorbitol | | | Ergosterol | |
|----------------|-------------------|---------|----------|------------|----------|
| | Control | Absence | Presence | Absence | Presence |
| Citral | MIC ₅₀ | + | 32 | 32 | 32 |
| | BIC ₅₀ | + | 64 | 64 | 64 |
| | BEC ₅₀ | + | 128 | 128 | 128 |
| Thymol | MIC ₅₀ | + | 16 | 32 | 16 |
| | BIC ₅₀ | + | 32 | 64 | 32 |
| | BEC ₅₀ | + | 128 | 128 | 128 |
| Amphotericin B | MIC ₅₀ | + | NA | NA | 1 |
| | BIC ₅₀ | + | NA | NA | 4 |
| | BEC ₅₀ | + | NA | NA | 8 |

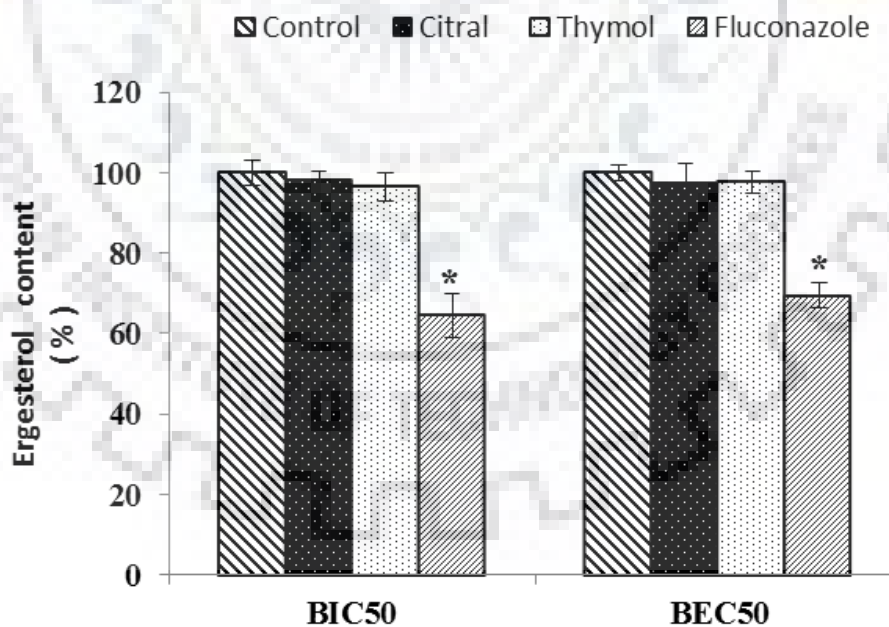


Figure 4.6 Percentage of ergosterol content in *C. tropicalis* biofilm. Error bars denote standard deviation (SD). * $p < 0.05$, ** $p < 0.01$, *** $p < 0.005$ when compared with the control

4.2.2 Ergosterol content was unaltered in the presence of citral and thymol

The total ergosterol content was measured to determine the changes in the presence and absence of citral and thymol. The content of ergosterol was not significantly altered when exposed to citral and thymol at their respective BIC₅₀ and BEC₅₀ values. However, there was a decrease in the ergosterol content when the biofilm cells were treated with fluconazole, a well-established inhibitor of ergosterol biosynthesis (Figure 4.6). A significant reduction of the ergosterol content was observed in the *C. tropicalis* biofilm cells during fluconazole treatment at BIC₅₀ (128µg/mL) and BEC₅₀ (256µg/mL) with a percent of 35.57% and 30.58%, respectively. However, no significant reduction was detected at BIC₅₀ and BEC₅₀ values of citral and thymol.

4.2.3 FE-SEM and CLSM analysis displayed damage to the biofilm in the presence of citral and thymol

The morphological changes of preformed *C. tropicalis* biofilm and their cellular surfaces in the presence of BEC₅₀ (128µg/mL) of citral and thymol were investigated. The morphologies of the biofilm with and without treatment were observed when proceeded with the visualization of mature biofilm through FE-SEM and CLSM analysis. During FE-SEM imaging, control (0µg/mL) biofilm displayed complex structure with clustered cells surrounded by the extracellular matrix as shown in Figure 4.7 A. However, during the treatment of amphotericin B (4µg/mL); BEC₅₀ (128µg/mL) of citral and thymol, the biofilm exhibited deformed morphology with cells having porous outer membrane as represented in Figure 4.7 B-D, respectively.

During CLSM analysis, the combination of fluorescent dyes Con-A (selectively binds mannose and glucose residues of cell wall polysaccharides) and FUN-1 (cytoplasmic probe for cell viability) was used. CLSM images of control biofilm revealed dense and compact structure which was green with Con-A staining cell wall and red with FUN-1 staining live cells, conversely, with yellowish-green in colour in the presence of both Con-A and FUN-1 i.e. dual stain. However, when treated with citral and thymol at BEC₅₀ i.e. 128µg/mL, reduction in dense live cells and more green cells/ broken cell walls as debris was observed as in Figure 4.8.

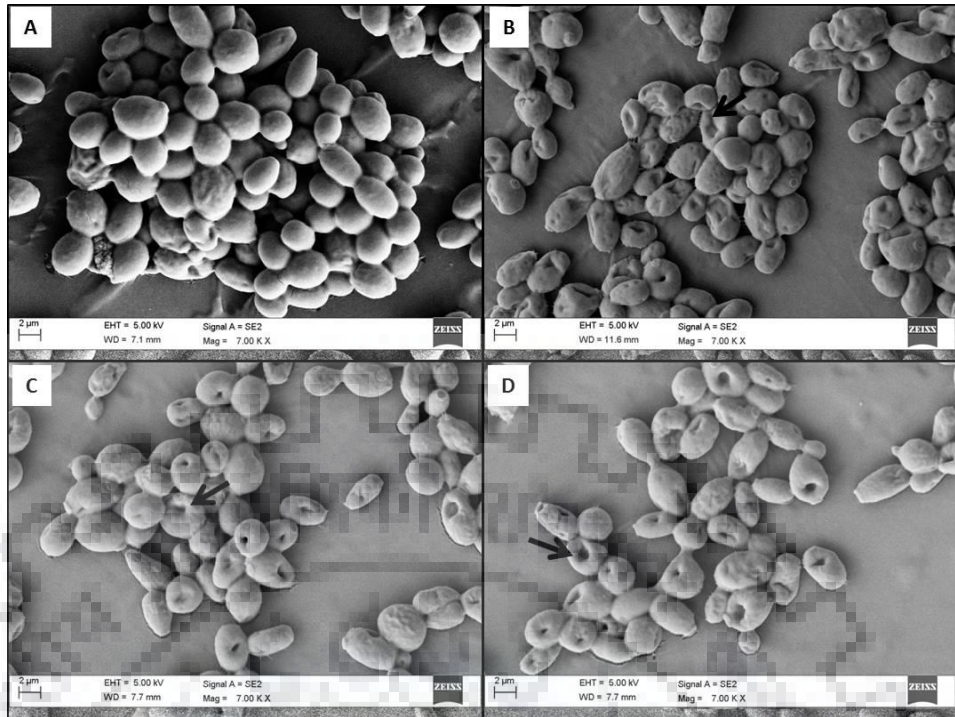


Figure 4.7 Images through field emission scanning electron microscopy (FE-SEM) (Magnification: 7000 \times , Bar: 2 μ m) of *C. tropicalis* biofilm: A. control (1% DMSO) with densely clustered healthy cells; B. amphotericin B (4 μ g/mL); C. citral (128 μ g/mL); and D. thymol (128 μ g/mL), cells are more porous and flaccid with looser cell surface. # Black arrows show pores in the cells

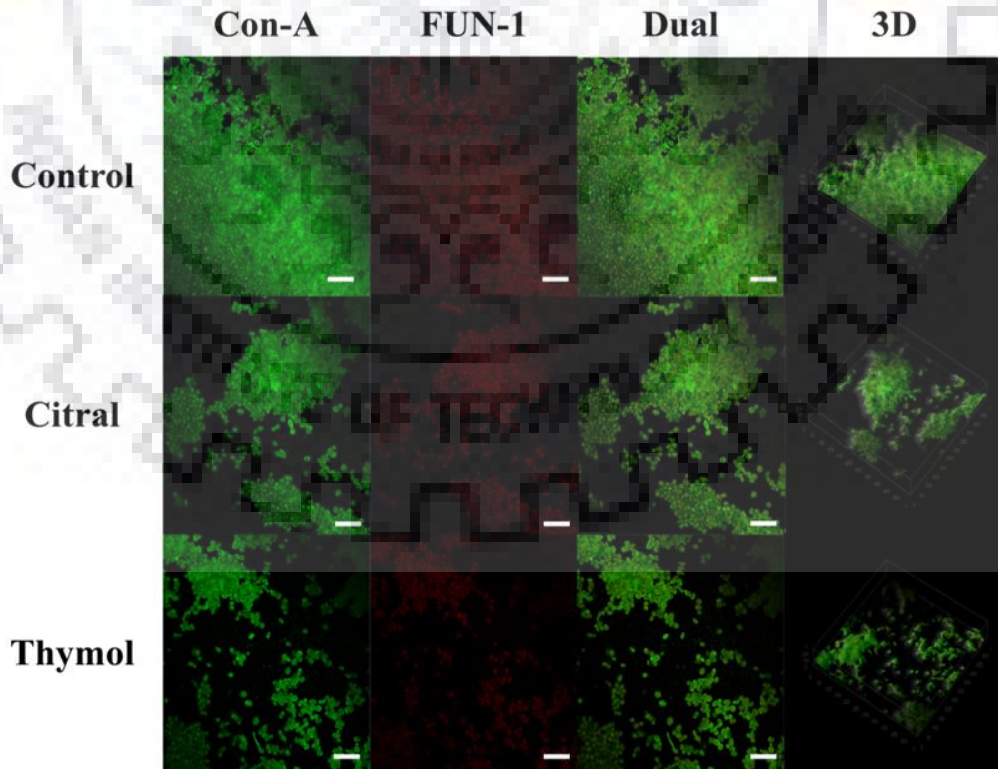


Figure 4.8 Confocal laser scanning microscopic images (CLSM) of *C. tropicalis* biofilm; dual stained: CON-A (Excitation: 488, Emission: 505), staining polysaccharide walls, green and FUN-1 (Excitation: 470, Emission: 590), staining metabolically active cells, red; thus dually staining yellowish-green colour of healthy biofilm as control (1% DMSO). Power field: 40 \times ; Scale Bar: 50 μ m

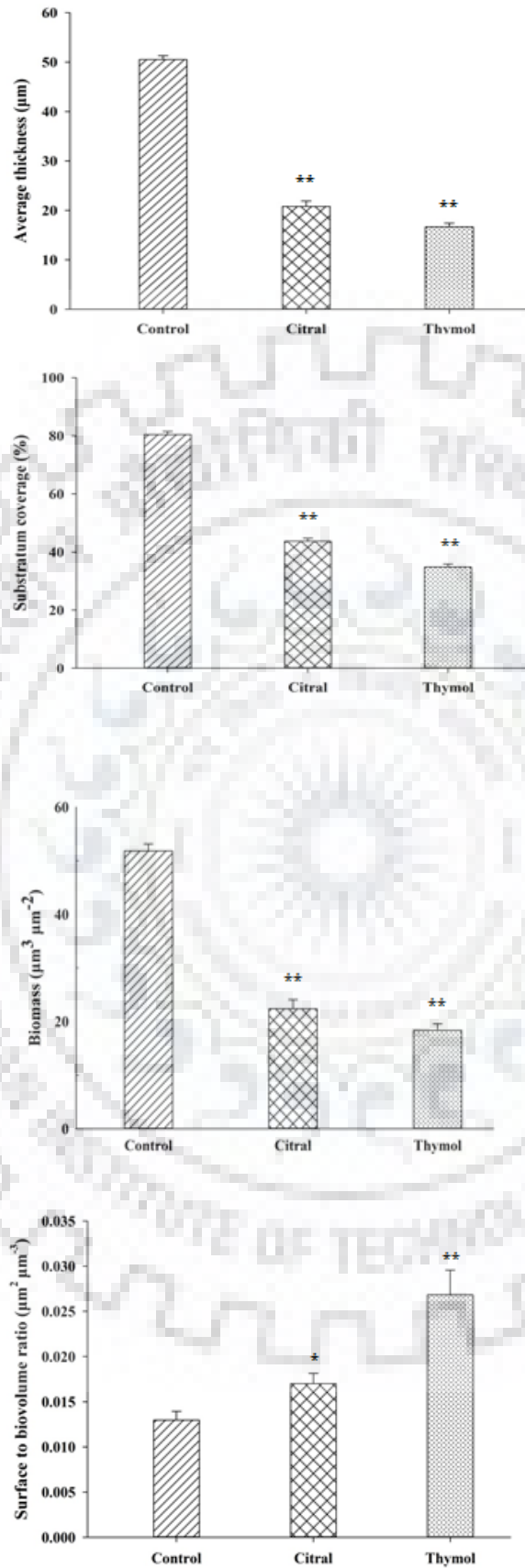


Figure 4.9 COMSTAT analysis of *C. tropicalis* biofilm. Error bars denote standard deviation (SD). *p < 0.05, **p < 0.01, ***p < 0.005 when compared with the control

Furthermore, COMSTAT analysis depicted the lower biomasses in the presence of both citral and thymol, less thickened biofilm at the matured stage and lesser substratum coverage when compared to the healthy biofilm. Also, the surface to bio-volume ratio was increased showing less biofilm formation during treatment as represented in Figure 4.9.

4.2.4 Impairment of the plasma membrane integrity of *C. tropicalis* biofilm cells in the presence of citral and thymol

Terpenes are long known for their fungicidal as well as fungistatic components. Here, the effect of citral and thymol on *C. tropicalis* biofilm cells was documented to be fungicidal. The fungicidal effect of citral and thymol was recognized as depicted in Figure 4.10. The biofilm cells of *C. tropicalis*, when incubated with citral, thymol, and amphotericin B were studied for membrane permeabilization. *C. tropicalis* biofilm cell membrane is impermeable to PI and hinders its uptake during healthy conditions. However, when the cell membrane is compromised PI uptake assay will indicate the fungal membrane permeabilization of the *C. tropicalis* biofilm cells in the presence of antifungal agents. The fungicidal effects of citral, thymol, and amphotericin B were studied using FACS analysis where PI uptake by cells was monitored to confirm the cytotoxicity of effect on *C. tropicalis* biofilm cells.

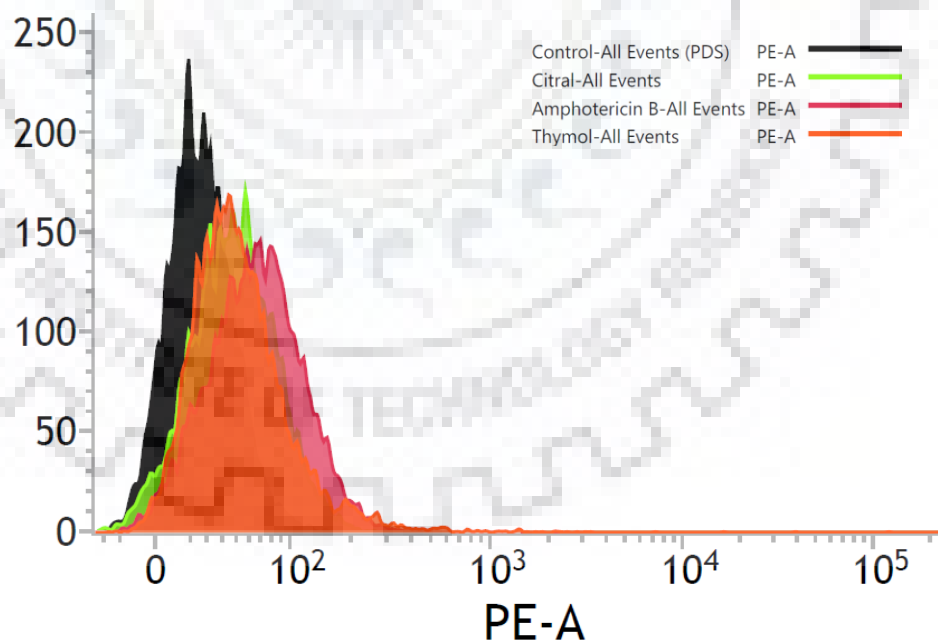


Figure 4.10 Fungicidal effects of citral and thymol on *C. tropicalis* biofilm cells

The PI staining of the cells and broadening of PE-A corresponds to cellular death. The obtained data thus suggested the toxicity of amphotericin B slightly higher than citral and thymol. Also, citral and thymol required more doses (16µg/mL and 8µg/mL, respectively) to

kill the biofilm cells in comparison to amphotericin B (4µg/mL). Therefore, citral and thymol act in a fungicidal manner when introduced to the biofilm cells of *C. tropicalis* as drug similar to that of amphotericin B.

4.2.5 Citral and thymol generated reactive oxygen species (ROS)

Here, thymol has shown significant increment in the ROS production than citral as represented in Figure 4.11. The production of ROS determines the status of mitochondrial dysfunction in the presence of antimicrobial agents. The measurement of ROS generation was done by employing CM-H2DCFDA fluorescent molecule which is sensitive to redox changes. *C. tropicalis* biofilm cells were incubated with citral, thymol, and amphotericin B at their respective BIC₅₀ and BEC₅₀. The positive result explained one of the factors introduced by citral and thymol during treatment. Therefore, the antibiofilm activity of citral and thymol corresponds to the oxidative stress which could be a cellular response against these components.

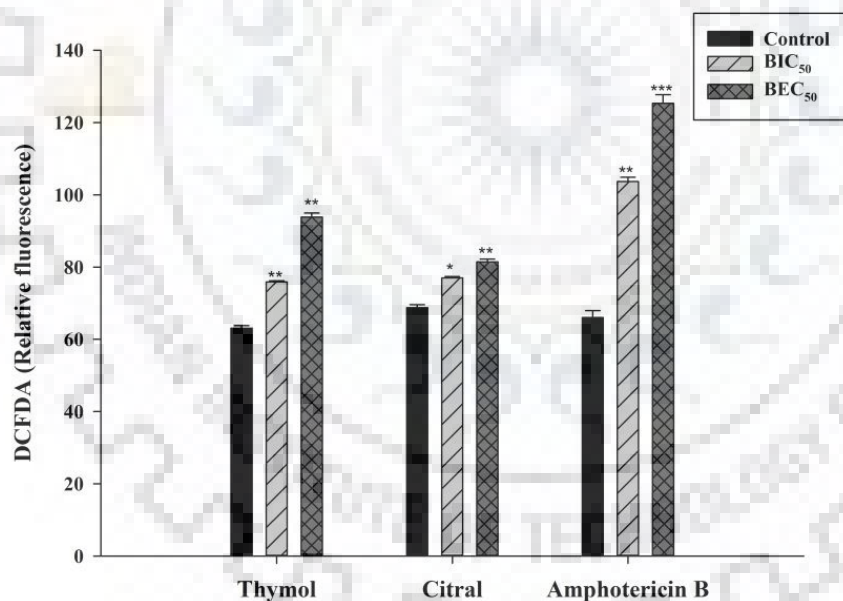


Figure 4.11 Graphical representation of the DCFDA fluorescence of *C. tropicalis* biofilm representing reactive oxygen species (ROS) production during treatment of amphotericin B, citral and thymol. Error bars denote standard deviation (SD). *p < 0.05, **p < 0.01, *** p < 0.005 when compared with the control

4.2.6 Enzymatic activities of catalase (CAT), peroxidase (POD) and superoxide dismutase (SOD) during citral and thymol treatment

As discussed earlier, the levels of ROS of *C. tropicalis* biofilm tends to elevate in response to citral and thymol. Henceforth, the antioxidant enzyme activities of CAT, POD and

SOD which are responsible for eradication these ROS, were assessed. The activities of all the three antioxidant enzymes were increased by 1.5 – 2.5 folds in comparison to control (Figure 4.12 A-C). A significant rise in the enzymatic activities of CAT, POD and SOD was observed in comparison to that of control.

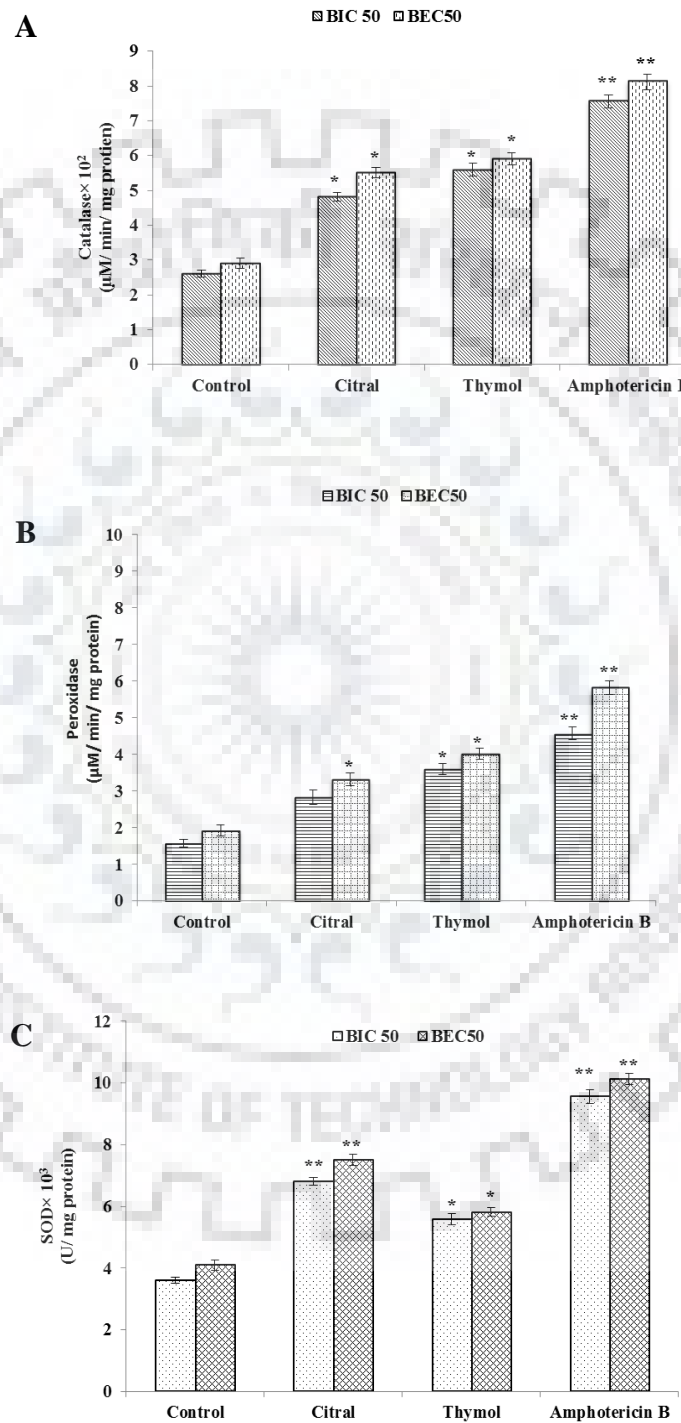


Figure 4.12 Elevation in the activities of antioxidant enzymes in response to citral and thymol: A. Catalase (CAT); B. Peroxidase (POD); and C. Superoxide dismutase (SOD). Error bars denote standard deviation (SD). *p < 0.05, **p < 0.01, *p < 0.005 when compared with the control**

4.2.7 Occurrence of lipid peroxidation in the presence of citral and thymol

The lipid peroxidation is a consequence of oxidative stress with an increase in the level of ROS. In the presence of citral and thymol, the level of lipid peroxidation in *C. tropicalis* biofilm cells were elevated as calculated using TBARS assay which indicated the significant increase in the amounts of MDA (Figure 4.13).

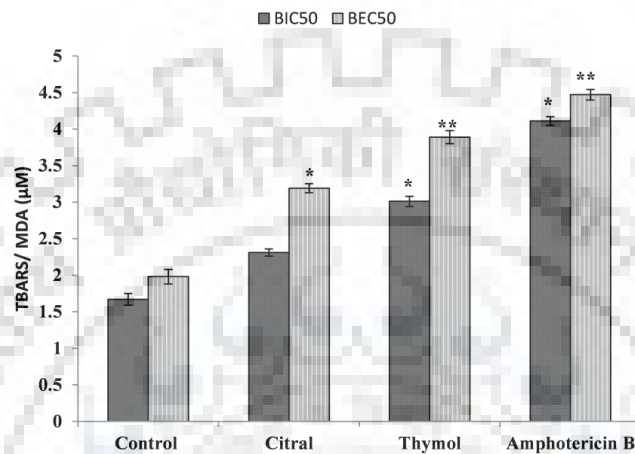


Figure 4.13 Lipid peroxidation in the presence of citral and thymol. Error bars denote standard deviation (SD). *p < 0.05, **p < 0.01, ***p < 0.005 when compared with the control

4.2.8 DNA damage in *C. tropicalis* biofilm cells on treating with citral and thymol

The alkaline yeast comet assay was applied to study the protective capacity of DNA against oxidative stress induction by citral and thymol. *C. tropicalis* biofilm cells when treated with citral (64µg/mL), thymol (32µg/mL), H₂O₂ (5mM) were considered.

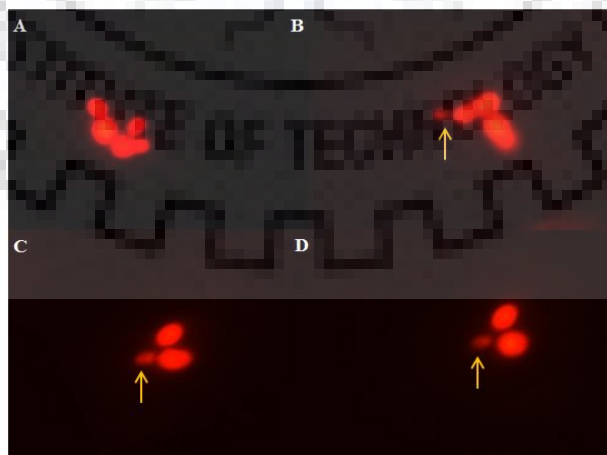


Figure 4.14 DNA damage visualization through comet tailing: A. control (0µg/mL); B. citral (64µg/mL); C. thymol (32µg/mL); and D. H₂O₂ (5mM). # Yellow arrow indicates the comet tail

The damage to the DNA in *C. tropicalis* biofilm cells was visualized through comet tailing during treatment in comparison to a positive control (H₂O₂ (5 mM)) and negative control (0 µg/ mL). The control cell with no treatment displayed no tailing in the biofilm cells whereas treated cells had distinct comet tail similar to the positive control (Figure 4.14).

4.2.9 Citral upregulated *ERG11/ CYT450* genes whereas thymol upregulated *CNB1* and *SOD1* genes

The relative gene expression of *ENO1*, *ALD5*, *ERG11*, *CYT450*, *KGD2*, *SOD1*, and *CNB1*, responsible for major antifungal tolerance mechanism were evaluated as depicted in Figure 4.15.

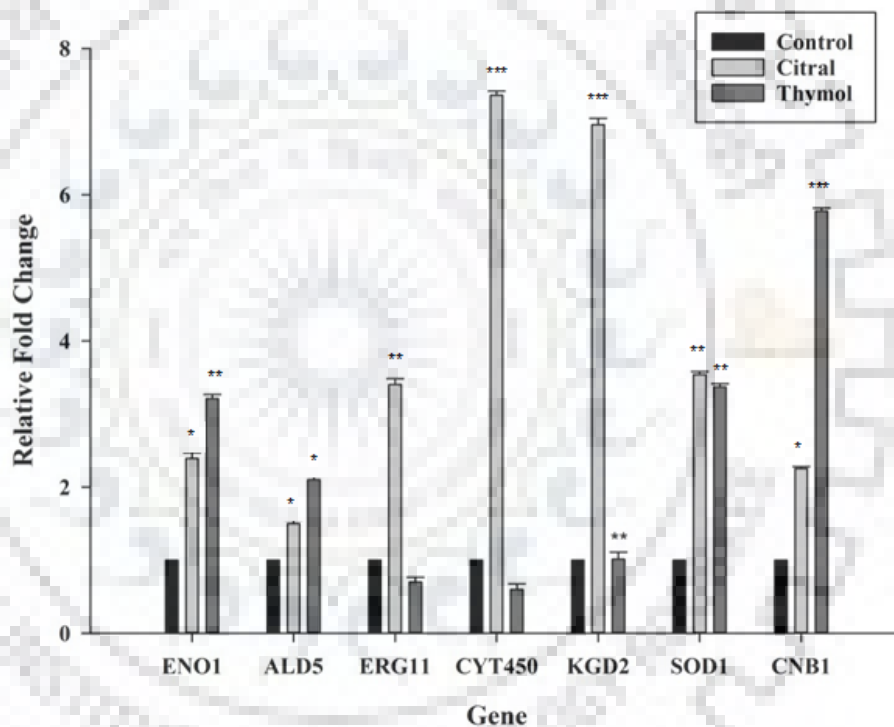


Figure 4.15 Effect of citral and thymol on the relative expression of the selected genes in *C. tropicalis*. Error bars represent standard deviation (SD). * $p \leq 0.05$, ** $p \leq 0.01$, and *** $p \leq 0.005$ in comparison to the control

4.3 *In silico* molecular modelling and docking analysis of lanosterol-14- α -demethylase (Erg11p) from *C. tropicalis* with citral

As mentioned before, the activity of citral is not through direct ergosterol binding but could possibly involve in the hindrance of ergosterol biosynthesis. The *in silico* screening of natural compounds have accelerated the process of drug discovery which assists in the

development of alternative drugs in reduced time. Considering the above facts, in the present study, the homology model of well-known azole drug target Erg11p of *C. tropicalis* was employed to unravel the interaction between citral and lanosterol-14- α -demethylase (Erg11p).

4.3.1 Protein sequence was retrieved from NCBI database

CtErg11p, a total of 528 amino acids, was retrieved in FASTA format from NCBI database (Figure 4.16). The sequences of similar proteins to the query *CtErg11p* were acquired through PDB search using BLASTp resulting in a large number of sequences. The best two matches of the query (*CtErg11p*) were taken into consideration. Both the sequences were of same gene Erg11p bound to heme (porphyrin ring) and two different azole drugs. The *CaErg11p* complexed with itraconazole (PDB ID: 5V5Z) and posaconazole (PDB ID: 5FSA), respectively, were considered the best templates for the query sequence. 5V5Z was bound to itraconazole and had 537 amino acids whereas; 5FSA was bound to posaconazole and had 490 amino acids along with heme ligand in both.

```
>AMR44151.1 cytochrome P450 lanosterol 14-alpha-demethylase [Candida tropicalis]
MAIVDTAIDGINYFLSLSLTQQITILVVFPIYNIWQLLYSLRKDRVPMVFW
IPWFGSAASYGMQPYEFFEKCRKLYGDIVFSFMLLGKVMVTVYLGPKGHEFIYN
AKLSDVSAEEAYTHLTTPVFGKGVYIDCPNSRLMEQKKFAKFALTTDSFKTY
VPKIREEVLNYFVNDVSFKTKERDHGVASVMKTQPEITIFTASRCLFGDEMRS
SFDRSFAQLYADLDKGFTPIVFPNLPPLPHYWRRDAAQRKISAHYMKIKRR
RESGDIDPKRDLIDSLVNSTYKDGVMKMTDQEIANLLIGVLMGGQHTSASTSA
WFLHLAEQPQLQDDLYEELTNLLKEKGGDLNDLTYEDLQKLPLVNNTIKET
LRMHMPLHSIFRKVMNPLRVPNTKYVIPKGHYVLVSAGYAHTSDRWFEHPE
HFNPRRWESDDTKASAVSFNSEDTVDYGFYKISKGVSSPYLPFGGGRHRCIGE
QFAYVQLGTILTTYIYNFKWRLNGDKVPDVDYQSMVTLPLEPAEIVWEKRDT
CMV
```

Figure 4.16 FASTA sequence of the query *CtErg11p* retrieved from NCBI (528 amino acids)

4.3.2 Query and template sequence alignment and prediction of secondary structure

The secondary structure of the modelled protein is defined as described previously (Kabsch and Sander, 1983). The overall structure and secondary patterns observed was similar to that of *CaErg11p*. The multiple sequence alignment (MSA) file was prepared using FASTA sequences of all three in .txt format and was converted into a .aln file.

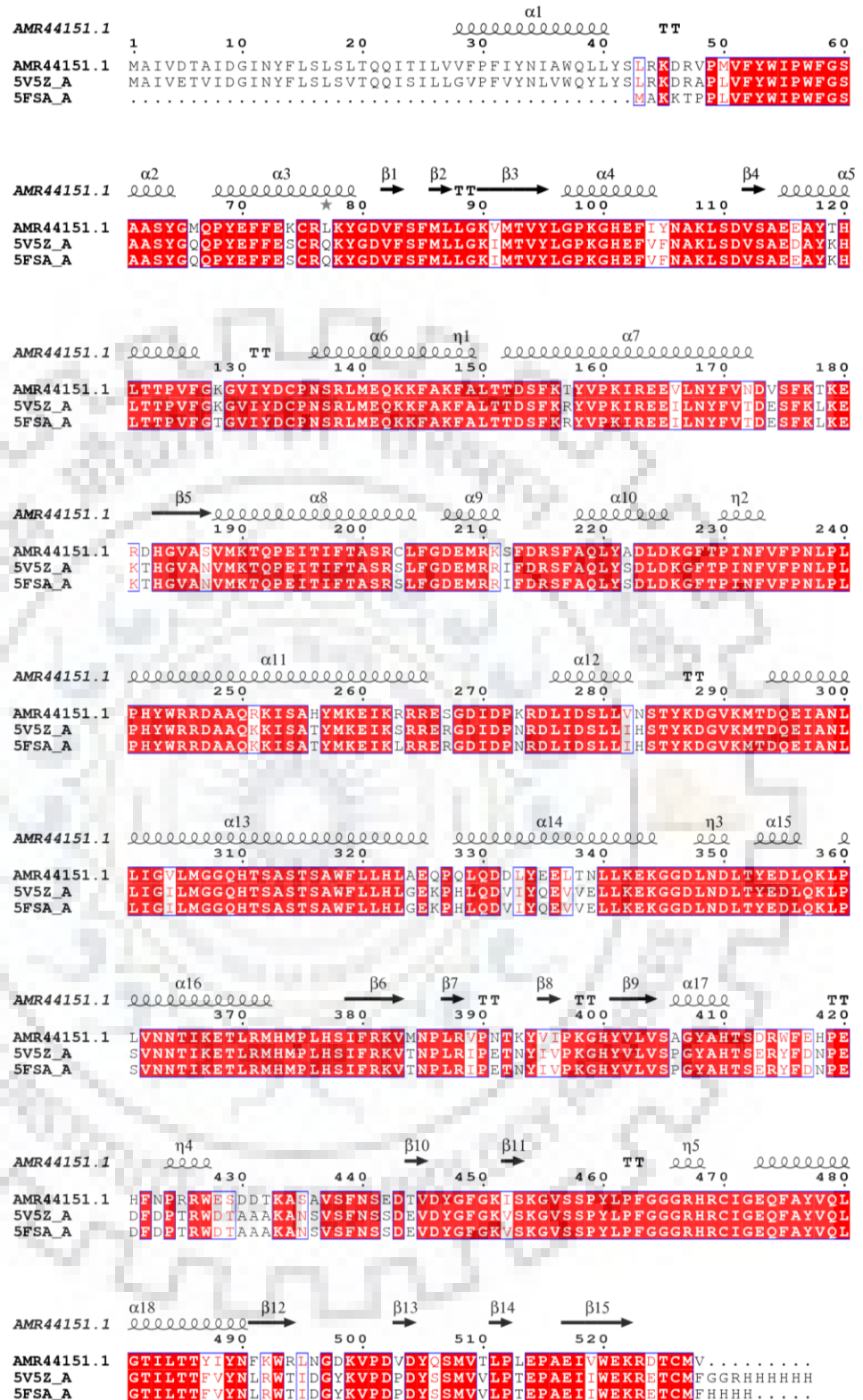
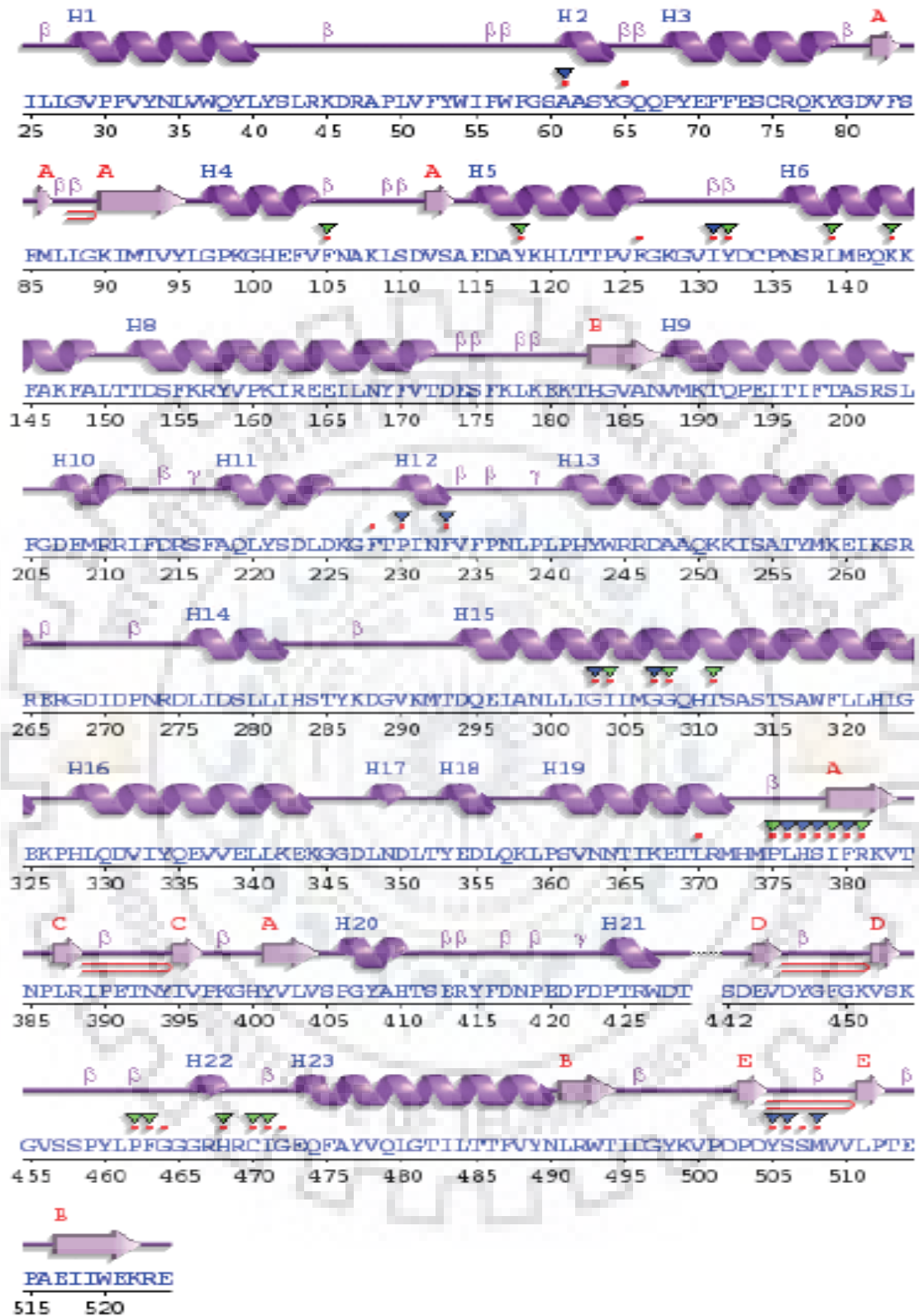


Figure 4.17 Multiple sequence alignment (MSA) of the deduced amino acid sequence of *C. tropicalis* Erg11p with 5V5Z and 5FSA with helix (coil) and β -sheets (arrow)

A



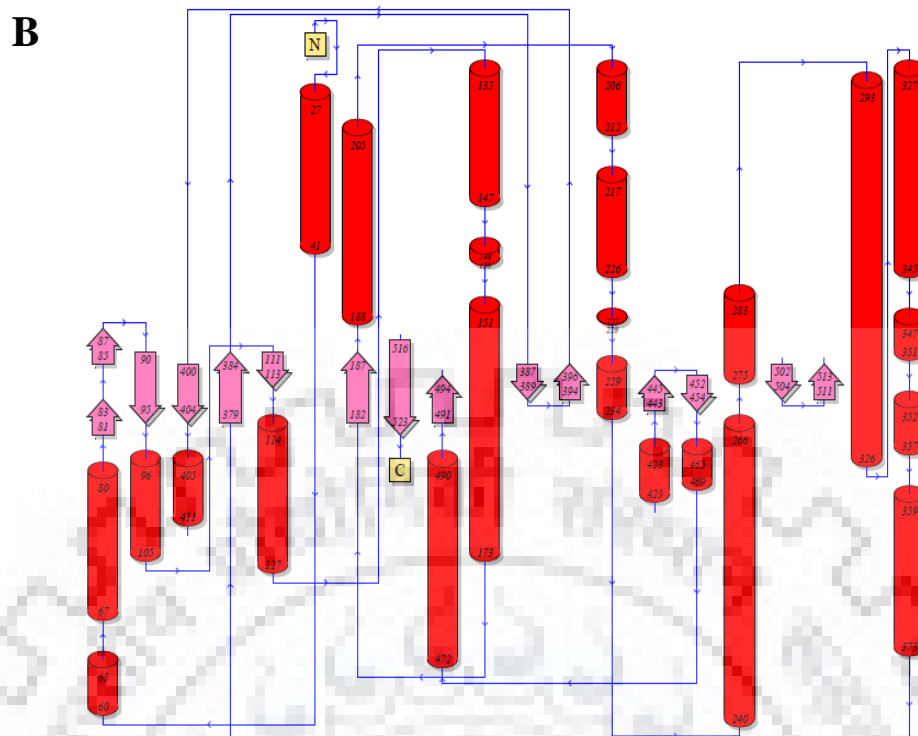


Figure 4.18 Secondary structure of *CtErg11p* predicted using PDBsum represented as **A. cartoon**; primary sequence comprising of helix (ribbon) and β -sheets (solid lines) and **B. graphical image**; helix (pink coloured arrow) and β -sheets (red coloured cylinder)

5V5Z and 5FSA templates have the sequence homology with 83.11% and 83.09% identity, respectively. The resulting .aln file was considered for secondary structure predictions (Table 4.4). The predicted secondary structure through sequence alignment of *CtErg11p* is mostly identical to that of 5V5Z as shown in Figure 4.17. The secondary structure was composed of 5 β -sheets, 4 β -hairpins, 1 β - bulge, 15 β -strands, 23 α -helices, 40-helix interacts, 38 β - turns and 4 γ -turns (Figure 4.18).

Table 4.4 Amino acid residues present in the principal motifs of the protein

| Motifs | Amino acid position |
|--------------------|---------------------|
| a6-1 sheet | 374-381 |
| I helix | 295-317 |
| Meander1 | 131-137 |
| B _{helix} | 120-130 |
| a1-5-B' loop | 114-119 |
| FG loop | 210-260 |
| F helix | 220-231 |
| A6-2 sheet | 507-512 |

4.3.3 Homology modelling and structure validation of *CtErg11p*

The three-dimensional model (3D) of *CtErg11p* was constructed for the ligand support on the basis of the crystallographic structure of *CaErg11p* (5V5Z) as depicted in Figure 4.19. 3D model structures were retrieved, and the quality of each model was analysed using SAVES server. SAVES server was used to determine the stereochemical properties of the modelled *CtErg11p* through ProSA plot, Verify-3D, ERRAT plot and Ramachandran plot (Colovos and Yeates, 1993; Lovell *et al.*, 2003; Wiederstein and Sippl, 2007).

In the PROCHECK result, the generated model was correctly passed and Verify 3D results were revealed. Verify_3D has depicted 95.82% of the residues with an average 3D–1D score greater than 0.2. These results demonstrated that the folding energy patterns of the predicted *CtErg11p* model is in complete agreement and also supported the correctness of the predicted model. Furthermore, ProSA server provides the Z score value which lies within the range of scores generally found for the protein native 3D structures, determined by NMR and X-ray crystallography (Figure 4.20). ProSA gives Z-score of -9.41 and -9 for the *CtErg11p* model and the template 5V5Z, respectively. Z-scores values of all experimentally determined protein chains in the current PDB were used to check whether Z-score of the *CtErg11p* is within the range of scores typically found for similar-sized native proteins.

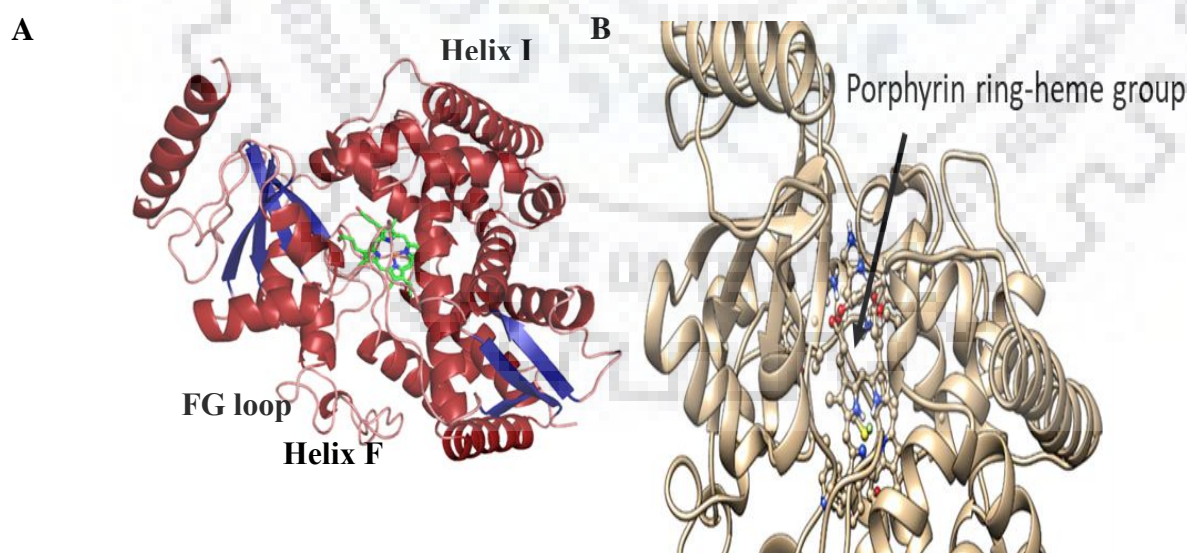


Figure 4.19 A. Molecular model; cartoon representation of the generated 3D model of *CtErg11p*; helices (firebrick coloured), β -strands (deep blue coloured) and connecting loops (salmon coloured) and porphyrin ring (green coloured). B. porphyrin ring of *CtErg11p*

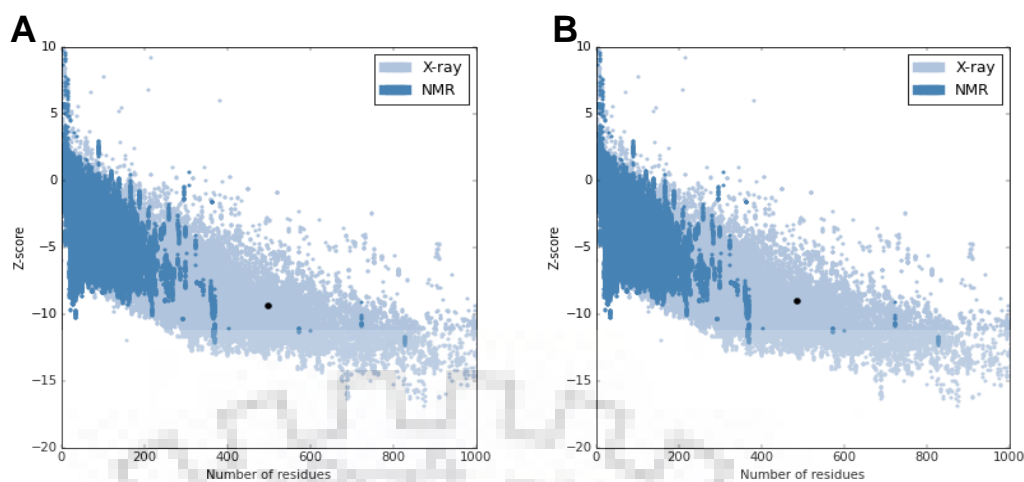


Figure 4.20 ProSA-web Z-scores of the predicted 3D model of *CtErg11p* (black dot) in relation to all proteins deposited in Protein Data Bank determined by X-ray crystallography (light blue) or NMR (dark blue) with respect to their length, the plot showing only chains with less than 1000 residues and a Z-score >10

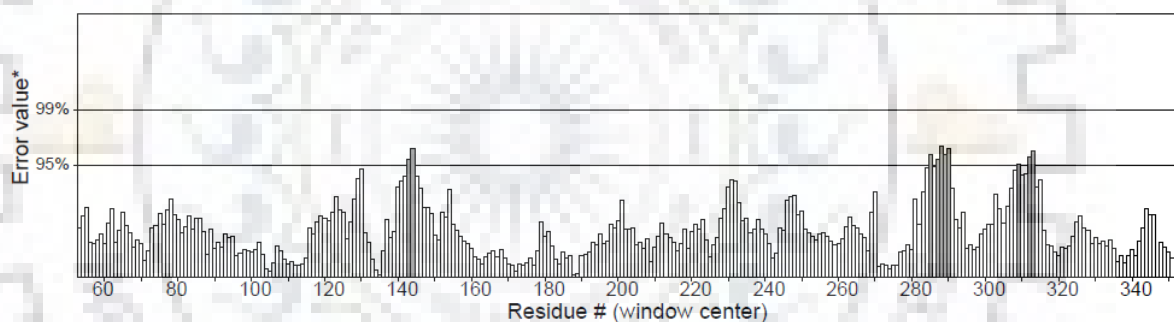


Figure 4.21 ERRAT plot of the *CtErg11p* showing the overall quality factor or ERRAT score of the model

In the ERRAT plot analysis, the overall quality factor value of the *CtErg11p* model was found 94.6% which indicated the good quality of the predicted model, where good resolution structures always show value ~ 95% or higher value (Figure 4.21). Furthermore, Ramachandran plot of the generated 3D model clearly indicated that the backbone dihedral angles Φ and Ψ in the *CtErg11p* model were reasonably accurate (Figure 4.22). The residues in the outliers could be ignored due to their absence near the active site and ligand non-binding. Root mean square deviation (RMSD) was calculated to be 0.11Å between the main chain atom of *CtErg11p* and template (5V5Z) showing close homology and ensured the reliability of the predicted model.

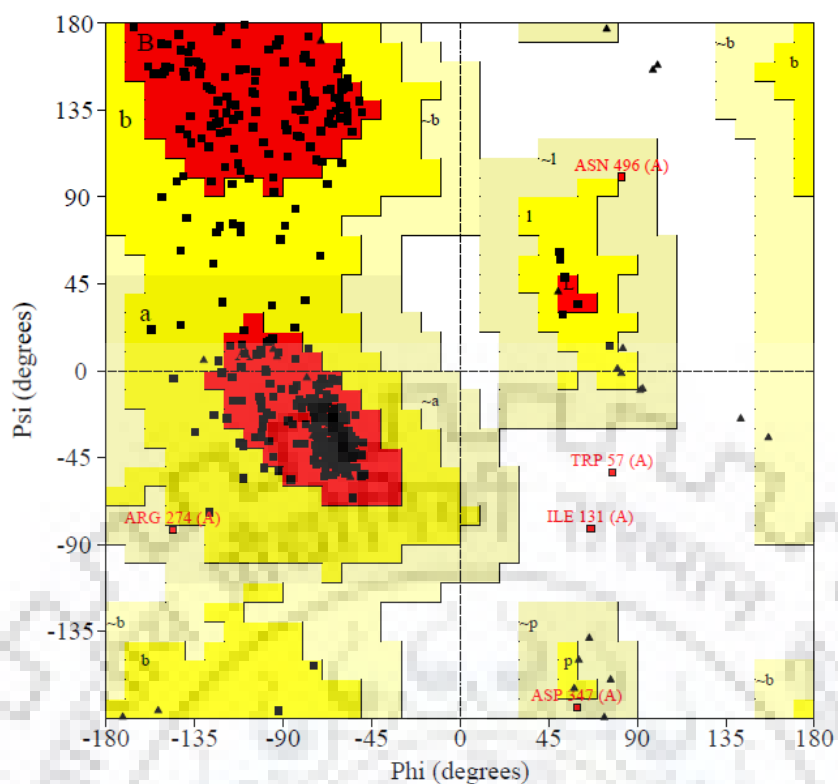


Figure 4.22 Ramachandran plot of the predicted 3D model of *CtErg11p*

Table 4.5 Ramachandran plot statistics I

| | No. of Residues | Percentage |
|--|-----------------|-------------|
| Most favoured regions [A, B, L] | 394 | 89.1% |
| Additional allowed regions [a, b, l, p] | 43 | 9.7% |
| Generously allowed regions [~a, ~b, ~l, ~p] | 3 | 0.7% |
| Disallowed region [XX] | 2 | 0.5% |
| Number of non-glycine and non-proline residue | 442 | 100% |
| End-residues (exclusive Gly and Pro) | 3 | |
| Glycine residues | 29 | |
| Proline residues | 27 | |
| Total no. of residues | 501 | |

Table 4.6 Ramachandran Plot statistics II

| Dihedral angles | |
|-----------------------------------|-------|
| Phi-psi distribution | -0.04 |
| Chi1-chi2 distribution | -0.17 |
| Chi1 only | -0.02 |
| Chi3 & chi4 | -0.51 |
| Omega | -0.88 |
| Main-chain covalent forces | |
| Main-chain bond length | 0.61 |
| Main chain Bond-angles | -0.20 |
| Overall average | -0.14 |

Table 4.7 Main-chain parameters plot statistics

| Stereo-chemical parameters | No. of data points | Parameter value | Typical value | Bandwidth | No. of bandwidths from mean | |
|-----------------------------------|---------------------------|------------------------|----------------------|------------------|------------------------------------|--------|
| Percentage of residues in A, B, L | 442 | 89.1 | 88.2 | 10.0 | 0.1 | Inside |
| Omega angle st dev | 498 | 7.2 | 6.0 | 3.0 | 0.4 | Inside |
| Bad contacts/ 100 residues | 5 | 1.0 | 1.0 | 10.0 | -0.0 | Inside |
| Zeta angle st. dev | 471 | 2.0 | 3.1 | 1.6 | -0.7 | Inside |
| H-bond energy st. dev | 337 | 0.8 | 0.7 | 0.2 | 0.4 | Inside |
| Overall G-factor | 501 | -0.1 | -0.2 | 0.3 | 0.1 | Inside |

The Ramachandran plot was assessed using SAVES server. Ramachandran plot statistics I was based on the analysis of 118 crystal structures of resolution 2.0Å and R factor is greater than 20 (Table 4.5, Table 4.6, Table 4.7). A good quality model would expect to have approximately 90% in the most favoured region (A, B, L) and additional allowed regions.

4.3.4 Specification of the model selected for docking studies

The heme group in the *CtErg11p* model was bound inside the active site of the protein through hydrogen, van der Waal's and hydrophobic linkages. The hydrophobic residues such as PHE-156, LEU-376, LEU-167, VAL-500, PHE-491 and ILE-488 which were present in the core of the protein were associated with the heme ring. The CYS-470 was the principal amino acid residue in the cysteine pocket which provides the axial thiolate ligand for the heme atom. TYR-132, LYS-156, ARG-388 were associated with the heme group through hydrogen bonding, which maintains the spatial arrangement deep in the protein.

4.3.5 Molecular docking studies of *CtErg11p*

The two isomers of citral namely neral and geranial and itraconazole, which were used for molecular docking studies are represented in Figure 4.23. The binding analysis was performed after docking both the ligands to the modelled 3D structure of *CtErg11p*. The isomers represent different bonding associations with amino acid residues of the *CtErg11p*.

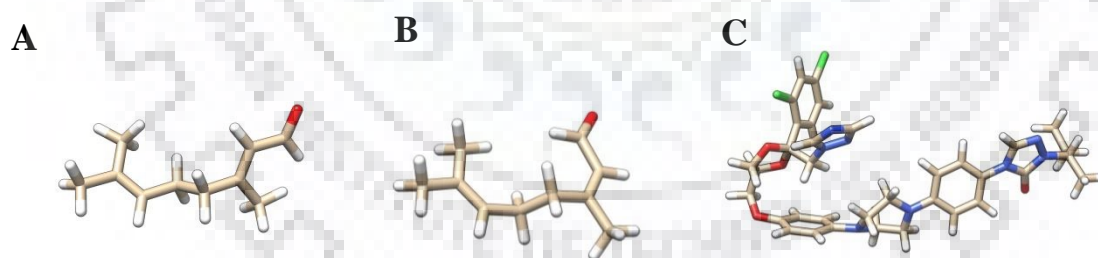


Figure 4.23 Modeled structures of citral isomers: A. geranial and B. neral and C. itraconazole

The binding analysis was performed after docking both the ligands to the modelled 3D structure of *CtErg11p*. The isomers represent different bonding associations with amino acid residues of the *CtErg11p* and are listed in Table 4.8. Neral binds to a total of eight residues yielding binding energy of - 6.3kcal/mol, whereas geranial binds to a total of six amino acid residues and has a binding energy of - 6.7kcal/mol. HEM-601 is bound to both the isomers through Pi-Sigma bond representing polar contacts to fix the isomers inside the binding pocket.

However, amino acid residues: TYR-118, TYR-132 with alkyl bonds; PHE-126, ILE-131 and also TYR-132 with Pi-alkyl bonds ; and THR-122, GLY-303 and LEU-376 with van der Waals forces are bound to neral whereas, TYR-118, LEU-121 and LEU-376 with alkyl bonds; and THR-122, TYR-132 with van der Waals forces to geranial shows close vicinity in 4 Å distance. These binding through hydrophobic interactions with the protein are continuous with the hydrophobic nature of citral.

Table 4.8 Binding parameters of citral in association with *CtErg11p*

| S. No. | Ligands | Binding Energy (kcal/mol) | Interacting Residues |
|--------|-------------------------|---------------------------|---|
| 1. | Itraconazole | -8.5 | van der Waals: TYR-64, GLY-65, LEU-87, TYR-118, LEU-121, THR-122, PHE-233, GLY-307, THR-311, SER378, TYR-505 Carbon Hydrogen Bond: HIS377, SER-507 Alkyl/Pi-Alkyl: PHE-58, ALA-62, PHE-126, ILE-131, PHE-228, PRO-230, LEU-376, MET-508. Amide-Pi/ Pi-Pi: ALA-61, TYR-132, PHE-380 |
| 2. | Neral (cis-citral) | -6.3 | van der Waals: THR-122, GLY-303, LEU-376 Alkyl/ Pi-Alkyl: TYR-118, PHE-126, ILE-131, TYR-132 Pi-Sigma: HEM-601 |
| 3. | Geranial (trans-citral) | -6.7 | van der Waals: THR-122, TYR-132 Alkyl/ Pi-Alkyl: TYR-118, LEU-121, LEU-376 Pi-Sigma: HEM-601 |

The docked models of neral and geranial are illustrated in Figure 4.24. The theoretical interactions of neral and geranial with *CtErg11p* are hydrophobic and can target the azole binding site in a similar way and may alter the ergosterol biosynthesis. Moreover, detailed practical studies are required to modulate the interaction through these compounds or modified forms of citral. This study predicts the probable interactive residues and binding affinities of the isomers of the citral and could help to elaborate on the mechanism of action of citral on *CtErg11p*.

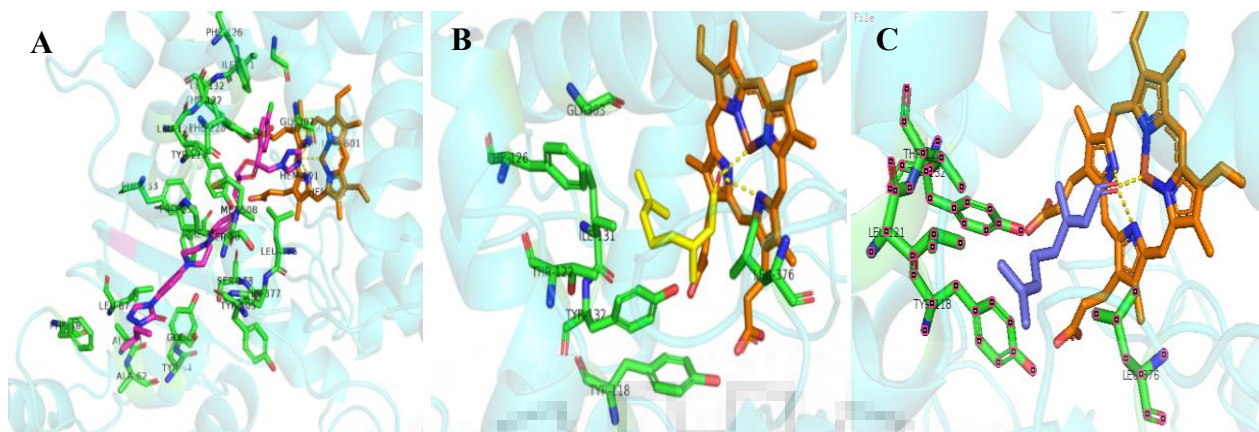


Figure 4.24 Docked poses of the *CtErg11p* A. itraconazole (pink stick); B. neral (yellow stick) and C. geranial (blue stick) depicting interactive amino acid residues (green stick) and porphyrin ring with heme (orange stick)

4.4 Delineating the differentially expressed proteins and variations in extracellular matrix of *C. tropicalis* biofilm in response to citral

In the present work, *C. tropicalis* biofilm has been exposed to the sub-lethal concentration of citral in order to elucidate the differences in the expression of the proteins in the presence of citral to that of the healthy biofilm cells using proteomics approach. Here, the one-dimensional and two-dimensional SDS-PAGE reference map of *C. tropicalis* comprehends the identified proteins which were specifically induced in the presence of citral. The proteins of interest were identified using mass spectrometry. Furthermore, the metabolic profiling of the extracellular matrix of *C. tropicalis* biofilm has also been interpreted with variations during the administration of citral.

4.4.1 Citral induces variation in the proteome of *C. tropicalis* biofilm cells

The differentially expressed proteins in the biofilm during the presence and absence of citral were examined through protein profiling of the whole-cell extract of *C. tropicalis* biofilm. 1D gel images (Figure 4.25) indicated four distinct bands at ~ 85kDa, ~ 45kDa, ~ 37kDa and ~ 21kDa, respectively, in the presence of citral when compared with untreated biofilm. The obtained protein bands were identified by high throughput mass spectrometry.

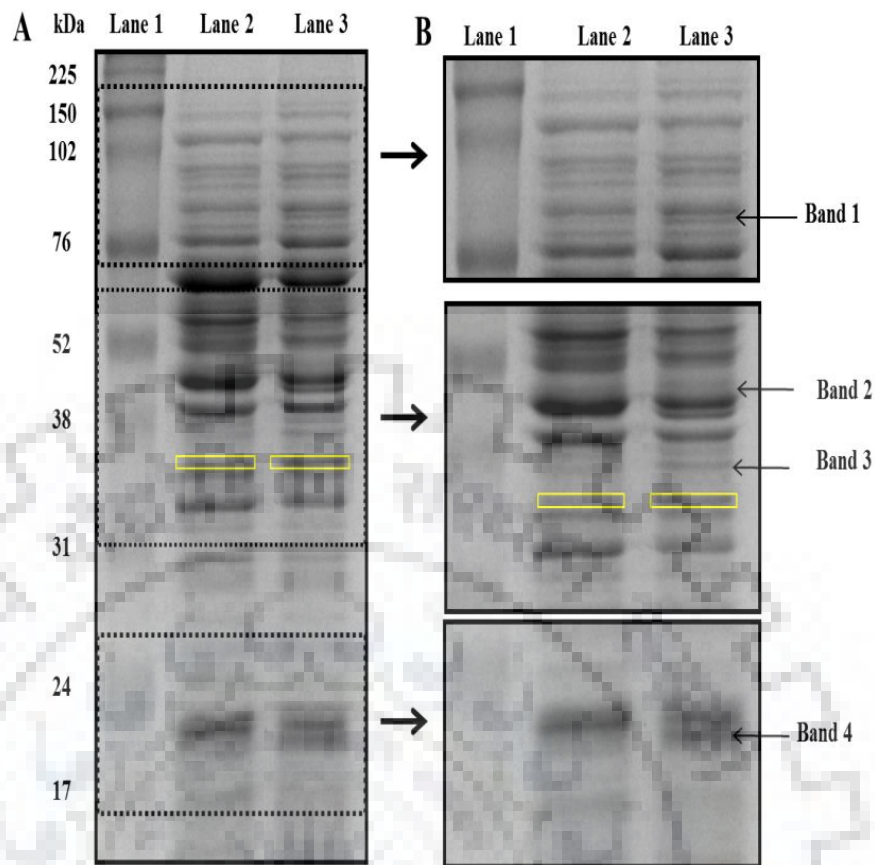


Figure 4.25 *C. tropicalis* proteins resolved using 1D gel electrophoresis. **A.** 1D gel image: Lane 1: molecular weight marker (kDa) as indicated on the left side; Lane 2: control biofilm; and Lane 3: citral (16µg/mL) **B.** zoomed subsets of the dotted box on the gel with distinct bands. Reference protein is shown in the yellow box. Differentially expressed proteins that were identified by mass spectrometer are correspondingly numbered in Table 4.9

Tandem Mass Spectrometry (MS/MS) has identified a reference protein and six proteins with differential expression through MASCOT Server. A reference protein: Glyceraldehyde-3-phosphate dehydrogenase (XP_002551368.1, Mw: 36.209kDa, Score: 87) with three peptides (R.DPINIPWG.K, K.EATYEEICAAV.K, K.IHVFQE.R) was observed with similar expression in both the samples. Additionally, out of the six differentially expressed proteins; two were associated with oxidative stress (Tsa1p, Psa2p), two with amino acid biosynthesis (Met6p, Gln1p), one with heme biosynthesis (Hem13p) and one with glucose metabolism (Eno1p). The differentially expressed proteins and their respective peptides are documented in Table 4.9.

Table 4.9 Summary of the identified proteins using 1D bands with differential expressions in response to citral

| Band No. | Accession No. ^a | Protein ^b | Functional description | Mw (kDa) | Score ^c | Identified peptides ^d |
|----------|----------------------------|--|-------------------------|----------|--------------------|--|
| 1 | XP_002546 146.1 | methionine-synthesizing 5-methyl tetrahydropteroyl triglutamate-homocysteine methyltransferase (Met6p) | amino-acid biosynthesis | 85.69 | 69 | K.GQITAEYEAFINKEIETV VR.F M.VQSSVLGFPR.M R.YVRPPIIVGDVDRPK.A K.YDLAPIDVLFAMGR.G K.AGVDDVIQVDEPALR.E R.SDYLNWAAQSFR.V K.AIENLPVAGFHFDVFR.V |
| 2 | XP_002548 866.1 | enolase1 (Eno1p) | glucose metabolism | 46.984 | 118 | R.SGETEDTFIADLSVGLR.N K.IQIVGDDLTVTNPIR.I K.VNQIGTLTESIQAANDSY AAGWGVMVSHR.S |
| 2 | XP_002545 775.1 | glutamine synthetase (Gln1p) | amino-acid biosynthesis | 42.090 | 60 | K.VLAEYVWIDAEGNTR.S |
| 3 | XP_002548 314.1 | coproporphyrinogen III oxidase (Hem13p) | heme biosynthesis | 37.087 | 41 | M.VSPDQIHDTSFPIRER.M K.GGVNISIVHGKLPQAVT R.M |
| 4 | XP_002547 929.1 | peroxiredoxin (Tsa1p) | oxidative-stress | 21.839 | 76 | R.DYGVLIEEEGVALR.G K.DAQVLFASDSEYTWLA WTNVAR.K |
| 4 | XP_002545 791.1 | protoplast secreted protein 2 precursor (Pst2p) | oxidative-stress | 21.228 | 160 | K.MHAPAKPDYPIASAETLT QYDAFLFGIPTR.F K.IAIEYSTYGHITQLSR.A K.AFALQSNLEEIHGASAYG AGTFAGADGSR.Q K.VAIIISLYHHVAQLAEEE K.K |

^aProtein accession numbers according to NCBI protein database; ^bProtein named and description according to the *C. tropicalis* genomic database (CandidaDB); ^cScore based on NCBI Inr database using the MASCOT server as MALDI-TOF data (p < 0.05); ^dPeptides generated through Tandem Mass Spectrometry

4.4.2 Differential expression of the proteome during citral administration

The difference between the proteome of the biofilm cells of *C. tropicalis* in the untreated and citral-treated conditions has been elaborated. In two-dimensional PAGE, a total of 25 proteins were differentially expressed i.e. up- or downregulated by more than 1.5 times in whole proteome analysis of untreated and citral-treated *C. tropicalis* biofilm as represented in the two-dimensional gel electrophoresis (2DE) reference map (Figure 4.26).

Out of these 25 proteins, three were of amino acid biosynthesis; one nucleotide biosynthesis; three of carbohydrate metabolism; one of sterol biosynthesis; one heme biosynthesis; six involved in energy metabolism; five proteins were related to the oxidative stress and remaining five were belonging to the biofilm formation (Table 4.10).

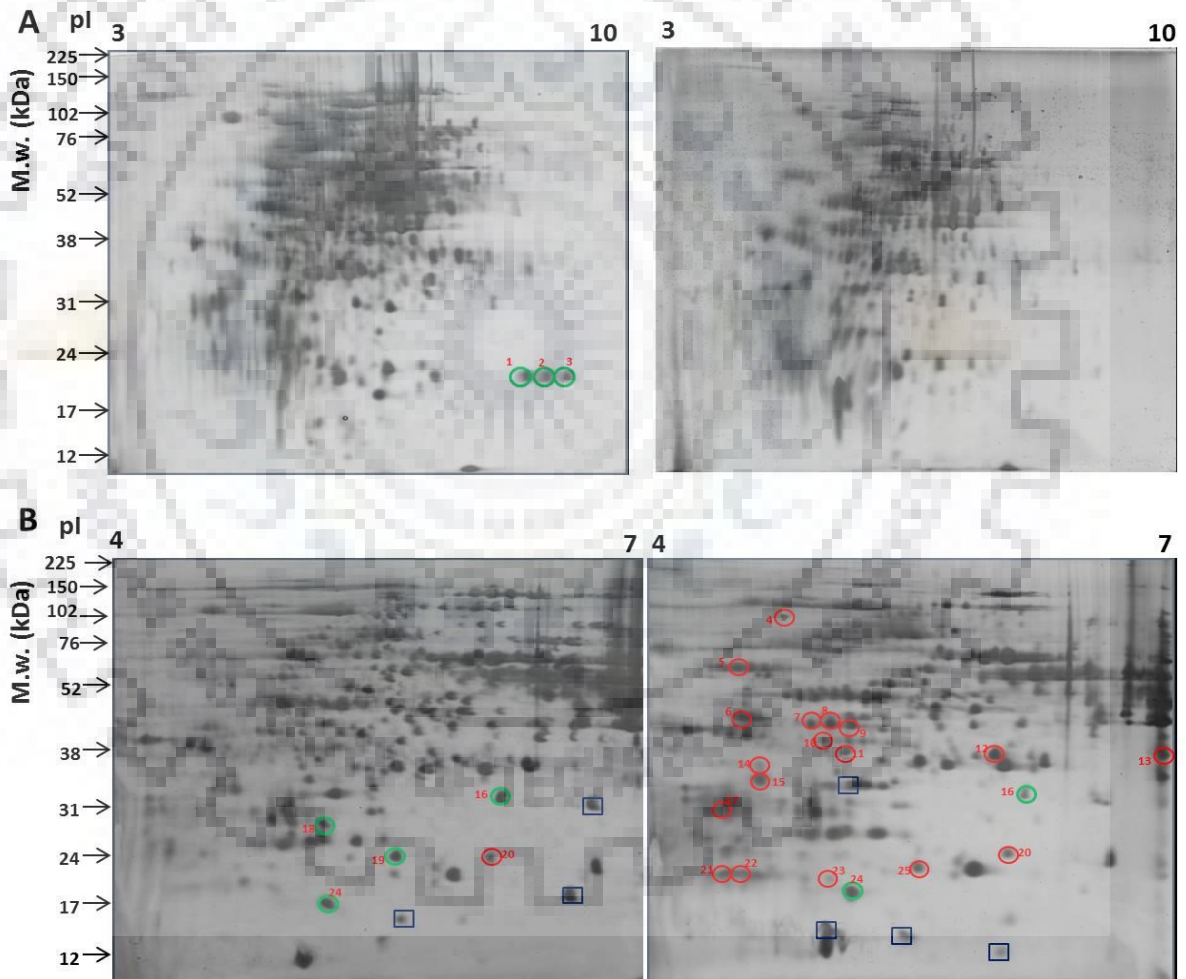


Figure 4.26 Two-dimensional gel electrophoresis (2DE) reference map of citral-induced differentially expressed proteins of *C. tropicalis* biofilm cells. A. Left: control; Right: citral (16µg/mL) and B. Left: control; Right: citral (16µg/mL). Red circled spots; green circled spots and blue squared spots represent up-regulated; down-regulated; and uncharacterized proteins, respectively

Table 4.10 Summary of the identified proteins using 2D spots in differential expressed proteome of *C. tropicalis* biofilm cells in the presence of citral

| Spot No. | Accession No. ^a | Protein ^b | pI | Mw (kDa) | Score ^c | Identified peptides ^d | Fold Change |
|--------------------------------|----------------------------|--|------|----------|--------------------|---|-------------|
| Amino acid biosynthesis | | | | | | | |
| 4 | XP_00254 6146.1 | methionine-synthesizing 5-methyl tetrahydropteroyl triglutamate-homocysteine methyltransferase (Met6p) | 5.43 | 85.69 | 69 | K.GQITAEYEAFINKEIET VVR.F M.VQSSVLGFPR.M R.YVRPPIIVGDVDRPK.A K.YDLAPIDVLFAMGR.G K.AGVDVIQVDEPALR.E R.SDYLNWAAQSFR.V K.AIENLPVAGFHFDFVR. V | 2.91 |
| 9 | XP_00254 5775.1 | glutamine synthetase (Gln1p) | 5.75 | 42.090 | 60 | K.VLAEYVWIDAEGNTR.S | 2.33 |
| 11 | gi:2419529 17 | prephenate dehydratase, putative (Pha2p) | 5.82 | 36.748 | 25 | R.DWFLQTSTPPK.F K.KNTTIVSSIMFTLNHDD PGALCDVLVK.F | 2.45 |
| Nucleotide biosynthesis | | | | | | | |
| 19 | XP_00254 7041.1 | xanthine phosphoribosyltransferase 1 (Xpt1p) | | 24.239 | 149 | K.IKDFKPDIIAIGGGGFIP AR.M | 0.71 |
| Carbohydrate metabolism | | | | | | | |
| 7 | XP_00254 8866.1 | enolase1 (Eno1p) | 5.54 | 46.984 | 118 | R.SGETEDTFIADLSVGLR. N K.IQIVGDDLTVTNPIR.I K.VNQIGTLTESIQAANDS YAAGWGVMVSHR.S | 2.17 |
| 16 | XP_00254 5430.1 | fructose-bisphosphate aldolase (Fba1p) | 6.20 | 33.867 | 87 | K.GVDNKDQAASIAGSIA AAHYIR.S | 1.02 |

| | | | | | | | |
|----------------------------|--------------------|---|------|--------|-----|---|------|
| 18 | XP_00254 6870.1 | phosphoglycerate mutase 1 (Gpm1p) | 5.63 | 27.491 | 58 | R.YNNIDPAVVPLAESLAL VIDR.L R.AIQTANIALSSADQLYV PVKR.S | 0.73 |
| Sterol biosynthesis | | | | | | | |
| 8 | gi:2557301 17 | diphosphomevalonate decarboxylase (Mvd1p/ Erg19p) | 5.68 | 40.704 | 82 | K.KDTPSTTGMQATVQTS DLFAHR.I K.RFEEMK.K K.SFGHVQGWK.K | 2.25 |
| Heme biosynthesis | | | | | | | |
| 10 | XP_00254 8314.1 | coproporphyrinogen III oxidase (Hem13p) | 5.69 | 37.087 | 41 | M.VSPDQIHDTSFPIRER.M K.GGVNISIVHGKLPQAV TR.M | 1.78 |
| Energy metabolism | | | | | | | |
| 1 | gi:4485281 06 | Dnm1 dynamin-related GTPase (Dnm1p) | 9.20 | 19.182 | 74 | K.RITQLSHQTVR.H K.VAKEVCELSLQFPK.A | 0.09 |
| 3 | gi:3442324 04 | DUF1783-domain-containing protein (Coa1p) | 9.65 | 22.309 | 34 | K.YAIVYGIGVTISCVVIFN YEK.T K.TSWPWYIGELNtvrgei DINFAVK.G | 0.11 |
| 6 | gi:2557208 19 | ATP synthase beta chain, mitochondrial precursor (Atp2p) | 4.89 | 44.505 | 107 | K.VVDLLAPYAR.G K.VALVFGQMNEPPGAR. A R.DEEGQDVLLFIDNIFR.F R.FTQAGSEVSALLGR.I | 2.16 |
| 17 | gi:9117813 6 | mitochondrial F-ATPase beta subunit (Atp4p) | 4.88 | 35.971 | 103 | R.IINVVGEPIDDR.G K.VVDLLAPYAR.G K.VALVFGQMNEPPGAR. A R.DEEGQDVLLFIDNIFR.F | 2.89 |
| 21 | gi:2172423 | histidine- | 4.87 | 28.668 | 56 | K.NRANLNNISANHTDVF | 2.97 |

| | | | | | | | |
|----------------------------------|----------------|---|------|--------|-----|--|------|
| 7 | | tRNA synthetase (Hts1p) | | | | VMAFGGGEGWNGFLK.E | |
| 24 | gi:2557231 | nucleoside diphosphate kinase (Ndk1p) | 6.15 | 16.991 | 59 | R.GLISSILGR.F K.LVQPTESLLR.N R.GDFAIDMGR.N K.EINLWFK.K | 1.23 |
| Oxidative stress related | | | | | | | |
| 5 | gi:2236426 | histone deacetylase complex subunit, putative (Hda2p) | 5 | 77.934 | 140 | K.EFFTENYGLNMKEFWN LMHNDR.Q K.LARVDTDLTK.Q K.SLVEMTLHLFSSELLNT VRSK.R | 3.12 |
| 14 | gi:6849165 | potential oxidoreductase (Gre22p) | 5.21 | 37.951 | 70 | K.EVGVFIHSASPIPFATDS VEK.D | 1.63 |
| 22 | XP_002547929.1 | peroxiredoxin (Tsa1p) | 4.94 | 21.839 | 76 | R.DYGVLIIEEGVALR.G K.DAQVLFASDSEYTWL AWTNVAR.K | 1.86 |
| 23 | XP_002545791.1 | protoplast secreted protein 2 precursor (Pst2p) | 5.60 | 21.228 | 160 | K.MHAPAKPDYPIASAET LTQYDAFLFGIPTR.F K.IAIIESTYGHITQLSR.A K.AFALQSNLEEIHGASAY GAGTFAGADGSR.Q K.VAIIISLYHHVAQLAE EEK.K K.AFWDDTTGGLWAQ GAL HGK.Y | 1.59 |
| 25 | KGR03226.1 | Fe-Mn family superoxide dismutase (Sod2p) | 6.49 | 22.678 | 85 | K.LAGIQGSGWAFIVK.N K.ALWNVINWKEAER.R K.NIWNVINWK.T - .HHQTYVNNLNASIEQAV EAK.S | 3.23 |
| Biofilm specific proteins | | | | | | | |
| 2 | gi:2401316 | predicted | 9.49 | 26.851 | 37 | K.SKPKPKSK.A | 0.17 |

| | | | | | | | |
|----|--------------|--------------------------------------|------|--------|----|---|------|
| | 06 | protein | | | | K.QAQPCK.K | |
| 12 | gi:7100149 | alcohol dehydrogenase (Adh1p) | 6.32 | 38.211 | 45 | R.ELCLSLGATDYFDYK.K | 3.20 |
| 13 | gi:2388823 | conserved hypothetical protein | 7.05 | 36.325 | 39 | R.DNTISMEINIDLLVQTL KNFDK.A R.IPVKILR.D | 3.14 |
| 15 | gi:3583692 | zinc metalloproteinase (Ape1p) | 5.46 | 46.376 | 38 | K.NGAGPTILLR.A | 2.79 |
| 20 | XP_002547485 | RAN-like GTP binding protein (Gsp1p) | 6.53 | 24.470 | 27 | R.VCENIPIVLCGNK.V K.NLQYYDISAKSNYNFE KPFLWLAR.K | 2.91 |

^aProtein accession numbers according to NCBI protein database; ^bProtein named and description according to the *C. tropicalis* genomic database (CandidaDB); ^cScore based on NCBI nr database using the MASCOT server as MALDI-TOF data ($p < 0.05$); ^dPeptides generated through Tandem Mass Spectrometry

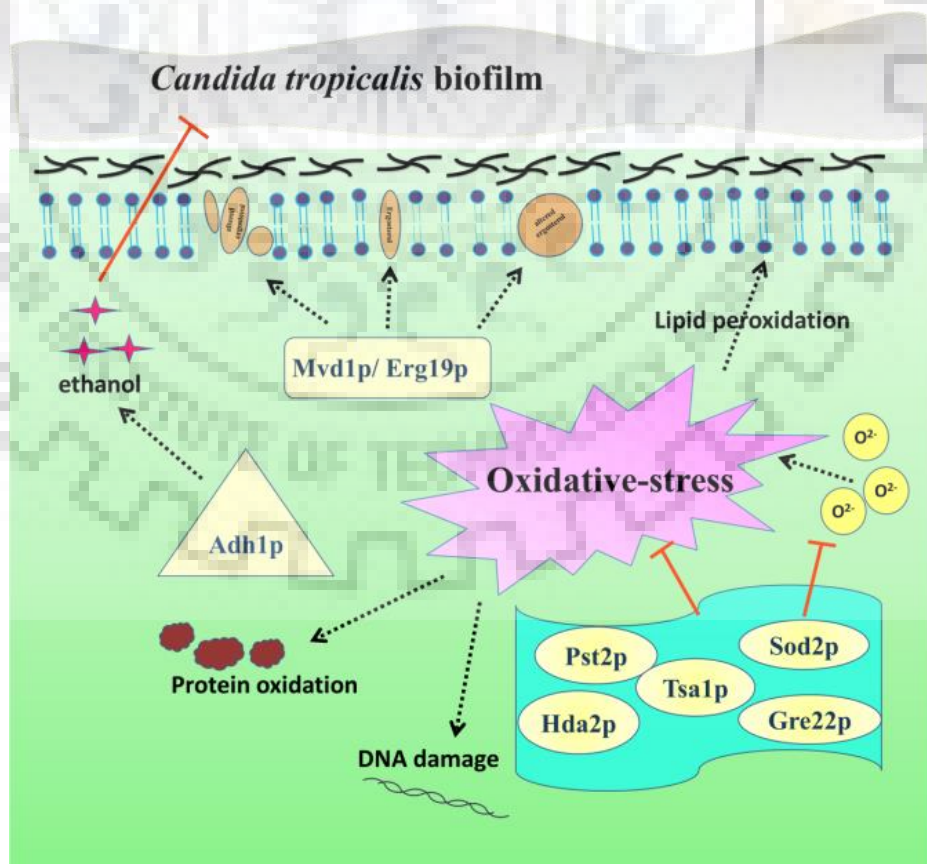


Figure 4.27 Schematic representation of proposed multiple mode of action of citral

In this study, the expression profile of stress-responsive proteins in association with the biofilm during citral administration has revealed differential expression. The action of terpenes is a multifaceted response and leads to cellular damage due to various factors including oxidative damage, upregulation of biofilm-specific proteins, overexpression of ergosterol biosynthesis proteins and variations in amino acid and carbohydrate metabolism etc. (Figure 4.27).

4.4.3 Variations in metabolic profiling of extracellular matrix in the biofilm of *C. tropicalis*

The metabolic alterations were visualized between citral-treated and untreated samples using orthogonal partial least squares-discriminant analysis (OPLS-DA) after mean centering and scaling of unit variance. The variables with variable importance in the projection (VIP) value 1 were considered to be relevant for group discrimination (Sogin *et al.*, 2014). The seven samples each of treated and untreated biofilm cells were selected to establish the OPLS-DA model for the selection of differential metabolites (Figure 4.28).

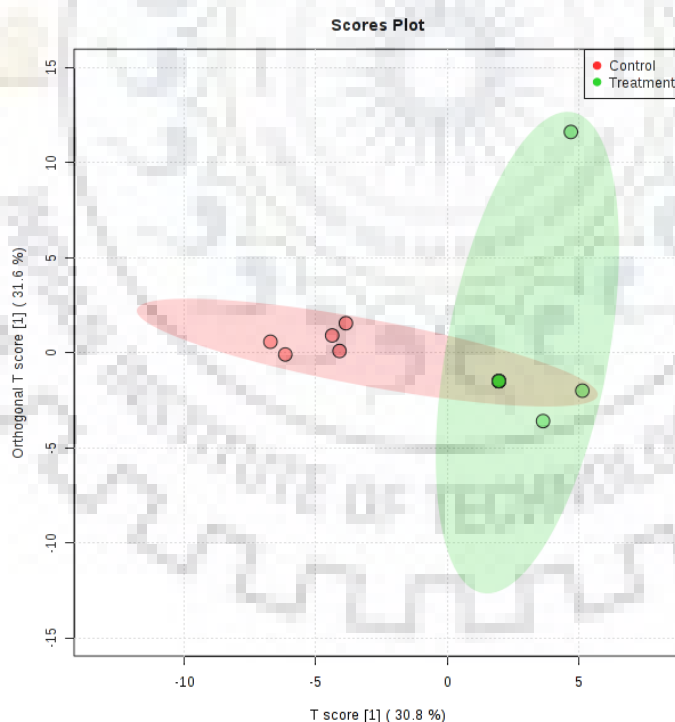


Figure 4.28 OPLS-DA model comparisons between control and citral-treated samples

After normalization of the data, OPLS-DA was performed to identify the metabolites discrimination between the two groups i.e. citral-treated and untreated. The corresponding

up- and down-regulated trend as shown by several peaks which comprehended the selected differential metabolites variation between citral-treated and untreated samples (Figure 4.29).

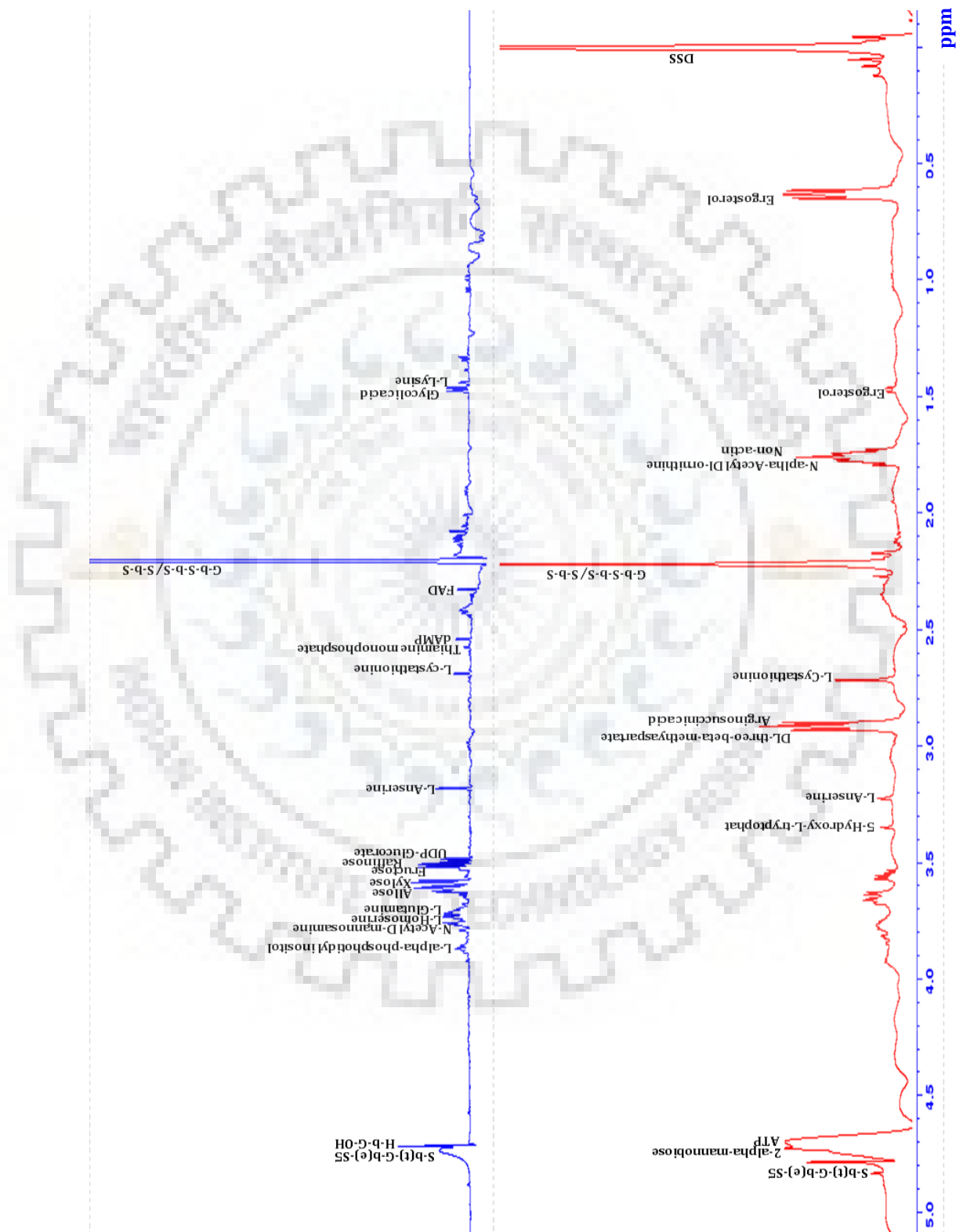


Figure 4.29 1D ¹H-NMR profiling of extracellular matrix in the biofilm of *C. tropicalis*

The metabolic profiling of the extracellular matrices displayed distinguished pattern between the two above-mentioned samples. Here, the cell wall components were found to be increased in the presence of citral. Furthermore, the presence of ergosterol in the spectrum also indicates the damage to the cell membrane and release of ergosterol in the extracellular components. Other metabolites including allose, xylose, fructose, raffinose, L- α -phosphatidyl inositol, N-acetyl-D-mannosamine, L-homoserine, UDP-glucurate, L-anserine, thiamine monophosphate, dAMP, FAD, L-glutamine, L-lysine and glycolic acid were distressed during citral treatment. On the other hand, 2 α -mannobiose, ATP, DL-threo- β -methylaspartate, arginosuccinic acid, L-cystathione, N- α -acetyl DL-ornithine, 5-hydroxy-L-tryptophan and non-actin were increased in the extracellular matrix.



Effective antifungal and antibiofilm activities of terpenes against *C. tropicalis*

The process of biofilm formation includes initial adherence of the planktonic cells to the substratum, followed by micro-colony formation. The increase in the metabolic activity of *Candida* species during proliferation leads to release of the extracellular matrix which finally stabilizes the growth at maturation (Gulati and Nobile, 2016). The mature biofilm is a complex structure composed of densely packed cells surrounded with extracellular matrix acting as the reservoir under stressful conditions and is responsible for the dispersal of cells during infection (Ramage, Vandewalle, *et al.*, 2001; Chandra and Mukherjee, 2015). Here, the activities of selected terpenes were tested against *C. tropicalis* in a rich nutritious medium which mimics a model for clinical settings to determine the effective reduction of the fungal contamination in yeast and biofilm forms. The terpenes were showing deficit in viable cells of *C. tropicalis* upon administration conforming antifungal activity of terpenes. The time-kill curves elucidated the fungicidal activities of these terpenes when compared to the healthy cells along with amphotericin B (Figure 4.4). In literature, essential oils and their active components have established killing effect against fungal pathogens, for instance, carvacrol a major component of essential oils from *Origanum* species, *Satureja hortensis*, *Thymus* species and *Thymbra capitata* exhibit potent fungicidal activity against fluconazole-resistant isolates of *Candida* (Chami *et al.*, 2004; Dalleau *et al.*, 2008).

The cell surface hydrophobicity is also a crucial factor that assists the fungal cells to get aggregated on various surfaces and initiate the formation of biofilm. Therefore, a decrease in it will directly impact the adhesion of fungal cells on biofilm-forming materials. Here in the presence of each terpene, the hydrophobicity was significantly decreased (Table 4.2). Few earlier studies have described a positive correlation between *Candida* adhesion to the plastic surface; denture acrylic surfaces; and buccal epithelial cells and cell surface hydrophobicity (Klotz, Drutz and Zajic, 1985; Samaranayake *et al.*, 1995; Panagoda, Ellepola and Samaranayake, 1998; Ellepola and Samaranayake, 2001). The biomass and formation of the biofilm have also been associated with cell surface hydrophobicity (Blanco *et al.*, 2010; Silva-Dias *et al.*, 2015). Moreover, *C. albicans* can regulate the cell surface hydrophobicity on the basis of its growth phase as well as nutritional and environmental conditions (Hazen, Plotkin and Klimas, 1986). Lately, a variety of natural extracts and their constituents such as human

serum, eugenol, tyrosol, magnolol, and honokiol, *Lactobacillus*-derived biosurfactant, extracts of *Piper betle* and *Brucea javanica* have demonstrated a positive effect on cell surface hydrophobicity, adhesion and biofilm-forming abilities of *Candida* yeast cells (Harun *et al.*, 2013; de Paula *et al.*, 2014; Ding *et al.*, 2014; Ceresa *et al.*, 2015; Monteiro *et al.*, 2015; Sun, Liao and Wang, 2015). Furthermore, the reduction of adhesion and biofilm-forming abilities has also shown a positive correlation for *Candida* species as reported previously (Borecka-Melkusova and Bujdakova, 2008; Harun *et al.*, 2013; de Paula *et al.*, 2014). A significant decrease in the adherence of *Candida* cells to salivary pellicle (up to 86%) and mammalian human larynx epidermoid carcinoma (HEp-2) cells (up to 68.9%) was observed as a result of the decline in the hydrophobicity (> 40%).

Furthermore, citral and thymol have displayed effective antifungal activity in comparison to the other terpenes (Table 4.1). Two and four-fold higher concentrations were needed to eradicate mature biofilm than to inhibit its formation in the case of citral and thymol, respectively. Also, thymol is more effective in the inhibition of biofilm formation and becomes comparatively less effective on preformed biofilm due to the recalcitrant nature of the mature biofilm. Furthermore, the extracellular matrix limits the penetration of antimicrobial agents into the biofilm as suggested by the observed inhibitory concentrations of citral and thymol during biofilm formation. This could be partly because of diffusion limitation affected by the 3-dimensional structure, but primarily due to absorption or reaction of the antimicrobial agent within extracellular matrix components. The results suggested that the absorption and consumption of thymol were more in comparison to citral (Stewart, 2015). This may occur in the surrounding part of the biofilm and thus, neutralizes the more reactive antifungal agent such as thymol in this case. A previous report with the azole group of standard drugs such as fluconazole has demonstrated that the BEC was eight-fold higher than BIC (Sandai *et al.*, 2016).

Scanning electron micrographs of *C. tropicalis* biofilm have demonstrated the presence of dense cells surrounded with extracellular matrix during healthy biofilm formation (Figure 4.2). However, during administration of terpenes the cell surfaces were damaged (Figure 4.5). The deformation of the cells and loss of cell membrane integrity have been reported as the mechanisms of antimicrobial activity (Basak, Das and Das, 2014). These morphological alterations of the cells could be associated with the loss of cell membrane integrity ultimately resulting in cell death (Haque *et al.*, 2016). In FE-SEM (Figure 4.7) and CLSM (Figure 4.8), the indentation of cell surfaces and decreased metabolic activity with lesser viable was clearly observed in the treated biofilm cells when compared to untreated ones. In CLSM, intense green

fluorescence resulting from Con-A binding to cell wall polysaccharides outlined the cell walls of the yeast, whereas red colour appeared due to FUN-1 staining localized in dense aggregates in the cytoplasm of metabolically active cells (Millard *et al.*, 1997). Thus, areas of red fluorescence represent metabolically active cells and green fluorescence indicated cell wall-like polysaccharides, whereas yellow areas represent dual staining (Ceresa *et al.*, 2018). Further, the membrane integrity of the biofilm cells in the presence of citral and thymol were also seemed to be compromised (Figure 4.10). The damage to the cell membrane was also documented as antifungal activity of certain β -lactam substituted polycyclic fused pyrrolidine/pyrrolizidine compound 3 to *C. albicans* cells (Gowri *et al.*, 2016). The fluconazole treatment on fluconazole-sensitive *C. tropicalis* strains with fluconazole caused the yeast cell membrane disruption and the effect was stronger in comparison to the fluconazole-resistant strains as demonstrated by the PI exclusion assay (da Silva *et al.*, 2013). Whereas, the fluconazole-resistant strains when exposed to the azole only did not cause any reduction in the number of viable cells in comparison to the control.

Multifactorial mechanisms of citral and thymol involved in *C. tropicalis* biofilm inhibition

The ergosterol binding assay confirmed that both citral and thymol does not bind directly to the membrane ergosterol content whereas, only thymol affects the cell wall or its assembly as suggested by the sorbitol assay (Table 4.3). However, the content of the ergosterol was constant in the presence of both citral and thymol. Recent studies have revealed that citral inhibits ergosterol biosynthesis in *C. albicans* and *Penicillium italicum* but does not bind directly to the ergosterol. Similarly, recent studies have also documented the non-binding of the citral and thymol to the ergosterol content of the *C. tropicalis* cell membrane in planktonic cells. However, a four-fold increase of ICs was observed with positive control drug amphotericin B, whose interaction with ergosterol is well established (Tao, OuYang and Jia, 2014; Sousa *et al.*, 2016). Cyt450p (cytochrome P-450) dependent enzyme Erg11p (lanosterol 14 α -demethylase) is a specific target to azole resistance and was checked for their involvement in the tolerance of citral and thymol as antifungals. The increment in the expression of the *ERG11/ CYT450* and *CNBI* was observed with the treatment of citral but was not seemed in the presence of thymol (Figure 4.15). Also, *CYT450*, an azole binding protein has shown augmented expression than *ERG11*. The upregulation of *ERG11* has only a minor effect on drug tolerance and does not exceed a factor of three or five. Also, upregulation of *CYT450* in the presence of citral corresponds to the activation of drug tolerance mechanism similar to that of fluconazole (Cowen *et al.*, 2015). Thus, the increased expression of *ERG11* and *CYT450* in

the presence of citral explains the role in the assembly of the cell membrane. *CNBI* (calcineurin regulatory subunit) which is required for cell wall integrity and drug tolerance has also shown increased expression in the presence of citral as well as thymol. *C. tropicalis* calcineurin mutants have shown susceptibility to the antifungal agents targeting the cell wall and serve as a negative regulator of calcium tolerance function. Increased expression of *CNBI* in the presence of thymol indicates its plausible role in cell wall synthesis or assembly, which corroborated the sorbitol assay.

The observed augmentation in the expression of *CYT450* and *ERG11* indicated the role of citral during the process of ergosterol biosynthesis. The protein-ligand binding analysis can provide valuable insights for future studies (Pérot *et al.*, 2010). Therefore to get insights of the interactions of citral with *CtErg11p*, *in silico* docking studies were performed. The overall structure and secondary patterns of *CtErg11p* was observed to be similar to that of *CaErg11p*. The N-terminal domain is membrane-spanning which folds in 16 helices and 12 β -sheets. A conserved insertion in *Erg11p* was also identified in *C. tropicalis* with 6 residue gap between α -4 and beta 3-1 which has also been observed in *C. albicans*, *T. cruzi* and *C. neoformans* (Ji *et al.*, 2000). However, the sequence from Q22 to L40 was predicted to be a strongly hydrophobic helix. Another long insertion inside fungal *Erg11p* was found in α -K and α -L region. However, this insertion was far from the active site and had no influence in the catalysis. Other small insertions were also present on the surface of *Erg11p* which are unlike to cause any perturbation in the protein backbone or folding for its activity. Moreover, the active site of the molecule is packed with heme which was surrounded by the helix I, β -1 and β -6.

CaErg11p has been successfully crystallized and characterized in native form as well as complexed with itraconazole (PDB ID: 5V5Z) and posaconazole (PDB ID: 5FSA), respectively (Hargrove *et al.*, 2017). For the homology modelling, the backbone dihedral angles, phi and psi were reasonable and could be further elaborated in molecular docking simulations. The bond angles and the bond values were not significantly different from those of *C. albicans* and *T. cruzi* but not as *S. cerevisiae* and *C. neoformans* (Lamb, Kelly and Kelly, 1998). The compatibility between environment of the amino acid residues and the sequences are the most important factor for the procedure of model validation. The profile 3D score was found to be 95, compared to the expected high score of 150 and expected low score of 50. The profile 3D score was found to be compatible within the limits of the acceptable value (Sheng *et al.*, 2009). The confirmatory structures were ascertained by constrained and systematic search method. The results of the distances between the citral stereoisomers and amino acid residues of *Erg11p*

were in acceptable range. The best geometrical fit of the inhibitory molecules is a result of the energy difference between the molecules and global minimum energy conservation.

Several residues like GLY-303, HIS-310, helix I are said to be the contact residues within 8 Å distance. These residues play pivotal role in catalysis and substrate specificity. The helix and terminal helix b' forms the variable region which creates a dome over the pocket of active site establishing the size of the active site. In *C. albicans*, the distance of the substrate and the heme group is within 5Å distances which was present in a deep and hydrophobic cleft (Höltje and Fattorusso, 1998). The methyl group of the substrate was bound to the hydrophobic patches composed of amino acids with van der Waals interaction. VAL-04, VAL-125, VAL-130 residues played important role in fitting the substrate inside the pocket. Both neral and geranial showed similar region of binding as the substrate. The region consists of helix I, meander I, b-6-1, and the amino acid made the dome of the cleft. As there were no bulky groups inside the citral molecule, there was less steric hindrance as compared to the azole pharmacophore. The space between the helix I, and the FG Loop in the active site of Erg11p was enough for the accommodation of the compound with lesser binding energies.

The highly conserved region in the Erg11p of *C. tropicalis* were also found to be the conserved residues such as LYS-143, LYS-147, N-terminal end of the helix C, GLU-398, β 2-2, β 1-3, ARG-469, ARG-467 and the identical cysteine residue pocket. This feature has been conserved within various Erg11p (Hargrove *et al.*, 2017). These motifs also play important role in the identification of the reductases. Other electron donors like PHE-463 and HIS-468 also plays a vital role in the redox reaction system. The substrate-binding pocket was present in much interior of *CtErg11p*. A long channel was present making the heme group accessible. The hydrophobic nature of substrate was accessed with the presence of interior hydrophobic amino acids would only be accessed through the long channel as depicted by the model. In the N-terminal region, amino acids LEU-88 and ILE-195 acted as a flap over the channel making the substrate approachable. The hydrophobic structure of the channel helps in the entry of the substrate and its travel towards the active site of the molecule. The surface access channel was composed of the amino acids present in the FG loop.

The substrate-binding site was situated in the interior of Erg11p which was only accessible through a long channel. The modeled structure was found to have striking dissimilarity with the *Cryptococcus neoformans* structure whereas it resembles the structure of *C. albicans* with respect to the long channel 1 and 2 (Ji *et al.*, 2000). Channel 1 was found to be parallel to the heme group whereas channel 2 was found to be perpendicular to the heme group

and the entrance was blocked by the flexible FG loop and helix A. The substrate access channel was also comprised of I helix and BC loop to block the channel. The hydrophobic patches facilitated the interaction of the protein with the heme and the substrate passing through the hydrophobic channel. The hydrophobic patches include helices E, I and L. Helix I comprised of 35 amino acids which includes a region to allow the binding of water and oxygen molecules resulted in the formation of hydrophilic center and hydrophobic N and C terminals. The hydrophilic segment included helix A, beta 1-5, N-terminal residues of helix C and F, C terminal residues of helix G, beta -5, helix G, B, helix J and helix K. These bindings through hydrophobic interactions with Erg11p were continuous with the hydrophobic nature of citral. Numerous studies show that P450s interact with the electron donor at the proximal site through electrostatic linkages (Hargrove *et al.*, 2017).

The acidic partners donate electrons to provide negative charges. P450s are the counter positively charged partners. The sites on the proximal part of the protein which acted as reducing-oxidizing element were in the helices J, C, K, K, β 1-3 β 1-4 β 5 and β 2 and the cysteine residue pocket. GLY-481 located in the cysteine pocket also plays an important role in the arrangement of the heme group, whose substitution, caused fluconazole resistance (Rodero *et al.*, 2003). The side chains of PHE-475 provide the enclosure of the cysteine pocket in combination with ILE-471 and ALA-476. The cysteine pocket serves the purpose of redox reaction of the heme ion in association with the conserved basic residues. LYS-147 and the N-terminal end of the C-helix forms a salt bridge with the D ring of the propionate, while ARG-469 build hydrogen bond with the D ring propionate.

Literature demonstrated that the fluconazole and itraconazole similarly binds to the active site of the molecule, where the halogenated phenyl side groups interact with the same highly hydrophobic amino acid structures in the cleft through various hydrophobic residues. Although, the phenyl groups possessed much steric hindrance in the narrow hydrophobic channel, where the active site is located, the residues CYS-135 and GLY-307 changed the docking ligand conformation by lowering the binding energies. The phenyl ring of the inhibitors in close proximity to the aromatic side chains TYR-132 probably engages a pi-pi stacking interaction between them. The long side chains of itraconazole and ketoconazole create steric hindrances, whereas, due short side chains of fluconazole and small molecule citral showed similar antimicrobial properties as their special orientation is similar in nature. Although citral is smaller than fluconazole, yet the special arrangement of fluconazole is more effective than citral. This can be due to higher hydrophobic interactions with the active site

residues of the protein. Only 2- 3 carbons from both neral and geranial have shown to have hydrogen or van der Waals interaction with the hydrophobic surface of the protein. In azoles, interactions with n1, n3-4, the phenyl rings, and chlorines are responsible for the active site binding and inhibition of the molecule. The chirality of the pharmacophores is also important for the inhibitor binding as in the case of azoles which might also be essential in citral binding.

The unsaturated aldehydic residue of the citral could help in its antifungal activity. Previous studies have revealed that the aldehydic or alcoholic groups in the inhibitors are more potent than the first generation aldehydic compounds without any hydroxyl group at c3 positions (Höltje and Fattorusso, 1998). The length of the Fe-N bond is less than 2.1Å and also the posaconazole complex is 2.2-2.5Å, whereas, the length of citral, heme and the hydrophobic residues were less than 4Å. The basicity is an important criterion for binding and higher selectivity. The FG arm of *C. tropicalis* is found to linger than that of *C. albicans* and *T. cruzi* (Hargrove *et al.*, 2017). The domain lid of FG loop plays a pivotal role in the access of the substrate, whereas the PHE-234 and PHE-213 of the *C. albicans* correspond to PHE-228 of *C. tropicalis*. It has also been proposed that the compact FG loop of the protein is responsible for the inhibition. The most conserved domain being B-helix and the BC loop and these clefts interact with the sterol substrates. Less than 0.5Å distances were found in *albicans/ fumagatis* and *albicans/ cruzi*. The heme group of the protein moiety has weaker hydrogen bond between the porphyrin ring structures and tyrosines of the Erg11p. Also, a reverse proton delivery pairing ASP-225 in helix F and HIS-310 in helix I was noticed. The surface-exposed residues of the salt bridges influence the enzymatic properties of Erg11p. Along with the FG loop and Helix F, Helix I was the core structure of Erg11p. It was situated in the distal part of the heme, parallel to the heme plane carrying two proton delivery residues namely HIS-310 and THR-311 in *C. albicans* (Ji *et al.*, 2000). Similar to the protozoa Erg11p orthologue, I -helix could be considered in whole as disordered loop structure, which is present similarly in the active Erg11p of *C. albicans*, causing drastically weaker inhibition. The helical loop structure is energetically weak and hence is more flexible.

The dominant antifungal mechanism of both citral and thymol was also subjected to the production of reactive oxygen species (ROS) within the cells and under biofilm conditions (Figure 4.11). Mono-terpene phenols such as thymol irrationally increase the production of ROS in *C. albicans*, which negatively affects the antioxidant system (Khan *et al.*, 2015). These ROS productions further corroborate DNA damage and defective repair machinery due to oxidative stress (Chang *et al.*, 2011). During the treatment with citral and thymol, the

antioxidant enzymes were also activated in the *C. tropicalis* biofilm cells as a protective response against enhanced ROS levels to limit the cellular damage (Figure 4.12). During increase in oxidative stress, the adaptations such as activation of antioxidant defence system are required for the cell survival (Chauhan, Latge and Calderon, 2006). Indeed, the equilibrium between ROS generation and antioxidant defenses regulates the extent of oxidative stress and cell survival fate (Belenky and Collins, 2011; Goel and Mishra, 2018). During RT-PCR analysis, the expression of *SOD1* (copper-zinc superoxide dismutase) was significantly augmented in the presence of both citral and thymol, respectively, however, the expression of *KGD2* was only increased in the presence of citral but was not affected when treated with thymol (Figure 4.15). *SOD1* mitigates the generation of ROS by quenching fatal superoxides restoring the redox balance essential for cell survival. Antifungal drugs increase oxidative stress which induces adaptive response resulting in an increased expression of *SOD1* (Linares *et al.*, 2013). *ALD5* (aldehyde dehydrogenase) gene was also overexpressed in the case of both citral and thymol, indicating its role in the tolerance mechanism. *ALD5* is a redox-related gene involved in oxidative stress defence. The overexpression of *ALD5* verifies the activation of the anti-oxidative system to restore the redox balance during the antifungal activity of these agents as in agreement with the previous study of drug resistance (Sun *et al.*, 2013).

Biological macromolecules such as lipids and nucleic acids can be damaged through ROS (Antunes *et al.*, 1996; Stadtman and Berlett, 1997). ROS can react mostly with unsaturated fatty acid chains and few saturated lipids during peroxidation yielding lipid alcohols, lipid peroxides and aldehydic by-products. The MDA results have demonstrated the lipid peroxidation in biofilm cells of *C. tropicalis* similar to those in *S. cerevisiae* (Manfredini *et al.*, 2005). Therefore, the increment of TBARS signifies oxidative stress inside the cells in the presence of citral and thymol (Figure 4.13). The comet tailing in the cells corresponds to the damage to DNA (Figure 4.14). Hence, the biofilm cells when treated with citral and thymol have shown DNA damage making it to be genotoxic. The damage to the DNA including breakage of strands, crosslinking of DNA, incomplete excision repair sites in single strands and alkali-labile sites could be seen through the comet assay which is sensitive, rapid and widely adapted technique to detect DNA damage (Tice *et al.*, 2000; Kirf *et al.*, 2010).

The upregulation of two other genes namely, *ENO1* and *KGD2* were also observed when treated with citral and thymol (Figure 4.15). The null mutants of *ENO1* (enolase), involved in virulence and drug resistance, have demonstrated various degrees of increased antifungal drug susceptibility compared to SC5314 strain, reporting the role of *ENO1* in the

drug resistance mechanism (Ko *et al.*, 2013). However, *KGD2* encodes the dihydro lipoyl lysine-residue succinyltransferase component of 2-oxoglutarate dehydrogenase complex serves as a novel immunogenic protein that could be associated with the pathogenesis of *C. tropicalis* (Lee *et al.*, 2014). Moreover, detailed studies are required to enlighten the alterations in *ENO1* and *KGD2* expression during citral and thymol treatment.

Citral induced differential expression of proteome in *C. tropicalis* biofilm cells

Furthermore, the proteomics approach was utilized to elucidate the proteome expression profile in the presence and absence of citral (Figure 4.26). The use of one and two dimensional gel electrophoresis has successfully been implemented in studying protein profiling during altered conditions (Rogers *et al.*, 2006). The fungal biofilm exhibited changes in the expression of various proteins associated with antifungal tolerance (Li *et al.*, 2015). Biofilm usually develops resistance to cope with the stress caused by antifungal drugs (Cannon *et al.*, 2007). Since very long citral has been found as a good antimicrobial agent against various microorganisms, therefore, researchers are now exploring the effect of citral on other microorganisms and their biofilm. The effect of citral on the biofilm of *C. tropicalis* is still in infancy and has not been studied in detail. However, from previous study it has been demonstrated that the citral has variable effects in comparison to that of thymol against *C. tropicalis* biofilm (Chatrath *et al.*, 2019). In the present study, a total of twenty-five proteins have been identified to be differentially expressed in the presence of citral using mass spectrometry (Table 4.10).

The amino-acid deficiency in stress is vastly documented and relates to the cellular mechanism of survival during drug treatment. Here, methionine-synthesizing 5-methyl tetrahydro-pteroyl triglutamate—homocysteine methyltransferase (Met6p) and glutamine synthetase (Gln1p) were found to be overexpressed in the proteome of citral-treated biofilm along with prephenate dehydratase (Pha2p). The increased expression of these proteins can convince the consumption of their products during stress; therefore, the production was increased at the cellular level. In higher plants, fungi and some prokaryotes represent cobalamin-independent methionine synthases, whereas human methionine synthase is cobalamin-dependent. Therefore, the development of novel antifungal agents which targets cobalamin-independent methionine synthase can be an effective approach for specific inhibition (Suliman, Appling and Robertus, 2007). Similarly, the over-expression of Gln1p in the present study also directs to further elaborate diverse aspects in hindering these pathways.

This stimulates the development of specific novel inhibitory molecules against these enzymes. Several enzymes of these pathways are already proven drug targets (Alcazar-Fuoli, 2016).

Xanthine phosphoribosyl transferase 1 (Xpt1p), required for nucleotide biosynthesis, was depleted in the presence of citral. The involvement of Xpt1p was observed in the salvage synthesis of purine nucleotides i.e. GMP and XMP from precursors, guanine and xanthine, respectively (Guetsova *et al.*, 1999). Such observation reveals the decrease in salvage pathway of purine biosynthesis upon treatment.

The metabolism of carbohydrate is also essential for the survival of the cell during drug treatment. The differential expression of the proteins like Eno1p, Fba1p and Gpm1p during treatment with citral corresponds to their role in drug tolerance. Eno1p is highly recognized antigen found during biofilm formation. In glycolysis, the hydrolysis of fructose-1, 6-bisphosphate into glyceraldehyde-3-phosphate is catalysed by fructose-bisphosphate aldolase (Fba1p) and 3-phosphoglycerate is converted into 2-phosphoglycerate by phosphoglycerate mutase 1 (Gpm1p) following the conversion of 2-phosphoglycerate into phosphoenolpyruvate by enolase1 (Eno1p). The decrease of Fba1p and Gpm1p in the presence of citral indicated lower carbohydrate metabolism whereas, increased Eno1p corresponds to the earlier studies where Eno1 was considered as antigen secreted by biofilm cells (Montagnoli *et al.*, 2004). Citral has induced the expression of Eno1p, indicating its usage for *in vivo* antibody generation during infections in correspondence to the investigations when mice vaccinated with Eno1p of *C. albicans*, showed an increase in antibody resulting in higher survival rate than non-vaccinated mice (Montagnoli *et al.*, 2004). Clinical use of citral in combination with conventional drugs might escalate their efficacy through antibody production by the host cells.

Diphosphomevalonate decarboxylase (Mvd1p/ Erg19p) required in ergosterol biosynthesis was documented to be overexpressed in the presence of citral. Ergosterol is an integral part of the fungal cell membrane and identified drug target for various conventional drugs. The biosynthesis of sterol compounds is necessary for the production of the required amount of ergosterol to sustain the cell membrane. Mvd1p/ Erg19p reportedly contributes to the flux regulation through the mevalonate pathway and shows high transcriptional level in response to the antifungal drugs (Bergès, Guyonnet and Karst, 1997; Bammert and Fostel, 2000). The increment in the expression of Mvd1p/ Erg19p depicted the fast production of the sterol compounds in the presence of citral rather than untreated cells. Similarly, the presence of ergosterol has also been reported in the extracellular matrix of the biofilm indicating damage to the cell membrane and its release in the extracellular matrix. Coproporphyrinogen III oxidase

(Hem13p) involved in heme biosynthesis was also over expressed during citral treatment. A previous study has suggested that heme plays a vital role in sterol biosynthesis and transcriptional regulation of several processes related genes (Parks and Casey, 1995).

Additionally, the requirement of energy has also been augmented during stress when treated with the antifungal agents. Here, the expressions of six proteins which are involved in energy metabolism are found to be differentially expressed. Dnm1p, Coa1p, and Ndk1 were seen to be under expressed, however, Atp2p, Atp4p, and Hts1p were over expressed in the presence of citral as an antifungal agent. Mitochondria are the energy production house of the eukaryotic cell, therefore necessary in energy metabolism. The mitochondrial morphology is controlled by dynamin-related GTPase (Dnm1p) protein. Dnm1p mutations lead to the formation of the mitochondrial compartment into a planar net of interconnected tubules during mitochondrial fission (Bleazard *et al.*, 1999). Cytochrome oxidase (Coa1p) is associated with the cytochrome c oxidase assembly in the inner mitochondrial membrane of yeast. The mutants of Coa1p cells display respiratory deficiency and have a low level of copper in mitochondria (Pierrel *et al.*, 2007). Furthermore, the reduced production of these proteins in the presence of citral indicated damage to the mitochondrial structure negatively affecting its function. Nucleoside diphosphate kinase (Ndk1p) proteins are vital for the division of cell, growth, metabolism of macromolecules and DNA/ RNA synthesis. It forms NTPs energy molecules by phosphorylation of NDPs such as converting ADP into ATP (Jong and Ma, 1991). The depletion in Ndk1p specifies one of the effects when treated with citral.

Whereas, over expression of ATP synthase (Atp2p/ Atp4p) when treated with citral, indicated the efficient combat made by biofilm cells of *C. tropicalis* in order to survive. The mitochondrial F₁-F₀ ATP-synthase complexes catalyze the synthesis of ATP from ADP by acquiring P_i through the electrochemical gradient of the proton. It can also reversibly hydrolyze ATP (Vinogradov, 1999). The increased amount of ATP in the extracellular matrix indicated high energy requirement and consumption of ATP during citral treatment. Histidine-tRNA synthetase (Hts1p) mutants displayed respiratory deficiency as this mitochondrial synthetase is required for mitochondrial DNA synthesis (Natsoulis, Hilger and Fink, 1986).

Oxidative stress tolerance is widely proclaimed process of the cells to deal with an antifungal agent. The upregulation of oxidative stress-responsive protein in the presence of citral indicates the participation of ROS within the biofilm cells. The defense mechanism of biofilm involves increased production of anti-oxidative proteins to resist the damage caused by these ROS. In the presence of citral, Hda2p, Gre22p, Tsa1p, Pst2p and Sod2p were upregulated

in the proteome of *C. tropicalis* biofilm. Historically, histone acetylation (Hda2p) was directly linked to the activation of the transcriptional process; however, recent researches indicated versatile functions by its modifications and catalytic enzymes (Carrozza *et al.*, 2003). The diverse functionality includes DNA repair, gene silencing as well as cellular growth and development due to highly conserved complexes of acetyltransferase. Also, Gre22p, a potential oxidoreductase has been upregulated in the presence of citral. This protein was also documented in higher levels in the azole-resistant clinical isolates of *C. albicans* (Thomas, Bachmann and Lopez-Ribot, 2006). The four eisosome proteins (Pst1p, Pst2p, Pst3p, and Ycp4p) have recently shown novel antioxidant function in *C. albicans* (Li *et al.*, 2015). The protoplast secreted protein 2 (Pst2p) was also identified with overexpression in the presence of citral. Furthermore, the release of ROS in response to stress is checked by antioxidant enzymes. Here, the upregulation of Sod2p, a mitochondrial superoxide dismutase explains the check on these harmful species within *C. tropicalis* biofilm cells (Lambou *et al.*, 2010).

The thioredoxin redox system including peroxiredoxin (Tsa1p) can protect the biofilm cells from ROS playing a vital role to defend the cells against oxidative stress. Tsa1p plays an important role in the survival of cells under oxidative stress created by the host immune response. Shin *et al.* reported that *C. albicans TSA1* mutants show higher levels of H₂O₂ which indicated the Tsa1p ability to neutralize this peroxide (Shin *et al.*, 2005). Tsa1 was also overexpressed in *C. tropicalis* in response to citral suggesting that it may have caused the inhibition of biofilm by developing the oxidative stress condition. Similarly, the upregulation of Tsa1p in *C. glabrata* represented one of the rescue mechanisms during oxidative stress (Rogers *et al.*, 2006). The damage to the DNA is severe to the cell as the cell survival is altered. In *C. albicans*, the upregulation of the various oxidative stress-related proteins has indicated that the higher antifungal tolerance is contributed by anti-oxidant biomarkers including alkyl hydroperoxide reductase, thioredoxin peroxidase, and thioredoxin (Seneviratne *et al.*, 2008).

The biofilm specific proteins are particularly important in the tolerance of antifungal agents. Here, a total of four biofilm specific proteins were found to be overexpressed. The three proteins namely, Adh1p, Ape1p and Gsp1p were upregulated in the presence of citral. Alcohol dehydrogenase (Adh1p) which is widely responsible for the biofilm formation of *Candida*, can also contribute in the negative feedback regulation of the biofilm *in vitro* as well as *in vivo* which restricts the biofilm-forming ability in an ethanol-dependent manner (Mukherjee *et al.*, 2006). This specific protein if overexpressed can produce ethanol in immense amount and ultimately damage the biofilm. In the presence of citral, the upregulation enlightens the use of

citral as formulation supplements of conventional drugs. A study has reported an important role of proteolytic enzymes such as zinc metallopeptidase (Ape1p) in fungal physiology and development. It digests the protein substrates externally by secreted proteases for survival and growth of pathogenic species (Yike, 2011). The overproduction of RAN-like GTP binding protein (Gsp1p) is also related to the switching of the fungal lifestyle. The biofilm form of *C. tropicalis* is different from planktonic yeast and therefore, transforms through Ran-GTPase related switch (Braunwarth *et al.*, 2003). Hence, the biofilm of *C. tropicalis* has augmented production of Gsp1p perhaps to survive in stressed conditions created during treatment with citral.

The extracellular matrices in *C. tropicalis* biofilm majorly consist of hexosamine with lower carbohydrates, proteins and lipids (Al-Fattani and Douglas, 2006). Moreover, the consumption of sugar molecules such as allose, xylose, fructose, raffinose and proteins within the cell could be linked with their diminished presence in the extracellular matrix during citral treatment. Also, the metabolites L-glutamine and L-lysine were decreased in the treated samples and tryptophan hydroxylation as 5-hydroxy-L-tryptophan was observed to be increased indicating the oxidative stress to the biofilm cell in response to citral. Amino acids such as tryptophan can accommodate the ROS under stressful condition by forming hydroxyl moieties (Davies, 2004; Peyrot and Ducrocq, 2008). The reduction in metabolic activity to conserve energy and nutrients can avoid stress and activation of the glyoxylate pathway required for the production of cell-wall carbohydrates and exopolymeric substances (Brown, Odds and Gow, 2007).

Recently, the mannans and its derivative are found to be effective antioxidants that can quench the ROS (Machová and Bystrický, 2013). Mannans are located in the cell wall of *C. tropicalis*. The increased amount of 2-alpha-mannobiose indicated the change in the extracellular composition of the *C. tropicalis* biofilm on citral treatment. Moreover, pentose and hexose sugar molecules are readily consumed during oxidative stress. These are observed to scavenge the free radicals in the cells for their survival (Spencer *et al.*, 2014). Due to the oxidative stress, the viability of the cells seem to be reduced and glycerol accumulation is induced (Gibson *et al.*, 2007).



CONCLUSION AND FUTURE PERSPECTIVES

Despite, *C. tropicalis* and *C. albicans* being different species of the same genus *Candida*, the former does have similar abilities of biofilm formation but varying rates of survival and tolerance against antifungal agents. The biofilm lifestyle, stress response, and antifungal tolerance are directly related to the endurance of the fungus in a hostile milieu. This reflects the probable physiological differences among different species and even strains. The present study concludes the following outcomes:

- Both citral and thymol have shown moderate anti-mycotic activity against *C. tropicalis* and its biofilm.
- Thymol was found to be more effective against *C. tropicalis* planktonic cells and biofilm inhibition than citral.
- During the eradication of the biofilm, thymol represented a relatively low and equivalent activity to that of citral.
- Interestingly, it was observed that citral, as an antifungal agent, targets the cell membrane whereas thymol aims the cell wall. These were evident by the differential expression of *ERG11/CYT450* and *CNBI* against citral and thymol.
- Exogenous ergosterol binding assay directed that the both citral and thymol does not bind directly to the ergosterol, however, sorbitol protection assay concluded that only thymol acts over the cell wall.
- The generation of ROS in the presence of both citral and thymol depicted their role in causing oxidative stress.
- Although both, citral and thymol exert similar antifungal activity yet different actions on the cell wall and membrane depicts their diverse mode of action.
- The molecular interactions between citral, heme group and participating amino acid residues of *CtErg11p* protein have been identified which leads to an understanding of the protein-ligand interaction.
- The varying proteome of *C. tropicalis* biofilm ensures its survival in a hostile environment. A total of twenty-five proteins have been identified to be differentially expressed in the presence of citral. Among these, the following proteins predicted multifactorial response of citral:
 1. The upregulation of *Adh1p* was particularly important as it acts in the inhibition of biofilm through an ethanol-dependent manner.

2. The occurrence of oxidative stress was dealt with the activation of antioxidant system as depicted by the increased expression of anti-oxidative proteins like Sod2p, Pst2p, Hda2p, Gre22p and Tsa1p.
3. The overexpression of Mvd1/ Erg19 also convinces the action of citral at the level of ergosterol biosynthesis.

The outcomes of this study may further be led by taking following points into consideration:

- Citral and thymol being US-FDA approved GRAS molecules can emerge as potent alternatives and implement for prompt clinical trials in nosocomial infection not only to be administered as drugs but could also be used to coat medical devices.
- *In silico* studies of citral-CtErg11p interactions may further be utilized in designing and synthesis of new citral based antifungal analogues for targeting the essential CtErg11p enzyme.
- *CNBI*, a potential gene, could be further exploited to decipher its function during administration of thymol as antifungal agent.
- Other identified proteins such as Pha2p, Hda2p and two uncharacterized biofilm specific proteins are required to study in detail to get insights about their role in the presence of citral.

BIBLIOGRAPHY

1. Agarwal, V., Lal, P., & Pruthi, V. (2010). Effect of plant oils on *Candida albicans*. *Journal of Microbiology, Immunology and Infection*, 43(5), 447-451.
2. Ahmad, A., Khan, A., Kumar, P., Bhatt, R. P., & Manzoor, N. (2011). Antifungal activity of *Coriaria nepalensis* essential oil by disrupting ergosterol biosynthesis and membrane integrity against *Candida*. *Yeast*, 28(8), 611-617.
3. Aiensaard, J., Aiumlamai, S., Aromdee, C., Taweechaisupapong, S., & Khunkitti, W. (2011). The effect of lemongrass oil and its major components on clinical isolate mastitis pathogens and their mechanisms of action on *Staphylococcus aureus* DMST 4745. *Research in Veterinary Science*, 91(3), e31-e37.
4. Al-Fattani, M. A., & Douglas, L. J. (2004). Penetration of *Candida* biofilms by antifungal agents. *Antimicrobial Agents and Chemotherapy*, 48(9), 3291-3297.
5. Al-Fattani, M. A., & Douglas, L. J. (2006). Biofilm matrix of *Candida albicans* and *Candida tropicalis*: chemical composition and role in drug resistance. *Journal of Medical Microbiology*, 55(8), 999-1008.
6. Albuquerque, P., & Casadevall, A. (2012). Quorum sensing in fungi—a review. *Medical Mycology*, 50(4), 337-345.
7. Alcazar-Fuoli, L. (2016). Amino acid biosynthetic pathways as antifungal targets for fungal infections. *Virulence*, 7(4), 376-378.
8. Alem, M. A. S., Oteef, M. D. Y., Flowers, T. H., & Douglas, L. J. (2006). Production of tyrosol by *Candida albicans* biofilms and its role in quorum sensing and biofilm development. *Eukaryotic Cell*, 5(10), 1770-1779.
9. Alnuaimi, A. D., O'Brien-Simpson, N. M., Reynolds, E. C., & McCullough, M. J. (2013). Clinical isolates and laboratory reference *Candida* species and strains have varying abilities to form biofilms. *FEMS Yeast Research*, 13(7), 689-699.
10. Alonso-Monge, R., Román, E., Arana, D. M., Pla, J., & Nombela, C. (2009). Fungi sensing environmental stress. *Clinical Microbiology and Infection*, 15(1), 17-19.
11. Altschul, S. F., Gish, W., Miller, W., Myers, E. W., & Lipman, D. J. (1990). Basic local alignment search tool. *Journal of Molecular Biology*, 215(3), 403-410.
12. Andes, D., Nett, J., Oschel, P., Albrecht, R., Marchillo, K., & Pitula, A. (2004).

Development and characterization of an *in vivo* central venous catheter *Candida albicans* biofilm model. *Infection Immunity*, 72(10), 6023-6031.

13. Andes, D. R. (2017). *In Vivo Candida* Device Biofilm Models. In *Candida albicans: Cellular and Molecular Biology*. Springer, 2nd Edition, 93-113.
14. Aneja, B., Azam, M., Alam, S., Perwez, A., Maguire, R., Yadava, U., Kavanagh, K., Daniliuc, C.G., Rizvi, M.M.A., Haq, Q. M. R., & Abid, M. (2018). Natural product-based 1, 2, 3-triazole/sulfonate analogues as potential chemotherapeutic agents for bacterial infections. *ACS Omega*, 3(6), 6912-6930.
15. Antunes, F., Salvador, A., Marinho, H. S., Alves, R., & Pinto, R. E. (1996). Lipid peroxidation in mitochondrial inner membranes. I. An integrative kinetic model. *Free Radical Biology and Medicine*, 21(7), 917-943.
16. Aspres, N., & Freeman, S. (2003). Predictive testing for irritancy and allergenicity of tea tree oil in normal human subjects. *Exogenous Dermatology*, 2(5), 258-261.
17. Bachmann, S. P., VandeWalle, K., Ramage, G., Patterson, T. F., Wickes, B. L., Graybill, J. R., & López-Ribot, J. L. (2002). *In vitro* activity of caspofungin against *Candida albicans* biofilms. *Antimicrobial Agents and Chemotherapy*, 46(11), 3591-3596.
18. Baillie, G. S., & Douglas, L. J. (2000). Matrix polymers of *Candida* biofilms and their possible role in biofilm resistance to antifungal agents. *Journal of Antimicrobial Chemotherapy*, 46(3), 397-403.
19. Baillie, G. S., & Douglas, L. J. (1999). Role of dimorphism in the development of *Candida albicans* biofilms. *Journal of Medical Microbiology*, 48(7), 671-679.
20. Bammert, G. F., & Fostel, J. M. (2000). Genome-wide expression patterns in *Saccharomyces cerevisiae*: comparison of drug treatments and genetic alterations affecting biosynthesis of ergosterol. *Antimicrobial Agents and Chemotherapy*, 44(5), 1255-1265.
21. Basak, G., Das, D., & Das, N. (2014). Dual role of acidic diacetate sophorolipid as biostabilizer for ZnO nanoparticle synthesis and biofunctionalizing agent against *Salmonella enterica* and *Candida albicans*. *Journal of Microbiology and Biotechnology*, 24(1), 87-96.
22. Baser, K. H. C., Demirci, F., & Bueno, J. (2017). Essential Oils against Microbial Resistance Mechanisms, Challenges and Applications in Drug Discovery. In *Essential*

Oils and Nanotechnology for Treatment of Microbial Diseases, CRC Press, 155-170.

23. Belenky, P., & Collins, J. J. (2011). Antioxidant strategies to tolerate antibiotics. *Science*, 334(6058), 915-916.
24. Belletti, N., Kamdem, S. S., Tabanelli, G., Lanciotti, R., & Gardini, F. (2010). Modeling of combined effects of citral, linalool and β -pinene used against *Saccharomyces cerevisiae* in citrus-based beverages subjected to a mild heat treatment. *International Journal of Food Microbiology*, 136(3), 283-289.
25. Bennett, J. W., & Klich, M. (2003). Mycotoxins. *Clinical Microbiology Reviews*, 16(3), 497-516.
26. Bergamo, V. Z., Donato, R. K., Dalla Lana, D. F., Donato, K. J. Z., Ortega, G. G., Schrekker, H. S., & Fuentefria, A. M. (2015). Imidazolium salts as antifungal agents: Strong antibiofilm activity against multidrug-resistant *Candida tropicalis* isolates. *Letters in Applied Microbiology*, 60(1), 61-71.
27. Bergès, T., Guyonnet, D., & Karst, F. (1997). The *Saccharomyces cerevisiae* mevalonate diphosphate decarboxylase is essential for viability, and a single Leu-to-Pro mutation in a conserved sequence leads to thermosensitivity. *Journal of Bacteriology*, 179(15), 4664-4670.
28. Biswas, S. K., & Chaffin, W. L. (2005). Anaerobic growth of *Candida albicans* does not support biofilm formation under similar conditions used for aerobic biofilm. *Current Microbiology*, 51(2), 100-104.
29. Bizerra, F. C., Nakamura, C. V., De Poersch, C., Estivalet Svidzinski, T. I., Borsato Quesada, R. M., Goldenberg, S., Krieger, M.A., & Yamada-Ogatta, S. F. (2008). Characteristics of biofilm formation by *Candida tropicalis* and antifungal resistance. *FEMS Yeast Research*, 8(3), 440-450.
30. Blanco, M. T., Sacristán, B., Lucio, L., Blanco, J., Pérez-Giraldo, C., & Gómez-García, A. C. (2010). Cell surface hydrophobicity as an indicator of other virulence factors in *Candida albicans*. *Revista Iberoamericana de Micología*, 27(4), 195-199.
31. Bleazard, W., McCaffery, J. M., King, E. J., Bale, S., Mozdy, A., Tieu, Q., Nunnari, J. & Shaw, J. M. (1999). The dynamin-related GTPase Dnm1 regulates mitochondrial fission in yeast. *Nature Cell Biology*, 1(5), 298.
32. Borecka-Melkusova, S., & Bujdakova, H. (2008). Variation of cell surface hydrophobicity and biofilm formation among genotypes of *Candida albicans* and

- Candida dubliniensis* under antifungal treatment. *Canadian Journal of Microbiology*, 54(9), 718-724.
33. Bound, D. J., Murthy, P. S., & Srinivas, P. (2016). 2, 3-Dideoxyglucosides of selected terpene phenols and alcohols as potent antifungal compounds, *Food Chemistry*, 210, 371-380.
34. Božovic, M., Garzoli, S., Sabatino, M., Pepi, F., Baldisserotto, A., Andreotti, E., Romagnoli, C., Mai, A., Manfredini, S., & Ragno, R. (2017). Essential oil extraction, chemical analysis and anti-*candida* activity of *Calamintha nepeta* (L.) Savi subsp. *glandulosa* (Req.) Ball- New approaches. *Molecules*. 22(2), 203.
35. Braunwarth, A., Fromont-Racine, M., Legrain, P., Bischoff, F. R., Gerstberger, T., Hurt, E., & Künzler, M. (2003). Identification and characterization of a novel RanGTP-binding protein in the yeast *Saccharomyces cerevisiae*. *Journal of Biological Chemistry*, 278(17), 15397-15405.
36. Brown, A. J. P., Odds, F. C., & Gow, N. A. R. (2007). Infection-related gene expression in *Candida albicans*. *Current Opinion in Microbiology*, 10(4), 307-313.
37. Brown, J. T., Hegarty, P. K., & Charlwood, B. V. (1987). The toxicity of monoterpenes to plant cell cultures. *Plant Science*, 48(3), 195-201.
38. Brul, S., & Coote, P. (1999). Preservative agents in foods: mode of action and microbial resistance mechanisms. *International Journal of Food Microbiology*, 50(1-2), 1-17.
39. Bruns, S., Seidler, M., Albrecht, D., Salvenmoser, S., Remme, N., Hertweck, C., Brakhage, A.A., Kniemeyer, O., & Müller, F. C. (2010). Functional genomic profiling of *Aspergillus fumigatus* biofilm reveals enhanced production of the mycotoxin gliotoxin. *Proteomics*, 10(17), 3097-3107.
40. Burt, S. A., Ojo-Fakunle, V. T. A., Woertman, J., & Veldhuizen, E. J. A. (2014). The natural antimicrobial carvacrol inhibits quorum sensing in *Chromobacterium violaceum* and reduces bacterial biofilm formation at sub-lethal concentrations. *PloS One*, 9(4), e93414.
41. Calvo, A. M., Wilson, R. A., Bok, J. W., & Keller, N. P. (2002). Relationship between secondary metabolism and fungal development. *Microbiology and Molecular Biology Reviews*, 66(3), 447-459.
42. Cannas, S., Mollicotti, P., Usai, D., Maxia, A., & Zanetti, S. (2014). Antifungal, anti-biofilm and adhesion activity of the essential oil of *Myrtus communis* L. against

- Candida* species. *Natural Product Research*, 28(23), 2173-2177.
43. Cannon, R. D., Lamping, E., Holmes, A. R., Niimi, K., Tanabe, K., Niimi, M., & Monk, B. C. (2007). *Candida albicans* drug resistance - Another way to cope with stress. *Microbiology*, 153(10), 3211-3217.
 44. Carrozza, M. J., Utley, R. T., Workman, J. L., & Cote, J. (2003). The diverse functions of histone acetyltransferase complexes. *TRENDS in Genetics*, 19(6), 321-329.
 45. Castellani, A. (1912). Observations on the fungi found in tropical bronchomycosis. *The Lancet*, 179(4610), 13-15.
 46. Cavalheiro, M., & Teixeira, M. C. (2018). *Candida* biofilms: threats, challenges, and promising strategies. *Frontiers in Medicine*, 5, 28.
 47. Ceresa, C, Tessarolo, F., Caola, I., Nollo, G., Cavallo, M., Rinaldi, M., & Fracchia, L. (2015). Inhibition of *Candida albicans* adhesion on medical-grade silicone by a *Lactobacillus*-derived biosurfactant. *Journal of Applied Microbiology*, 118(5), 1116-1125.
 48. Ceresa, Chiara, Tessarolo, F., Maniglio, D., Caola, I., Nollo, G., Rinaldi, M., & Fracchia, L. (2018). Inhibition of *Candida albicans* biofilm by lipopeptide AC7 coated medical-grade silicone in combination with farnesol. *AIMS Bioengineering*, 5(3), 192-208.
 49. Chakrabarti, A., Sood, P., Rudramurthy, S. M., Chen, S., Kaur, H., Capoor, M., Chhina, D., Rao, R., Eshwara, V.K., & Xess, I. (2015). Incidence, characteristics and outcome of ICU-acquired candidemia in India. *Intensive Care Medicine*, 41(2), 285-295.
 50. Chami, N., Bennis, S., Chami, F., Aboussekhra, A., & Remmal, A. (2005). Study of anticandidal activity of carvacrol and eugenol in vitro and in vivo. *Oral Microbiology and Immunology*, 20(2), 106-111.
 51. Chami, N., Chami, F., Bennis, S., Trouillas, J., & Remmal, A. (2004). Antifungal treatment with carvacrol and eugenol of oral candidiasis in immunosuppressed rats. *Brazilian Journal of Infectious Diseases*, 8(3), 217-226.
 52. Chander, J., Singla, N., Sidhu, S. K., & Gombar, S. (2013). Epidemiology of *Candida* blood stream infections: experience of a tertiary care centre in North India. *The Journal of Infection in Developing Countries*, 7(9), 670-675.
 53. Chandki, R., Banthia, P., & Banthia, R. (2011). Biofilms: A microbial home. *Journal of Indian Society of Periodontology*, 15(2), 111.

54. Chandra, J., Kuhn, D. M., Mukherjee, P. K., Hoyer, L. L., McCormick, T., & Ghannoum, M. A. (2001). Biofilm formation by the fungal pathogen *Candida albicans*: development, architecture, and drug resistance. *Journal of Bacteriology*, 183(18), 5385-5394.
55. Chandra, J., & Mukherjee, P. K. (2015). *Candida* biofilms: development, architecture, and resistance. *Microbiology Spectrum*, 3(4).
56. Chandra, J., Mukherjee, P. K., & Ghannoum, M. A. (2008). *In vitro* growth and analysis of *Candida* biofilms. *Nature Protocols*, 3(12), 1909-1924.
57. Chandra, J., Patel, J. D., Li, J., Zhou, G., Mukherjee, P. K., McCormick, T. S., Anderson, J.M. & Ghannoum, M. A. (2005). Modification of surface properties of biomaterials influences the ability of *Candida albicans* to form biofilms. *Applied and Environmental Microbiology*, 71(12), 8795-8801.
58. Chang, S. T., Chen, P. F., & Chang, S. C. (2001). Antibacterial activity of leaf essential oils and their constituents from *Cinnamomum osmophloeum*. *Journal of Ethnopharmacology*, 77(1), 123-127.
59. Chang, W. Q., Wu, X. Z., Cheng, A. X., Zhang, L., Ji, M., & Lou, H. X. (2011). Retigeric acid B exerts antifungal effect through enhanced reactive oxygen species and decreased cAMP. *Biochimica et Biophysica Acta (BBA)-General Subjects*, 1810(5), 569-576.
60. Chatrath, A., Gangwar, R., Kumari, P., & Prasad, R. (2019). *In vitro* anti-biofilm activities of citral and thymol against *Candida tropicalis*. *Journal of Fungi*, 5(1), 13.
61. Chatrath, A., Kumari, P., Gangwar, R., & Prasad, R. (2018). Investigation of differentially expressed proteins of *Candida tropicalis* biofilm in response to citral. *Journal of Proteomics and Bioinformatics*, 11(2), 57-61.
62. Chauhan, N., Latge, J. P., & Calderone, R. (2006). Signaling and oxidant adaptation in *Candida albicans* and *Aspergillus fumigatus*. *Nature Reviews Microbiology*, 4, 435-444.
63. Chavan, P. S., & Tupe, S. G. (2014). Antifungal activity and mechanism of action of carvacrol and thymol against vineyard and wine spoilage yeasts. *Food Control*, 46, 115-120.
64. Chen, Y. L., Brand, A., Morrison, E. L., Silao, F. G. S., Bigol, U. G., Malbas, F. F., Nett, J.E., Andes, D.R., Solis, N.V., Filler, S. G., & Averette, A. (2011). Calcineurin controls drug tolerance, hyphal growth, and virulence in *Candida dubliniensis*.

Eukaryotic Cell, 10(6), 803-819.

65. Chen, Y., Zeng, H., Tian, J., Ban, X., Ma, B., & Wang, Y. (2013). Antifungal mechanism of essential oil from *Anethum graveolens* seeds against *Candida albicans*. *Journal of Medical Microbiology*, 62(8), 1175-1183
66. Chifiriuc, C., Grumezescu, V., Grumezescu, A. M., Saviuc, C., Lazăr, V., & Andronescu, E. (2012). Hybrid magnetite nanoparticles/*Rosmarinus officinalis* essential oil nanobiosystem with antibiofilm activity. *Nanoscale Research Letters*, 7(1), 209.
67. Cho, J., & Lee, D. G. (2011). The antimicrobial peptide arenicin-1 promotes generation of reactive oxygen species and induction of apoptosis. *Biochimica et Biophysica Acta (BBA)-General Subjects*, 1810(12), 1246-1251.
68. Chouhan, S., Sharma, K., & Guleria, S. (2017). Antimicrobial activity of some essential oils—present status and future perspectives. *Medicines*, 4(3), 58.
69. Chung, P. Y., & Toh, Y. S. (2014). Anti-biofilm agents: recent breakthrough against multi-drug resistant *Staphylococcus aureus*. *Pathogens and Disease*, 70(3), 231-239.
70. Cleveland, A. A., Farley, M. M., Harrison, L. H., Stein, B., Hollick, R., Lockhart, S. R., Magill, S.S., Derado, G., Park, B.J., & Chiller, T. M. (2012). Changes in incidence and antifungal drug resistance in candidemia: results from population-based laboratory surveillance in Atlanta and Baltimore, 2008-2011. *Clinical Infectious Diseases*, 55(10), 1352-1361.
71. CLSI. (2017). Reference method for broth dilution antifungal susceptibility testing of yeasts: approved standard - fourth edition. CLSI document M27. Clinical and Laboratory Standards Institute.
72. Colovos, C., & Yeates, T. O. (1993). ERRAT: an empirical atom-based method for validating protein structures. *Protein Science*, 2(9), 1511-1519.
73. Cotoras, M., Castro, P., Vivanco, H., Melo, R., & Mendoza, L. (2013). Farnesol induces apoptosis-like phenotype in the phytopathogenic fungus *Botrytis cinerea*. *Mycologia*, 105(1), 28-33.
74. Cowen, L. E., Sanglard, D., Howard, S. J., Rogers, P. D., & Perlin, D. S. (2015). Mechanisms of antifungal drug resistance. *Cold Spring Harbor Perspectives in Medicine*, 5(7), a019752.
75. Credito, K., Lin, G., & Appelbaum, P. C. (2007). Activity of daptomycin alone and in combination with rifampin and gentamicin against *Staphylococcus aureus* assessed by

- time-kill methodology. *Antimicrobial Agents and Chemotherapy*, 51(4), 1504-1507.
76. Cromie, G. A., Tan, Z., Hays, M., Sirr, A., Jeffery, E. W., & Dudley, A. M. (2017). Transcriptional profiling of biofilm regulators identified by an overexpression screen in *Saccharomyces cerevisiae*. *G3: Genes, Genomes, Genetics*, 7(8), 2845-2854.
77. Croteau, R. (1977). Site of monoterpene biosynthesis in *Majorana hortensis* leaves. *Plant Physiology*, 59(3), 519-520.
78. Crump, J. A., & Collignon, P. J. (2000). Intravascular catheter-associated infections. *European Journal of Clinical Microbiology and Infectious Diseases*, 19(1), 1-8.
79. da Silva, C. R., de Andrade Neto, J. B., Sidrim, J. J. C., Ângelo, M. R. F., Magalhães, H. I. F., Cavalcanti, B. C., Brilhante, R.S.N., Macedo, D.S., de Moraes, M.O., Lobo, M. D. P., & Grangeiro, T.B. (2013). Synergistic effects of amiodarone and fluconazole on *Candida tropicalis* resistant to fluconazole. *Antimicrobial Agents and Chemotherapy*, 57(4), 1691-1700.
80. da Silva, N. B., de Lucena Rangel, M., Almeida, B. B., de Castro, R. D., Valença, A. M. G., & Cavalcanti, A. L. (2017). Antifungal activity of the essential oil of *Cymbopogon citratus* (DC) Stapf. An *in vitro* study. *Journal of Oral Research*, 6(12), 319-323.
81. Dalleau, S., Cateau, E., Bergès, T., Berjeaud, J. M., & Imbert, C. (2008). *In vitro* activity of terpenes against *Candida* biofilms. *International Journal of Antimicrobial Agents*, 31(6), 572-576.
82. Daniels, K. J., Srikantha, T., Lockhart, S. R., Pujol, C., & Soll, D. R. (2006). Opaque cells signal white cells to form biofilms in *Candida albicans*. *The EMBO Journal*, 25(10), 2240-2252.
83. Davies, M. J. (2004). Reactive species formed on proteins exposed to singlet oxygen. *Photochemical & Photobiological Sciences*, 3(1), 17-25.
84. de Paula, S. B., Bartelli, T. F., Di Raimo, V., Santos, J. P., Morey, A. T., Bosini, M. A., Nakamura, C.V., Yamauchi, L.M., & Yamada-Ogatta, S. F. (2014). Effect of eugenol on cell surface hydrophobicity, adhesion, and biofilm of *Candida tropicalis* and *Candida dubliniensis* isolated from oral cavity of HIV-infected patients. *Evidence-Based Complementary and Alternative Medicine*, 2014, 505204.
85. De Toledo, L. G., Ramos, M. A. D. S., Spósito, L., Castilho, E. M., Pavan, F. R., Lopes, É. D. O., É., Zocolo, G., Silva, F., Soares, T., dos Santos, A. G., & Bauab, T. (2016). Essential oil of *Cymbopogon nardus* (L.) Rendle: A strategy to combat fungal infections

- caused by *Candida* species, *International Journal of Molecular Sciences*, 17(8), 1252.
86. Del Nobile, M. A., Lucera, A., Costa, C., & Conte, A. (2012). Food applications of natural antimicrobial compounds. *Frontiers in Microbiology*, 3, 287.
87. Del Re, B., Sgorbati, B., Miglioli, M., & Palenzona, D. (2000). Adhesion, autoaggregation and hydrophobicity of 13 strains of *Bifidobacterium longum*. *Letters in Applied Microbiology*, 31(6), 438-442.
88. Deorukhkar, S. C., Saini, S., & Mathew, S. (2014). Non-*albicans* *Candida* infection: an emerging threat. *Interdisciplinary Perspectives on Infectious Diseases*, 2014, 615958.
89. Di Pasqua, R., Betts, G., Hoskins, N., Edwards, M., Ercolini, D., & Mauriello, G. (2007). Membrane toxicity of antimicrobial compounds from essential oils. *Journal of Agricultural and Food Chemistry*, 55(12), 4863-4870.
90. Di Santo, R. (2010). Natural products as antifungal agents against clinically relevant pathogens. *Natural Product Reports*, 27(7), 1084-1098.
91. Ding, X., Liu, Z., Su, J., & Yan, D. (2014). Human serum inhibits adhesion and biofilm formation in *Candida albicans*. *BMC Microbiology*, 14(1), 80.
92. Dominguez, E. G., & Andes, D. R. (2017). *Candida* Biofilm Tolerance: Comparison of Planktonic and Biofilm Resistance Mechanisms. In *Candida albicans: Cellular and Molecular Biology*, Springer, 77-92.
93. Donlan, R. M., & Costerton, J. W. (2002). Biofilms: survival mechanisms of clinically relevant microorganisms. *Clinical Microbiology Reviews*, 15(2), 167-193.
94. Dorman, H. J. D., & Deans, S. G. (2000). Antimicrobial agents from plants: antibacterial activity of plant volatile oils. *Journal of Applied Microbiology*, 88(2), 308-316.
95. Douglas, L. J. (2003). *Candida* biofilms and their role in infection. *Trends in Microbiology*, 11(1), 30-36.
96. Ellepola, A. N. B., & Samaranayake, L. P. (2001). Investigative methods for studying the adhesion and cell surface hydrophobicity of *Candida* species: an overview. *Microbial Ecology in Health and Disease*, 13(1), 46-54.
97. Escalante, A., Gattuso, M., Pérez, P., & Zacchino, S. (2008). Evidence for the mechanism of action of the antifungal phytolaccoside B isolated from *Phytolacca tetramera* Hauman. *Journal of Natural Products*, 71(10), 1720-1725.

98. Espina, L., Gelaw, T. K., de Lamo-Castellví, S., Pagán, R., & García-Gonzalo, D. (2013). Mechanism of bacterial inactivation by (+)-limonene and its potential use in food preservation combined processes. *PLoS One*, 8(2), e56769.
99. Eswar, N., Eramian, D., Webb, B., Shen, M.-Y., & Sali, A. (2008). Protein structure modeling with MODELLER. In *Structural proteomics*, Springer, 145-159.
100. Fanning, S., & Mitchell, A. P. (2012). Fungal biofilms. *PLoS Pathogens*, 8(4), e1002585.
101. Freires, I. D. A., Murata, R. M., Furletti, V. F., Sartoratto, A., De Alencar, S. M., Figueira, G. M., de Oliveira Rodrigues, J.A., Duarte, M.C.T., & Rosalen, P. L. (2014). *Coriandrum sativum* L. (Coriander) essential oil: antifungal activity and mode of action on *Candida* spp., and molecular targets affected in human whole-genome expression. *PLoS One*, 9(6), e99086.
102. Friedman, M., Henika, P. R., Mandrell, R. E. (2016). Bactericidal Activities of Plant Essential Oils and Some of Their Isolated Constituents against *Campylobacter jejuni*, *Escherichia coli*, *Listeria monocytogenes*, and *Salmonella enterica*. *Journal of Food Protection*, 65(10), 1545-1560.
103. García-Sánchez, S., Aubert, S., Iraqui, I., Janbon, G., Ghigo, J.-M., & d'Enfert, C. (2004). *Candida albicans* biofilms: a developmental state associated with specific and stable gene expression patterns. *Eukaryotic Cell*, 3(2), 536-545.
104. Georgopapadakou, N. H., & Walsh, T. J. (1994). Human mycoses: drugs and targets for emerging pathogens. *Science-AAAS-Weekly Paper Edition-including Guide to Scientific Information*, 264(5157), 371-373.
105. Ghalem, B. R. (2017). Essential oils as antimicrobial agents against some important plant pathogenic bacteria and fungi. In *Plant-Microbe Interaction: An Approach to Sustainable Agriculture*, Springer, 271-296.
106. Gibson, B. R., Lawrence, S. J., Leclaire, J. P. R., Powell, C. D., & Smart, K. A. (2007). Yeast responses to stresses associated with industrial brewery handling. *FEMS Microbiology Reviews*, 31(5), 535-569.
107. Girish Kumar, C. P., & Menon, T. (2006). Biofilm production by clinical isolates of *Candida* species. *Sabouraudia*, 44(1), 99-101.
108. Goel, S., & Mishra, P. (2018). Thymoquinone inhibits biofilm formation and has selective antibacterial activity due to ROS generation. *Applied Microbiology and*

- Biotechnology*, 102(4), 1955-1967.
109. Gouet, P., Courcelle, E., Stuart, D. I., & M^v© toz, F. (1999). ESPript: analysis of multiple sequence alignments in PostScript. *Bioinformatics* (Oxford, England), 15(4), 305-308.
 110. Gowri, M., Beaula, W. S., Biswal, J., Dhamodharan, P., Saiharish, R., Prasad, S. R., Pitani, R., Kandaswamy, D., Raghunathan, R., Jeyakanthan, J., Rayala, S. K., & Venkatraman, G. (2016). β -lactam substituted polycyclic fused pyrrolidine/pyrrolizidine derivatives eradicate *C. albicans* in an *ex vivo* human dentinal tubule model by inhibiting sterol 14- α demethylase and cAMP pathway. *Biochimica et Biophysica Acta (BBA) - General Subjects*, 1860(4), 636-647.
 111. Guetsova, M. L., Crother, T. R., Taylor, M. W., & Daignan-Fornier, B. (1999). Isolation and characterization of the *Saccharomyces cerevisiae* XPT1 gene encoding xanthine phosphoribosyl transferase. *Journal of Bacteriology*, 181(9), 2984-2986.
 112. Gulati, M., & Nobile, C. J. (2016). *Candida albicans* biofilms: development, regulation, and molecular mechanisms. *Microbes and Infection*, 18(5), 310–321.
 113. Gupta, R. K., & Gupta, P. (2017). Introduction to Opportunistic Infections. In *Pathology of Opportunistic Infections*, Springer, 1-4.
 114. Gusarov, I., Shatalin, K., Starodubtseva, M., & Nudler, E. (2009). Endogenous nitric oxide protects bacteria against a wide spectrum of antibiotics. *Science*, 325(5946), 1380-1384.
 115. Gyawali, R. & Ibrahim, S. A. (2014). Natural products as antimicrobial agents. *Food Control*, 46(2014), 412-429.
 116. Hammer, K. A., Carson, C. F., & Riley, T. V. (2004). Antifungal effects of *Melaleuca alternifolia* (tea tree) oil and its components on *Candida albicans*, *Candida glabrata* and *Saccharomyces cerevisiae*. *Journal of Antimicrobial Chemotherapy*, 53(6), 1081-1085.
 117. Hammer, Kate A, Carson, C. F., Riley, T. V., & Nielsen, J. B. (2006). A review of the toxicity of *Melaleuca alternifolia* (tea tree) oil. *Food and Chemical Toxicology*, 44(5), 616-625.
 118. Haque, E., Irfan, S., Kamil, M., Sheikh, S., Hasan, A., Ahmad, A., Lakshmi, V., Nazir, A., & Mir, S. S. (2016). Terpenoids with antifungal activity trigger mitochondrial dysfunction in *Saccharomyces cerevisiae*. *Microbiology*, 85(4), 436-443.
 119. Haque, F., Alfatah, M., Ganesan, K., & Bhattacharyya, M. S. (2016). Inhibitory effect

of sophorolipid on *Candida albicans* biofilm formation and hyphal growth. *Scientific Reports*, 6, 23575.

120. Hargrove, T. Y., Friggeri, L., Wawrzak, Z., Qi, A., Hoekstra, W. J., Schotzinger, R. J., York, J.D., Guengerich, F.P., & Lepesheva, G. I. (2017). Structural analyses of *Candida albicans* sterol 14 α -demethylase complexed with azole drugs address the molecular basis of azole-mediated inhibition of fungal sterol biosynthesis. *Journal of Biological Chemistry*, 292(16), 6728-6743.
121. Harrison, J. J., Rabiei, M., Turner, R. J., Badry, E. A., Sproule, K. M., & Ceri, H. (2006). Metal resistance in *Candida* biofilms. *FEMS Microbiology Ecology*, 55(3), 479-491.
122. Harrison, J. J., Turner, R. J., & Ceri, H. (2007). A subpopulation of *Candida albicans* and *Candida tropicalis* biofilm cells are highly tolerant to chelating agents. *FEMS Microbiology Letters*, 272(2), 172-181.
123. Harun, W., Aznita, W. H., Jamil, N. A., Jamaludin, N. H., & Nordin, M.-A.-F. (2013). Effect of *Piper betle* and *Brucea javanica* on the differential expression of hyphal wall protein (HWP1) in non-*Candida albicans* *Candida* (NCAC) species. *Evidence-Based Complementary and Alternative Medicine*, 2013, 397268.
124. Hawser, S P, Baillie, G. S., & Douglas, L. J. (1998). Production of extracellular matrix by *Candida albicans* biofilms. *Journal of Medical Microbiology*, 47(3), 253-256.
125. Hawser, Stephen P, & Douglas, L. J. (1995). Resistance of *Candida albicans* biofilms to antifungal agents *in vitro*. *Antimicrobial Agents and Chemotherapy*, 39(9), 2128-2131.
126. Hawser, Stephen P, & Douglas, L. J. (1994). Biofilm formation by *Candida* species on the surface of catheter materials *in vitro*. *Infection and Immunity*, 62(3), 915-921.
127. Hazen, K. C., Plotkin, B. J., & Klimas, D. M. (1986). Influence of growth conditions on cell surface hydrophobicity of *Candida albicans* and *Candida glabrata*. *Infection and Immunity*, 54(1), 269-271.
128. He, M., Du, M., Fan, M., & Bian, Z. (2007). *In vitro* activity of eugenol against *Candida albicans* biofilms. *Mycopathologia*, 163(3), 137-143.
129. Heffner, D. K., & Franklin, W. A. (1978). Endocarditis caused by *Torulopsis glabrata*. *American Journal of Clinical Pathology*, 70(3), 420-423.
130. Heydorn, A., Nielsen, A. T., Hentzer, M., Sternberg, C., Givskov, M., Ersboll, B. K., & Molin, S. (2000). Quantification of biofilm structures by the novel computer program

- COMSTAT. *Microbiology*, 146(10), 2395-2407.
131. Höltje, H. D., & Fattorusso, C. (1998). Construction of a model of the *Candida albicans* lanosterol 14- α -demethylase active site using the homology modelling technique. *Pharmaceutica Acta Helveticae*, 72(5), 271-277.
132. Hossain, F., Follett, P., Vu, K. D., Harich, M., Salmieri, S., & Lacroix, M. (2016). Evidence for synergistic activity of plant-derived essential oils against fungal pathogens of food. *Food Microbiology*, 53, 24-30.
133. Hu, Y., Zhang, J., Kong, W., Zhao, G., & Yang, M. (2017). Mechanisms of antifungal and anti-aflatoxigenic properties of essential oil derived from turmeric (*Curcuma longa* L.) on *Aspergillus flavus*. *Food Chemistry*, 220, 1-8.
134. Husain, F. M., Ahmad, I., Khan, M. S., Ahmad, E., Tahseen, Q., Khan, M. S., & Alshabib, N. A. (2015). Sub-MICs of *Mentha piperita* essential oil and menthol inhibits AHL mediated quorum sensing and biofilm of Gram-negative bacteria. *Frontiers in Microbiology*, 6, 420.
135. Hyldgaard, M., Mygind, T., & Meyer, R. L. (2012). Essential oils in food preservation: mode of action, synergies, and interactions with food matrix components. *Frontiers in Microbiology*, 3, 12.
136. İşcan, G., İşcan, A., & Demirci, F. (2016). Anticandidal effects of thymoquinone: mode of action determined by transmission electron microscopy (TEM). *Natural Product Communications*, 11(7), 1934578X1601100726.
137. Jahanshiri, Z., Shams-Ghahfarokhi, M., Allameh, A., & Razzaghi-Abyaneh, M. (2015). Inhibitory effect of eugenol on aflatoxin B 1 production in *Aspergillus parasiticus* by downregulating the expression of major genes in the toxin biosynthetic pathway. *World Journal of Microbiology and Biotechnology*, 31(7), 1071-1078.
138. Jain, N., Kohli, R., Cook, E., Gialanella, P., Chang, T., & Fries, B. C. (2007). Biofilm formation by and antifungal susceptibility of *Candida* isolates from urine. *Applied and Environmental Microbiology*, 73(6), 1697-1703.
139. James Bound, D., Murthy, P. S., & Srinivas, P. (2016). 2,3-Dideoxyglucosides of selected terpene phenols and alcohols as potent antifungal compounds. *Food Chemistry*, 210, 371-380.
140. Ji, H., Zhang, W., Zhou, Y., Zhang, M., Zhu, J., Song, Y., Lü, J., & Zhu, J. (2000). A three-dimensional model of lanosterol 14 α -demethylase of *Candida albicans* and its

- interaction with azole antifungals. *Journal of Medicinal Chemistry*, 43(13), 2493-2505.
141. Jin, Ye, Samaranayake, L. P., Samaranayake, Y., & Yip, H. K. (2004). Biofilm formation of *Candida albicans* is variably affected by saliva and dietary sugars. *Archives of Oral Biology*, 49(10), 789-798.
142. Jin, Y. Y. H. K., Yip, H. K., Samaranayake, Y. H., Yau, J. Y., & Samaranayake, L. P. (2003). Biofilm-forming ability of *Candida albicans* is unlikely to contribute to high levels of oral yeast carriage in cases of human immunodeficiency virus infection. *Journal of Clinical Microbiology*, 41(7), 2961-2967.
143. Jong, A. Y., & Ma, J. J. (1991). *Saccharomyces cerevisiae* nucleoside-diphosphate kinase: purification, characterization, and substrate specificity. *Archives of Biochemistry and Biophysics*, 291(2), 241-246.
144. Kabsch, W., & Sander, C. (1983). Dictionary of protein secondary structure: pattern recognition of hydrogen-bonded and geometrical features. *Biopolymers: Original Research on Biomolecules*, 22(12), 2577-2637.
145. Kalagatur, N. K., Mudili, V., Siddaiah, C., Gupta, V. K., Natarajan, G., Sreepathi, M. H., Vardhan, B. H., & Putcha, V. L. R. (2015). Antagonistic activity of *Ocimum sanctum* L. essential oil on growth and zearalenone production by *Fusarium graminearum* in maize grains. *Frontiers in Microbiology*, 6, 892.
146. Kalembe, D., & Kunicka, A. (2003). Antibacterial and antifungal properties of essential oils. *Current Medicinal Chemistry*, 10(10), 813-829.
147. Kavooosi, G., & Teixeira da Silva, J. A. (2012). Inhibitory effects of *Zataria multiflora* essential oil and its main components on nitric oxide and hydrogen peroxide production in glucose-stimulated human monocyte. *Food and Chemical Toxicology*, 50(9), 3079-3085.
148. Keren, I., Kaldalu, N., Spoering, A., Wang, Y., & Lewis, K. (2004). Persister cells and tolerance to antimicrobials. *FEMS Microbiology Letters*, 230(1), 13-18.
149. Keren, I., Shah, D., Spoering, A., Kaldalu, N., & Lewis, K. (2004). Specialized persister cells and the mechanism of multidrug tolerance in *Escherichia coli*. *Journal of Bacteriology*, 186(24), 8172-8180.
150. Khan, A., Ahmad, A., Akhtar, F., Yousuf, S., Xess, I., Khan, L. A., & Manzoor, N. (2011). Induction of oxidative stress as a possible mechanism of the antifungal action of three phenylpropanoids. *FEMS Yeast Research*, 11(1), 114-122.

151. Khan, A., Ahmad, A., Khan, L. A., Padoa, C. J., van Vuuren, S., & Manzoor, N. (2015). Effect of two monoterpene phenols on antioxidant defense system in *Candida albicans*. *Microbial Pathogenesis*, 80, 50-56.
152. Khan, M. S. A., & Ahmad, I. (2012). Biofilm inhibition by *Cymbopogon citratus* and *Syzygium aromaticum* essential oils in the strains of *Candida albicans*. *Journal of Ethnopharmacology*, 140(2), 416-423.
153. Kirf, D., Higginbotham, C. L., Rowan, N. J., & Devery, S. M. (2010). Cyto-and genotoxicological assessment and functional characterization of N-vinyl-2-pyrrolidone-acrylic acid-based copolymeric hydrogels with potential for future use in wound healing applications. *Biomedical Materials*, 5(3), 35002.
154. Klotz, S. A., Drutz, D. J., & Zajic, J. E. (1985). Factors governing adherence of *Candida* species to plastic surfaces. *Infection and Immunity*, 50(1), 97-101.
155. Knobloch, K, Weis, N., & Weigand, H. (1986). Mechanism of antimicrobial activity of essential oils. *Planta Medica*, 52(6), 556.
156. Knobloch, Karl, Pauli, A., Iberl, B., Weigand, H., & Weis, N. (1989). Antibacterial and antifungal properties of essential oil components. *Journal of Essential Oil Research*, 1(3), 119-128.
157. Ko, H. C., Hsiao, T. Y., Chen, C. T., & Yang, Y. L. (2013). *Candida albicans* ENO1 null mutants exhibit altered drug susceptibility, hyphal formation, and virulence. *Journal of Microbiology*, 51(3), 345-351.
158. Kohanski, M. A., Dwyer, D. J., Hayete, B., Lawrence, C. A., & Collins, J. J. (2007). A Common Mechanism of Cellular Death Induced by Bactericidal Antibiotics. *Cell*, 130(5), 797-810.
159. Kokkini, S., & Papageorgiou, V. P. (1987). Constituents of essential oils from *Mentha × villosa-nervata* Opiz. growing wild in Greece. *Flavour and Fragrance Journal*, 2(3), 119-121.
160. Kong, W., Huang, C., Chen, Q., Zou, Y., & Zhang, J. (2012). Nitric oxide alleviates heat stress-induced oxidative damage in *Pleurotus eryngii* var. *tuoliensis*. *Fungal Genetics and Biology*, 49(1), 15-20.
161. Kothavade, R. J., Kura, M. M., Valand, A. G., & Panthaki, M. H. (2010). *Candida tropicalis*: its prevalence, pathogenicity and increasing resistance to fluconazole. *Journal of Medical Microbiology*, 59(8), 873-880.

162. Krasner, R. I. (2002). *The microbial challenge: human-microbe interactions*. ASM Press.
163. Kuhn, D. M., George, T., Chandra, J., Mukherjee, P. K., & Ghannoum, M. A. (2002). Antifungal susceptibility of *Candida biofilms*: unique efficacy of amphotericin B lipid formulations and echinocandins. *Antimicrobial Agents and Chemotherapy*, 46(6), 1773-1780.
164. Kurtzman, C., Fell, J. W., & Boekhout, T. (2011). *The yeasts: a taxonomic study*. Elsevier.
165. LaFleur, M. D., Kumamoto, C. A., & Lewis, K. (2006). *Candida albicans* biofilms produce antifungal-tolerant persister cells. *Antimicrobial Agents and Chemotherapy*, 50(11), 3839-3846.
166. Lamb, D. C., Kelly, D. E., & Kelly, S. L. (1998). Molecular diversity of sterol 14 α -demethylase substrates in plants, fungi and humans. *FEBS Letters*, 425(2), 263-265.
167. Lambou, K., Lamarre, C., Beau, R., Dufour, N., & Latge, J. (2010). Functional analysis of the superoxide dismutase family in *Aspergillus fumigatus*. *Molecular Microbiology*, 75(4), 910-923.
168. Lang, G., Buchbauer, G. (2012). A review on recent research results (2008–2010) on essential oils as antimicrobials and antifungals. A review. *Flavour and Fragrance Journal*, 27(1), 13-39.
169. Laskowski, R. A., Hutchinson, E. G., Michie, A. D., Wallace, A. C., Jones, M. L., & Thornton, J. M. (1997). PDBsum: a Web-based database of summaries and analyses of all PDB structures. *Trends in Biochemical Sciences*, 22(12), 488-490.
170. Laverty, G., Gorman, S. P., & Gilmore, B. F. (2015). Biofilms and implant-associated infections. *Biomaterial and Medical Device Associated Infection*, 19-45.
171. Lee, P. Y., Gam, L. H., Yong, V. C., Rosli, R., Ng, K. P., & Chong, P. P. (2014). Immunoproteomic analysis of antibody response to cell wall-associated proteins of *Candida tropicalis*. *Journal of Applied Microbiology*, 117(3), 854-865.
172. Lee, Y. S., Kim, J., Shin, S. C., Lee, S. G., & Park, I. K. (2008). Antifungal activity of Myrtaceae essential oils and their components against three phytopathogenic fungi. *Flavour and Fragrance Journal*, 23(1), 23-28.
173. Leite, M. C. A., De Brito Bezerra, A. P., De Sousa, J. P., & De Oliveira Lima, E. (2015). Investigating the antifungal activity and mechanism(s) of geraniol against

- Candida albicans* strains. *Medical Mycology*, 53(3), 275-284.
174. Lesage, G., & Bussey, H. (2006). Cell wall assembly in *Saccharomyces cerevisiae*. *Microbiology and Molecular Biology Reviews*, 70(2), 317-343.
175. Lessing, F., Kniemeyer, O., Wozniok, I., Loeffler, J., Kurzai, O., Haertl, A., & Brakhage, A. A. (2007). The *Aspergillus fumigatus* transcriptional regulator AfYap1 represents the major regulator for defense against reactive oxygen intermediates but is dispensable for pathogenicity in an intranasal mouse infection model. *Eukaryotic Cell*, 6(12), 2290-2302.
176. Lewis, J. K., Wei, J., & Siuzdak, G. (2006). Matrix-Assisted Laser Desorption/Ionization Mass Spectrometry in Peptide and Protein Analysis. In *Encyclopedia of Analytical Chemistry: Applications, Theory and Instrumentation*, Wiley.
177. Lewis, K. (2005). Persister cells and the riddle of biofilm survival. *Biochemistry*, 70(2), 267-274.
178. Lewis, K. (2010). Persister cells. *Annual Review of Microbiology*, 64, 357-372.
179. Li, L., Naseem, S., Sharma, S., & Konopka, J. B. (2015). Flavodoxin-like proteins protect *Candida albicans* from oxidative stress and promote virulence. *PLoS Pathogens*, 11(9), e1005147.
180. Li, P., Seneviratne, C. J., Alpi, E., Vizcaino, J. A., & Jin, L. (2015). Delicate metabolic control and coordinated stress response critically determine antifungal tolerance of *Candida albicans* biofilm persisters. *Antimicrobial Agents and Chemotherapy*, 59(10), 6101-6112.
181. Linares, C. E. B., Giacomelli, S. R., Altenhofen, D., Alves, S. H., Morsch, V. M., & Schetinger, M. R. C. (2013). Fluconazole and amphotericin-B resistance are associated with increased catalase and superoxide dismutase activity in *Candida albicans* and *Candida dubliniensis*. *Revista Da Sociedade Brasileira de Medicina Tropical*, 46(6), 752-758.
182. Lindon, J. C., Nicholson, J. K., Holmes, E., & Everett, J. R. (2000). Metabonomics: metabolic processes studied by NMR spectroscopy of biofluids. *Concepts in Magnetic Resonance: An Educational Journal*, 12(5), 289-320.
183. Liu, R. H., Shang, Z. C., Li, T. X., Yang, M. H., Kong, L. Y. (2017). *In vitro* antibiofilm activity of Eucarobustol E against *Candida albicans*, *Antimicrobial agents and chemotherapy*, 61(8), 02707-16.

184. Liu, X., Ma, Z., Zhang, J., & Yang, L. (2017). Antifungal compounds against *Candida* infections from traditional Chinese medicine. *BioMed Research International*, 2017, 4614183.
185. Lovell, S. C., Davis, I. W., Arendall III, W. B., De Bakker, P. I. W., Word, J. M., Prisant, M. G., Richardson, J.S., & Richardson, D. C. (2003). Structure validation by $\text{C}\alpha$ geometry: ϕ , ψ and $\text{C}\beta$ deviation. *Proteins: Structure, Function, and Bioinformatics*, 50(3), 437-450.
186. Low, C. Y., & Rotstein, C. (2011). Emerging fungal infections in immunocompromised patients. *F1000 Medicine Reports*, 3, 14.
187. Lupetti, A., Danesi, R., Campa, M., Del Tacca, M., & Kelly, S. (2002). Molecular basis of resistance to azole antifungals. *Trends in Molecular Medicine*, 8(2), 76-81.
188. Lynch, A. S., & Robertson, G. T. (2008). Bacterial and Fungal Biofilm Infections. *Annual Review of Medicine*, 59, 415-428.
189. Machová, E., & Bystrický, S. (2013). Antioxidant capacities of mannans and glucans are related to their susceptibility of free radical degradation. *International Journal of Biological Macromolecules*, 61, 308-311.
190. Manfredini, V., Martins, V. D., Peralba, M. do C. R., & Benfato, M. S. (2005). Adaptive response to enhanced basal oxidative damage in sod mutants from *Saccharomyces cerevisiae*. *Molecular and Cellular Biochemistry*, 276(1-2), 175-181.
191. Marchese, A., Orhan, I. E., Daglia, M., Barbieri, R., Di Lorenzo, A., Nabavi, S. F., Gortzi, O., Izadi, M., & Nabavi, S. M. (2016). Antibacterial and antifungal activities of thymol: a brief review of the literature. *Food Chemistry*, 210, 402-414.
192. Martel, C. M., Parker, J. E., Bader, O., Weig, M., Gross, U., Warrillow, A. G. S., Kelly, D.E., & Kelly, S. L. (2010). A clinical isolate of *Candida albicans* with mutations in ERG11 (encoding sterol 14α -demethylase) and ERG5 (encoding C22 desaturase) is cross resistant to azoles and amphotericin B. *Antimicrobial Agents and Chemotherapy*, 54(9), 3578-3583.
193. Maurya, I. K., Thota, C. K., Sharma, J., Tupe, S. G., Chaudhary, P., Singh, M. K., Thakur, I.S., Deshpande, M., Prasad, R., & Chauhan, V. S. (2013). Mechanism of action of novel synthetic dodecapeptides against *Candida albicans*. *Biochimica et Biophysica Acta (BBA)-General Subjects*, 1830(11), 5193-5203.
194. Merks, I. J. M., & Svendsen, A. B. (1989). Occurrence and possible role of glycosidic

- bound eugenol and 2-methoxy-4-vinylphenol in the lignin biosynthesis of some Lamiaceae. *Planta Medica*, 55(1), 88-89.
195. Mesa-Arango, A. C., Trevijano-Contador, N., Román, E., Sánchez-Fresneda, R., Casas, C., Herrero, E., Argüelles, J.C., Pla, J., Cuenca-Estrella, M., & Zaragoza, O., (2014). The production of reactive oxygen species is an universal action mechanism of Amphotericin B against pathogenic yeasts and contributes to the fungicidal effect of this drug. *Antimicrobial Agents and Chemotherapy*, 58(4), 6627-6638.
196. Millard, P. J., Roth, B. L., Thi, H. P., Yue, S. T., & Haugland, R. P. (1997). Development of the FUN-1 family of fluorescent probes for vacuole labeling and viability testing of yeasts. *Applied and Environmental Microbiology*, 63(7), 2897-2905.
197. Miloshev, G., Mihaylov, I., & Anachkova, B. (2002). Application of the single cell gel electrophoresis on yeast cells. *Mutation Research/Genetic Toxicology and Environmental Mutagenesis*, 513(1-2), 69-74.
198. Khan, M. S. A., Ahmad, I., & Cameotra, S. S. (2013). Phenyl aldehyde and propanoids exert multiple sites of action towards cell membrane and cell wall targeting ergosterol in *Candida albicans*. *AMB Express*, 3(1), 54.
199. Montagnoli, C., Sandini, S., Bacci, A., Romani, L., & La Valle, R. (2004). Immunogenicity and protective effect of recombinant enolase of *Candida albicans* in a murine model of systemic candidiasis. *Medical Mycology*, 42(4), 319-324.
200. Monteiro, D. R., Feresin, L. P., Arias, L. S., Barão, V. A. R., Barbosa, D. B., & Delbem, A. C. B. (2015). Effect of tyrosol on adhesion of *Candida albicans* and *Candida glabrata* to acrylic surfaces. *Medical Mycology*, 53(7), 656-665.
201. Moralez, A. T. P., Perini, H. F., Furlaneto-Maia, L., Almeida, R. S., Panagio, L. A., & Furlaneto, M. C. (2016). Phenotypic switching of *Candida tropicalis* is associated with cell damage in epithelial cells and virulence in *Galleria mellonella* model, *Virulence* 7(4), 379-386.
202. Morris, G. M., Ruth, H., Lindstrom, W., Sanner, M. F., Belew, R. K., Goodsell, D. S., & Olson, A. J. (2009). Software news and updates AutoDock4 and AutoDockTools4: Automated docking with selective receptor flexibility. *Journal of Computational Chemistry*, 30(16), 2785-2791.
203. Muhammed, M., Kourkoumpetis, T., & Mylonakis, E. (2018). *Critical care secrets E-Book*. Elsevier

204. Mukherjee, P. K., Chandra, J., Kuhn, D. M., & Ghannoum, M. A. (2003). Mechanism of fluconazole resistance in *Candida albicans* biofilms: phase-specific role of efflux pumps and membrane sterols. *Infection and Immunity*, 71(8), 4333-4340.
205. Mukherjee, P. K., Chandra, J., Retuerto, M., Sikaroodi, M., Brown, R. E., Jurevic, R., Salata, R.A., Lederman, M.M., Gillevet, P.M., & Ghannoum, M. A. (2014). Oral mycobiome analysis of HIV-infected patients: identification of *Pichia* as an antagonist of opportunistic fungi. *PLoS Pathogens*, 10(3), e1003996.
206. Mukherjee, P. K., Mohamed, S., Chandra, J., Kuhn, D., Liu, S., Antar, O. S., Munyon, R., Mitchell, A.P., Andes, D., Chance, M. R., & Rouabhia, M. (2006). Alcohol dehydrogenase restricts the ability of the pathogen *Candida albicans* to form a biofilm on catheter surfaces through an ethanol-based mechanism. *Infection and Immunity*, 74(7), 3804-3816.
207. Natsoulis, G., Hilger, F., & Fink, G. R. (1986). The HTS1 gene encodes both the cytoplasmic and mitochondrial histidine tRNA synthetases of *S. cerevisiae*. *Cell*, 46(2), 235-243.
208. Nazzaro, F., Fratianni, F., Coppola, R., & Feo, V. De. (2017). Essential oils and antifungal activity. *Pharmaceuticals*, 10(4), 86.
209. Nazzaro, F., Fratianni, F., De Martino, L., Coppola, R., & De Feo, V. (2013). Effect of essential oils on pathogenic bacteria. *Pharmaceuticals*, 6(12), 1451-1474.
210. Negri, M., Silva, S., Henriques, M., & Oliveira, R. (2012). Insights into *Candida tropicalis* nosocomial infections and virulence factors. *European Journal of Clinical Microbiology and Infectious Diseases*, 31(7), 1399-1412.
211. Nett, J. E., & Andes, D. (2015). Fungal biofilms: in vivo models for discovery of anti-biofilm drugs. *Microbiology Spectrum*, 3(3), E30.
212. Nett, J. E., Cain, M. T., Crawford, K., & Andes, D. R. (2011). Optimizing a *Candida* biofilm microtiter plate model for measurement of antifungal susceptibility by XTT assay. *Journal of Clinical Microbiology*, 49(4), 1426-1433.
213. Nikawa, H., Nishimura, H., Yamamoto, T., Hamada, T., & Samaranayake, L. P. (1996). The role of saliva and serum in *Candida albicans* biofilm formation on denture acrylic surfaces. *Microbial Ecology in Health and Disease*, 9(1), 35-48.
214. Nikawa, Hiroki, Nishimura, H., Hamada, T., Kumagai, H., & Samaranayake, L. P. (1997). Effects of dietary sugars and saliva and serum on *Candida* biofilm formation on

- acrylic surfaces. *Mycopathologia*, 139(2), 87-91.
215. Nishijima, C. M., Ganey, E. G., Mazzardo-Martins, L., Martins, D. F., Rocha, L. R. M., Santos, A. R. S., & Hiruma-Lima, C. A. (2014). Citral: a monoterpene with prophylactic and therapeutic anti-nociceptive effects in experimental models of acute and chronic pain. *European Journal of Pharmacology*, 736, 16-25.
216. Nóbrega, R. de O., Teixeira, A. P. de C., Oliveira, W. A. de, Lima, E. de O., & Lima, I. O. (2016). Investigation of the antifungal activity of carvacrol against strains of *Cryptococcus neoformans*. *Pharmaceutical Biology*, 54(11), 2591-2596.
217. O'Boyle, N. M., Banck, M., James, C. A., Morley, C., Vandermeersch, T., & Hutchison, G. R. (2011). Open Babel: An Open chemical toolbox. *Journal of Cheminformatics*, 3(1), 33.
218. Ohkawa, H., Ohishi, N., & Yagi, K. (1979). Assay for lipid peroxides in animal tissues by thiobarbituric acid reaction. *Analytical Biochemistry*, 95(2), 351-358.
219. Onishi, J., Mainz, M., Thompson, J., Curotto, J., Dreikorn, S., Rosenbach, M., Douglas, C., Abruzzo, G., Flattery, A., Kong, L., & Cabello, A. (2000). Discovery of novel antifungal (1, 3)- β -D-glucan synthase inhibitors. *Antimicrobial Agents and Chemotherapy*, 44(2), 368-377.
220. Ortiz, M. I., González-García, M. P., Ponce-Monter, H. A., Castañeda-Hernández, G., & Aguilar-Robles, P. (2010). Synergistic effect of the interaction between naproxen and citral on inflammation in rats. *Phytomedicine*, 18(1), 74-79.
221. Oussalah, M., Caillet, S., & Lacroix, M. (2006). Mechanism of action of Spanish oregano, Chinese cinnamon, and savory essential oils against cell membranes and walls of *Escherichia coli* O157: H7 and *Listeria monocytogenes*. *Journal of Food Protection*, 69(5), 1046-1055.
222. Paiva, L. C. F., Vidigal, P. G., Donatti, L., Svidzinski, T. I. E., & Consolaro, M. E. L. (2012). Assessment of *in vitro* biofilm formation by *Candida* species isolates from vulvovaginal candidiasis and ultrastructural characteristics. *Micron*, 43(2-3), 497-502.
223. Panagoda, G. J., Ellepola, A. N. B., & Samaranyake, L. P. (1998). Adhesion to denture acrylic surfaces and relative cell-surface hydrophobicity of *Candida parapsilosis* and *Candida albicans*. *Apmis*, 106(7-12), 736-742.
224. Pandey, A., Madan, M., Goel, S., Asthana, A., & Sardana, V. (2012). Neonatal candidemia: A changing trend. *Indian Journal of Pathology and Microbiology*, 51(1),

132-133.

225. Pannanusorn, S., Fernandez, V., & Römling, U. (2013). Prevalence of biofilm formation in clinical isolates of *Candida* species causing bloodstream infection. *Mycoses*, 56(3), 264-272.
226. Pappas, P. G., Lionakis, M. S., Arendrup, M. C., Ostrosky-Zeichner, L., & Kullberg, B. J. (2018). Invasive candidiasis. *Nature Reviews Disease Primers*, 4, 18026.
227. Parahitiyawa, N. B., Samaranayake, Y. H., Samaranayake, L. P., Ye, J., Tsang, P. W. K., Cheung, B. P. K., Yau, J.Y.Y., & Yeung, S. K. W. (2006). Interspecies variation in *Candida* biofilm formation studied using the Calgary biofilm device. *Apmis*, 114(4), 298-306.
228. Park, M. J., Gwak, K. S., Yang, I., Kim, K. W., Jeung, E. B., Chang, J. W., & Choi, I. G. (2009). Effect of citral, eugenol, nerolidol and α -terpineol on the ultrastructural changes of *Trichophyton mentagrophytes*. *Fitoterapia*, 80(5), 290-296.
229. Parks, L. W., & Casey, W. M. (1995). Physiological implications of sterol biosynthesis in yeast. *Annual Review of Microbiology*, 49, 95-116.
230. Peixoto, L. R., Rosalen, P. L., Ferreira, G. L. S., Freires, I. A., de Carvalho, F. G., Castellano, L. R., & de Castro, R. D. (2017). Antifungal activity, mode of action and anti-biofilm effects of *Laurus nobilis* Linnaeus essential oil against *Candida* spp. *Archives of Oral Biology*, 73, 179-185.
231. Pekmezovic, M., Aleksic, I., Barac, A., Arsic-Arsenijevic, V., Vasiljevic, B., Nikodinovic-Runic, J., & Senerovic, L. (2016). Prevention of polymicrobial biofilms composed of *Pseudomonas aeruginosa* and pathogenic fungi by essential oils from selected Citrus species. *FEMS Pathogens and Disease*, 74(8), ftw102.
232. Perlin, D. S. (2011). Current perspectives on echinocandin class drugs, 6(4), 441-457.
233. Perlin, D. S., Seto-Young, D., & Monk, B. C. (1997). The Plasma Membrane H⁺-ATPase of Fungi: A Candidate Drug Target?. *Annals of the New York Academy of Sciences*, 834(1), 609-617.
234. Pérot, S., Sperandio, O., Miteva, M. A., Camproux, A. C., & Villoutreix, B. O. (2010). Druggable pockets and binding site centric chemical space: A paradigm shift in drug discovery. *Drug Discovery Today*, 15(15-16), 656-667.
235. Peyrot, F., & Ducrocq, C. (2008). Potential role of tryptophan derivatives in stress responses characterized by the generation of reactive oxygen and nitrogen species.

- Journal of Pineal Research*, 45(3), 235-246.
236. Pfaffl, M. W. (2001). A new mathematical model for relative quantification in real-time RT-PCR. *Nucleic Acids Research*, 29(9), e45.
237. Pfaller, M. A., Diekema, D. J., Gibbs, D. L., Newell, V. A., Ellis, D., Tullio, V., Rodloff, A., Fu, W., & Ling, T. A. (2010). Results from the artemis disk global antifungal surveillance study, 1997 to 2007: A 10.5-year analysis of susceptibilities of *Candida* species to fluconazole and voriconazole as determined by CLSI standardized disk diffusion. *Journal of Clinical Microbiology*, 48(4), 1366-1377.
238. Pfaller, M. A., Rhomberg, P. R., Messer, S. A., Jones, R. N., & Castanheira, M. (2015). Isavuconazole, micafungin, and 8 comparator antifungal agents' susceptibility profiles for common and uncommon opportunistic fungi collected in 2013: Temporal analysis of antifungal drug resistance using CLSI species-specific clinical breakpoints and prop. *Diagnostic Microbiology and Infectious Disease*, 82(4), 303-313.
239. Pfaller, M. A. (2012). Antifungal drug resistance: Mechanisms, epidemiology, and consequences for treatment. *American Journal of Medicine*, 125(1), S3-S13.
240. Pfaller, M. A., Moet, G. J., Messer, S. A., Jones, R. N., & Castanheira, M. (2011). *Candida* bloodstream infections: Comparison of species distributions and antifungal resistance patterns in community-onset and nosocomial isolates in the SENTRY Antimicrobial Surveillance Program, 2008-2009. *Antimicrobial Agents and Chemotherapy*, 52(2), 561-566.
241. Pierce, C. G., Uppuluri, P., Tristan, A. R., Wormley Jr, F. L., Mowat, E., Ramage, G., & Lopez-Ribot, J. L. (2008). A simple and reproducible 96-well plate-based method for the formation of fungal biofilms and its application to antifungal susceptibility testing. *Nature Protocols*, 3(9), 1494-1500.
242. Pierrel, F., Bestwick, M. L., Cobine, P. A., Khalimonchuk, O., Cricco, J. A., & Winge, D. R. (2007). Coa1 links the Mss51 post-translational function to Cox1 cofactor insertion in cytochrome c oxidase assembly. *The EMBO Journal*, 26(20), 4335-4346.
243. Pina-Vaz, C., Rodrigues, A. G., Pinto, E., Costa-de-Oliveira, S., Tavares, C., Salgueiro, L., L., Cavaleiro, C., Gonçalves, M.J., & Martinez-de-Oliveira, J. (2004). Antifungal activity of *Thymus* oils and their major compounds. *Journal of the European Academy of Dermatology and Venereology*, 18(1), 73-78.
244. Pitarch, A., Molero, G., Moteoliva, L., Thomas, D. P., López-Ribot, J. L., Nombela, C.,

- & Gil, C. (2007). Proteomics in *Candida* species. *Candida: Comparative and Functional Genomics*, 169-194.
245. Rabin, N., Zheng, Y., Opoku-Temeng, C., Du, Y., Bonsu, E., & Sintim, H. O. (2015). Biofilm formation mechanisms and targets for developing antibiofilm agents. *Future Medicinal Chemistry*, 7(4), 493-512.
246. Radford, D. R., Challacombe, S. J., & Walter, J. D. (1998). Adherence of phenotypically switched *Candida albicans* to denture base materials. *International Journal of Prosthodontics*, 11(1), 75-81.
247. Rajput, S. B., & Karuppaiyl, S. M. (2013). Small molecules inhibit growth, viability and ergosterol biosynthesis in *Candida albicans*. *SpringerPlus*, 2(1), 26.
248. Ramage, G., Wickes, B. L., & Lopez-Ribot, J. L. (2001). Biofilms of *Candida albicans* and their associated resistance to antifungal agents. *American Clinical Laboratory*, 20(7), 42.
249. Ramage, G., Mowat, E., Jones, B., Williams, C., & Lopez-Ribot, J. (2009). Our current understanding of fungal biofilms. *Critical Reviews in Microbiology*, 35(4), 340-355.
250. Ramage, G., Rajendran, R., Sherry, L., & Williams, C. (2012). Fungal biofilm resistance. *International Journal of Microbiology*, 2012, 528521.
251. Ramage, G., Saville, S. P., Wickes, B. L., & López-Ribot, J. L. (2002). Inhibition of *Candida albicans* biofilm formation by farnesol, a quorum-sensing molecule. *Applied Environmental Microbiology*, 68(11), 5459-5463.
252. Ramage, G., VandeWalle, K., Wickes, B. L., & López-Ribot, J. L. (2001). Standardized method for *in vitro* antifungal susceptibility testing of *Candida albicans* biofilms. *Antimicrobial Agents and Chemotherapy*, 45(9), 2475-2479.
253. Rammanee, K., & Hongpattarakere, T. (2011). Effects of tropical *Citrus* essential oils on growth, aflatoxin production, and ultrastructure alterations of *Aspergillus flavus* and *Aspergillus parasiticus*. *Food and Bioprocess Technology*, 4, 1050-1059.
254. Requena, R., Vargas, M., & Chiralt. (2019). Eugenol and carvacrol migration from PHBV films and antibacterial action in different food matrices. *Food Chemistry*, 277, 38-45.
255. Reynaud, A. H., Nygaard-Østby, B., Bøygard, G., Eribe, E. R., Olsen, I., & Gjermo, P. (2001). Yeasts in periodontal pockets. *Journal of Clinical Periodontology*, 28(9), 860-864.

256. Rice, E. L. (1987). Allelopathy: an overview. In *Allelochemical: Role in Agriculture in Forestry*. American Chemical Society Symposium Series, ACS Publications, 330, 8-22.
257. Robbins, N., Caplan, T., & Cowen, L. E. (2017). Molecular evolution of antifungal drug resistance. *Annual Review of Microbiology*, 71(1), 753-775.
258. Rodero, L., Mellado, E., Rodriguez, A. C., Salve, A., Guelfand, L., Cahn, P., Cuenca-Estrella, M., Davel, G., & Rodriguez-Tudela, J. L. (2003). G484S amino acid substitution in lanosterol 14- α demethylase (ERG11) is related to fluconazole resistance in a recurrent *Cryptococcus neoformans* clinical isolate. *Antimicrobial Agents and Chemotherapy*, 47(11), 3653-3656.
259. Rogers, P. D., Vermitsky, J. P., Edlind, T. D., & Hilliard, G. M. (2006). Proteomic analysis of experimentally induced azole resistance in *Candida glabrata*. *Journal of Antimicrobial Chemotherapy*, 58(2), 434-438.
260. Saddiq, A. A., Khayyat, S. A. (2010). Chemical and antimicrobial studies of monoterpene: Citral. *Pesticide Biochemistry and Physiology*, 98(1), 89-93.
261. Samaranayake, L. P., Hughes, A., & MacFarlane, T. W. (1984). The proteolytic potential of *Candida albicans* in human saliva supplemented with glucose. *Journal of Medical Microbiology*, 17(1), 13-22.
262. Samaranayake, L. P., & MacFarlane, T. W. (1981). The adhesion of the yeast *Candida albicans* to epithelial cells of human origin in vitro. *Archives of Oral Biology*, 26(10), 815-820.
263. Samaranayake, L. P., & MacFarlane, T. W. (1990). *Oral candidosis*. Wright Publishing Company.
264. Samaranayake, Y. H., Wu, P. C., Samaranayake, L. P., & So, M. (1995). Relationship between the cell surface hydrophobicity and adherence of *Candida krusei* and *Candida albicans* to epithelial and denture acrylic surfaces. *Apmis*, 103(7-8), 707-713.
265. Samaranayake, Y. H., Ye, J., Yau, J. Y. Y., Cheung, B. P. K., & Samaranayake, L. P. (2005). *In vitro* method to study antifungal perfusion in *Candida* biofilms. *Journal of Clinical Microbiology*, 43(2), 818-825.
266. Sandai, D., Tabana, Y. M., El Ouweini, A., & Ayodeji, I. O. (2016). Resistance of *Candida albicans* biofilms to drugs and the host immune system. *Jundishapur Journal of Microbiology*, 9(11), 1-7.
267. Sanglard, D. (2016). Emerging threats in antifungal-resistant fungal pathogens.

Frontiers in Medicine, 3(11), 1-10.

268. Sanglard, D., Coste, A., & Ferrari, S. (2009). Antifungal drug resistance mechanisms in fungal pathogens from the perspective of transcriptional gene regulation. *FEMS Yeast Research*, 9(7), 1029-1050.
269. Sardi, J. C. O., Scorzoni, L., Bernardi, T., Fusco-Almeida, A. M., & Mendes Giannini, M. J. S. (2013). *Candida* species: Current epidemiology, pathogenicity, biofilm formation, natural antifungal products and new therapeutic options. *Journal of Medical Microbiology*, 62(1), 10-24.
270. Seneviratne, C. J., Wang, Y., Jin, L., Abiko, Y., & Samaranayake, L. P. (2008). *Candida albicans* biofilm formation is associated with increased anti-oxidative capacities. *Proteomics*, 8(14), 2936-2947.
271. Serefko, A., Chudzik, B., & Malm, A. (2006). *In vitro* activity of caspofungin against planktonic and sessile *Candida* sp. cells. *Polish Journal of Microbiology*, 55(2), 133-137.
272. Sharma, N., & Tripathi, A. (2008). Effects of *Citrus sinensis* (L.) Osbeck epicarp essential oil on growth and morphogenesis of *Aspergillus niger* (L.) Van Tieghem. *Microbiological Research*, 163, 337-344.
273. Shen, Q., Zhou, W., Li, H., Hu, L., & Mo, H. (2016). ROS involves the fungicidal actions of thymol against spores of *Aspergillus flavus* via the induction of nitric oxide. *PLoS One*, 11(5), e0155647.
274. Sheng, C., Miao, Z., Ji, H., Yao, J., Wang, W., Che, X., Dong, G., Lü, J., Guo, W., & Zhang, W. (2009). Three-dimensional model of lanosterol 14 α -demethylase from *Cryptococcus neoformans*: Active-site characterization and insights into azole binding. *Antimicrobial Agents and Chemotherapy*, 53(8), 3487-3495.
275. Shevchenko, A., Tomas, H., Havli, J., Olsen, J. V, & Mann, M. (2006). In-gel digestion for mass spectrometric characterization of proteins and proteomes. *Nature Protocols*, 1(6), 2856-2860.
276. Shin, D. H., Jung, S., Park, S. J., Kim, Y. J., Ahn, J. M., Kim, W., & Choi, W. (2005). Characterization of thiol-specific antioxidant 1 (TSA1) of *Candida albicans*. *Yeast*, 22(11), 907-918.
277. Shin, J. H., Kee, S. J., Shin, M. G., Kim, S. H., Shin, D. H., Lee, S. K., Suh, S.P., & Ryang, D. W. (2002). Biofilm production by isolates of *Candida* species recovered from nonneutropenic patients: Comparison of bloodstream isolates with isolates from other

- sources. *Journal of Clinical Microbiology*, 40(4), 1244-1248.
278. Shreaz, S., Sheikh, R. A., Rimple, B., Hashmi, A. A., Nikhat, M., & Khan, L. A. (2010). Anticandidal activity of cinnamaldehyde, its ligand and Ni(II) complex: Effect of increase in ring and side chain. *Microbial Pathogenesis*, 49, 75-82.
279. Silva-Dias, A., Miranda, I. M., Branco, J., Monteiro-Soares, M., Pina-Vaz, C., & Rodrigues, A. G. (2015). Adhesion, biofilm formation, cell surface hydrophobicity, and antifungal planktonic susceptibility: relationship among *Candida* spp. *Frontiers in Microbiology*, 6, 205.
280. Silva, C. de B. da, Guterres, S. S., Weisheimer, V., & Schapoval, E. E. S. (2008). Antifungal activity of the lemongrass oil and citral against *Candida* spp. *Brazilian Journal of Infectious Diseases*, 12(1), 63-66.
281. Simpson, R. J. (2011). Preparation of extracts from yeast. *Cold Spring Harbor Protocols*, 2011(1), pdb-prot5545.
282. Singh, S., Malhotra, R., Grover, P., Bansal, R., Galhotra, S., Kaur, R., & Jindal, N. (2017). Antimicrobial resistance profile of Methicillin-resistant *Staphylococcus aureus* colonizing the anterior nares of health-care workers and outpatients attending the remotely located tertiary care hospital of North India. *Journal of Laboratory Physicians*. 9(4), 317-321.
283. Singh, S., Fatima, Z., & Hameed, S. (2016). Citronellal-induced disruption of membrane homeostasis in *Candida albicans* and attenuation of its virulence attributes. *Revista Da Sociedade Brasileira de Medicina Tropical*, 49(4), 465-472.
284. Siqueira Jr, J. F., & Sen, B. H. (2004). Fungi in endodontic infections. *Oral Surgery, Oral Medicine, Oral Pathology, Oral Radiology, and Endodontology*, 97(5), 632-641.
285. Smith, R. L., Cohen, S. M., Doull, J., Feron, V. J., Goodman, J. I., Marnett, L. J., Portoghese, P.S., Waddell, W.J., Wagner, B.M., & Adams, T. B. (2005). GRAS flavoring substances 22. *Food Technology*, 59(8), 24-62.
286. Sogin, E. M., Anderson, P., Williams, P., Chen, C. S., & Gates, R. D. (2014). Application of ¹H-NMR metabolomic profiling for reef-building corals. *PLoS One*, 9(10), e111274.
287. Sousa, J., Costa, A., Leite, M., Guerra, F., Silva, V., Menezes, C., Pereira, F., & Lima, E. (2016). Antifungal activity of citral by disruption of ergosterol biosynthesis in fluconazole resistant *Candida tropicalis*. *International Journal of Tropical Disease*

Health, 11(4), 1-11.

288. Spencer, J., Phister, T. G., Smart, K. A., & Greetham, D. (2014). Tolerance of pentose utilising yeast to hydrogen peroxide-induced oxidative stress. *BMC Research Notes*, 7(1), 151.
289. Srivastava, V., Singla, R. K., & Dubey, A. K. (2018). Emerging virulence, drug resistance and future anti-fungal drugs for *Candida* pathogens. *Current Topics in Medicinal Chemistry*, 18(9), 759-778.
290. Stadtman, E. R., & Berlett, B. S. (1997). Reactive oxygen-mediated protein oxidation in aging and disease. *Chemical Research in Toxicology*, 10(5), 485-494.
291. Stević, T., Berić, T., Šavikin, K., Soković, M., Godevac, D., Dimkić, & Stanković, S. (2014). Antifungal activity of selected essential oils against fungi isolated from medicinal plant. *Industrial Crops and Products*, 55, 116-122.
292. Stewart, P. S. (2015). Antimicrobial tolerance in biofilms. *Microbiol Spectrum*, 3(3).
293. Stochaj, W. R., Berkelman, T., & Laird, N. (2007). Mass spectrometry-compatible silver staining. *Cold Spring Harbor Protocols*, 2007(5), pdb-prot4742.
294. Suhr, M. J., & Hallen-Adams, H. E. (2015). The human gut mycobiome: pitfalls and potentials—a mycologist's perspective. *Mycologia*, 107(6), 1057-1073.
295. Suliman, H. S., Appling, D. R., & Robertus, J. D. (2007). The gene for cobalamin-independent methionine synthase is essential in *Candida albicans*: A potential antifungal target. *Archives of Biochemistry and Biophysics*, 467, 218-226.
296. Sun, L., Liao, K., & Wang, D. (2015). Effects of magnolol and honokiol on adhesion, yeast-hyphal transition, and formation of biofilm by *Candida albicans*. *PLoS One*, 10(2), e0117695.
297. Sun, X., Lu, H., Jiang, Y., & Cao, Y. (2013). CaIPF19998 reduces drug susceptibility by enhancing the ability of biofilm formation and regulating redox homeostasis in *Candida albicans*. *Current Microbiology*, 67(3), 322-326.
298. Taff, H. T., Nett, J. E., & Andes, D. R. (2012). Comparative analysis of *Candida* biofilm quantitation assays. *Sabouraudia*, 50(2), 214-218.
299. Tan, T. Y., Tan, A. L., Tee, N. W. S., Ng, L. S. Y., & Chee, C. W. J. (2010). The increased role of non-*albicans* species in candidaemia: results from a 3-year surveillance study. *Mycoses*, 53(6), 515-521.

300. Tao, N., OuYang, Q., & Jia, L. (2014). Citral inhibits mycelial growth of *Penicillium italicum* by a membrane damage mechanism. *Food Control*, 41, 116-121.
301. Tascini, C., Sozio, E., Corte, L., Sbrana, F., Scarparo, C., Ripoli, A., Bertolino, G., Merelli, M., Tagliaferri, E., Corcione, A., & Bassetti, M. (2018). The role of biofilm forming on mortality in patients with candidemia: a study derived from real world data. *Infectious Diseases*, 50(3), 214-219.
302. Taweechaisupapong, S., Aieamsaard, J., Chitropas, P., & Khunkitti, W. (2012). Inhibitory effect of lemongrass oil and its major constituents on *Candida* biofilm and germ tube formation. *South African Journal of Botany*, 81, 95–102.
303. Thaweboon, S., & Thaweboon, B. (2009). *In vitro* antimicrobial activity of *Ocimum americanum* L. essential oil against oral microorganisms. 40(5), 1025-1033.
304. Thein, Z. M., Samaranayake, Y. H., & Samaranayake, L. P. (2007). *In vitro* biofilm formation of *Candida albicans* and non-*albicans Candida* species under dynamic and anaerobic conditions. *Archives of Oral Biology*, 52(8), 761-767.
305. Thomas, D. P., Bachmann, S. P., & Lopez-Ribot, J. L. (2006). Proteomics for the analysis of the *Candida albicans* biofilm lifestyle. *Proteomics*, 6(21), 5795-5804.
306. Thomas, D. P., Pitarch, A., Monteoliva, L., Gil, C., & Lopez-Ribot, J. L. (2006). Proteomics to study *Candida albicans* biology and pathogenicity. *Infectious Disorders-Drug Targets (Formerly Current Drug Targets-Infectious Disorders)*, 6(4), 335-341.
307. Thota, N., Koul, S., Reddy, M. V, Sangwan, P. L., Khan, I. A., Kumar, A., Raja, A.F., Andotra, S.S., & Qazi, G. N. (2008). Citral derived amides as potent bacterial NorA efflux pump inhibitors. *Bioorganic & Medicinal Chemistry*, 16(13), 6535-6543.
308. Tice, R. R., Agurell, E., Anderson, D., Burlinson, B., Hartmann, A., Kobayashi, H., Miyamae, Y., Rojas, E., Ryu, J.C., & Sasaki, Y. F. (2000). Single cell gel/comet assay: guidelines for *in vitro* and *in vivo* genetic toxicology testing. *Environmental and Molecular Mutagenesis*, 35(3), 206-221.
309. Tolba, H., Moghrani, H., Benelmouffok, A., Kellou, D., & Maachi, R. (2015). Essential oil of Algerian *Eucalyptus citriodora*: Chemical composition, antifungal activity. *Journal de Mycologie Medicale*, 25(4), e128-e133.
310. Trindade, L. A., de Araújo Oliveira, J., de Castro, R. D., & de Oliveira Lima, E. (2015). Inhibition of adherence of *C. albicans* to dental implants and cover screws by *Cymbopogon nardus* essential oil and citronellal. *Clinical Oral Investigations*, 19(9),

2223-2231.

311. Tsui, C., Kong, E. F., & Jabra-Rizk, M. A. (2016). Pathogenesis of *Candida albicans* biofilm. *FEMS Pathogens and Disease*, 74(4), ftw018.
312. Tumbarello, M., Fiori, B., Treçarichi, E. M., Posteraro, P., Losito, A. R., De Luca, A., Sanguinetti, M., Fadda, G., Cauda, R., & Posteraro, B. (2012). Risk factors and outcomes of candidemia caused by biofilm-forming isolates in a tertiary care hospital. *PloS One*, 7(3), e33705.
313. Tyagi, A. K., & Malik, A. (2010). Liquid and vapour-phase antifungal activities of selected essential oils against *Candida albicans*: microscopic observations and chemical characterization of *Cymbopogon citratus*. *BMC Complementary and Alternative Medicine*, 10(1), 65.
314. Udayalaxmi, S. J., D'Souza, D. (2014). Comparison between virulence factors of *Candida albicans* and non-*albicans* species of *Candida* isolated from genitourinary tract. *Journal of clinical and diagnostic research: JCDR*, 8(11), DC15.
315. Ullmann, A. J., Sanz, M. A., Tramarin, A., Barnes, R. A., Wu, W., Gerlach, B. A., Krobot, K. J., Gerth, W. C. and Longitudinal Evaluation of Antifungal Drugs (LEAD I) Investigators. (2006). Prospective study of amphotericin B formulations in immunocompromised patients in 4 European countries. *Clinical Infectious Diseases*, 43(4), e29–e38.
316. Ultee, A., Bennik, M. H. J., & Moezelaar, R. (2002). The phenolic hydroxyl group of carvacrol is essential for action against the food-borne pathogen *Bacillus cereus*. *Applied Environmental Microbiology*, 68(4), 1561-1568.
317. Uppuluri, P., Chaturvedi, A. K., Srinivasan, A., Banerjee, M., Ramasubramaniam, A. K., Köhler, J. R., Kadosh, D., & Lopez-Ribot, J. L. (2010). Dispersion as an important step in the *Candida albicans* biofilm developmental cycle. *PLoS Pathogens*, 6(3), e1000828.
318. Usta, J., Kreydiyyeh, S., Barnabe, P., Bou-Moughlabay, Y., & Nakkashchmaisse, H. (2003). Comparative study on the effect of cinnamon and clove extracts and their main components on different types of ATPases. *Human & Experimental Toxicology*, 22(7), 355-362.
319. Van Acker, H., Van Dijck, P., & Coenye, T. (2014). Molecular mechanisms of antimicrobial tolerance and resistance in bacterial and fungal biofilms. *Trends in*

- Microbiology*, 22(6), 326-333.
320. Veien, N. K., Rosner, K., & Skovgaard, G. L. (2004). Is tea tree oil an important contact allergen? *Contact Dermatitis*, 50(6), 378-379.
321. Velluti, A., Sanchis, V., Ramos, A. J., Turon, C., & Marin, S. (2004). Impact of essential oils on growth rate, zearalenone and deoxynivalenol production by *Fusarium graminearum* under different temperature and water activity conditions in maize grain. *Journal of Applied Microbiology*, 96(4), 716-724.
322. Vieira, A. L. G., Linares, E., Augusto, O., & Gomes, S. L. (2009). Evidence of a Ca²⁺-NO-cGMP signaling pathway controlling zoospore biogenesis in the aquatic fungus *Blastocladiella emersonii*. *Fungal Genetics and Biology*, 46(8), 575-584.
323. Vinogradov, A. D. (1999). Mitochondrial ATP synthase: fifteen years later. *BIOCHEMISTRY C/C OF BIOKHMIIA*, (11), 1219-1229.
324. Vollbrecht, P., Janistyn, B., Gross, K., Bonzon, M., & Wagner, E. (1987). Forest decline-endogenous monoterpenes as mediators and amplifiers of environmental-stress. In *Experientia*, 43, 664-665.
325. Wagner, H. (2011). Synergy research: approaching a new generation of phytopharmaceuticals. *Fitoterapia*, 82(1), 34-37.
326. Wiederstein, M., & Sippl, M. J. (2007). ProSA-web: interactive web service for the recognition of errors in three-dimensional structures of proteins. *Nucleic Acids Research*, 35(suppl_2), W407-W410.
327. Williams, J. H., Phillips, T. D., Jolly, P. E., Stiles, J. K., Jolly, C. M., & Aggarwal, D. (2004). Human aflatoxicosis in developing countries: a review of toxicology, exposure, potential health consequences, and interventions. *The American Journal of Clinical Nutrition*, 80(5), 1106-1122.
328. Wösten, H. A. B. (2001). Hydrophobins: multipurpose proteins. *Annual Reviews in Microbiology*, 55(1), 625-646.
329. Wu, X. Z., Cheng, A. X., Sun, L. M., & Lou, H. X. (2008). Effect of plagiocin E, an antifungal macrocyclic bis(bibenzyl), on cell wall chitin synthesis in *Candida albicans*. *Acta Pharmacologica Sinica*, 29(12), 1478-1485.
330. Wu, Y., OuYang, Q., & Tao, N. (2016). Plasma membrane damage contributes to antifungal activity of citronellal against *Penicillium digitatum*. *Journal of Food Science and Technology*, 53(10), 3853-3858.

331. Xess, I., Jain, N., Hasan, F., Mandal, P., & Banerjee, U. (2007). Epidemiology of candidemia in a tertiary care centre of North India: 5-Year study. *Infection*, 35(4), 356-259.
332. Xie, X. M., Fang, J. R., & Xu, Y. (2004). Study of antifungal effect of cinnamaldehyde and citral on *Aspergillus flavus*. *Food Science*, 25(9), 32-34.
333. Yike, I. (2011). Fungal proteases and their pathophysiological effects. *Mycopathologia*, 171(5), 299-323.
334. Yutani, M., Hashimoto, Y., Ogita, A., Kubo, I., Tanaka, T., & Fujita, K. (2011). Morphological changes of the filamentous fungus *Mucor mucedo* and inhibition of chitin synthase activity induced by anethole. *Phytotherapy Research*, 25(11), 1707-1713.
335. Zhao, X., Daniels, K. J., Oh, S. H., Green, C. B., Yeater, K. M., Soll, D. R., & Hoyer, L. L. (2006). *Candida albicans* Als3p is required for wild-type biofilm formation on silicone elastomer surfaces. *Microbiology*, 152(8), 2287-2299.
336. Zore, G. B., Thakre, A. D., Jadhav, S., & Karuppayil, S. M. (2011). Terpenoids inhibit *Candida albicans* growth by affecting membrane integrity and arrest of cell cycle. *Phytomedicine*, 18(13), 1181-1190.

Publications out of this thesis work:

1. **Apurva Chatrath**, Rashmi Gangwar, Poonam Kumari, Ramasare Prasad (2019) In Vitro Anti-Biofilm Activities of Citral and Thymol Against *Candida tropicalis*. *Journal of Fungi*, 5(1), 13.
2. **Apurva Chatrath**, Poonam Kumari, Rashmi Gangwar, Ramasare Prasad (2018) Investigation of Differentially Expressed Proteins of *Candida tropicalis* Biofilm in Response to Citral. *Journal of Proteomics and Bioinformatics*, 11(2), 57-61.
3. **Apurva Chatrath**, Manish Chokker, Poonam Kumari, Rashmi Gangwar and Ramasare Prasad. Delineating the Differentially Expressed Proteome and Variations in Extracellular Matrix of *Candida tropicalis* Biofilm in Response to Citral. (In Communication).

Other related publications:

1. Poonam Kumari, Neha Arora, **Apurva Chatrath**, Rashmi Gangwar, Vikas Pruthi, Krishna Mohan Poluri and Ramasare Prasad (2019) Delineating the Biofilm Inhibition Mechanisms of Phenolic and Aldehydic Terpenes against *Cryptococcus neoformans*. *ACS Omega* 4(18), 17634-17648.
2. Anchal Sharma, Vijay Kumar, **Apurva Chatrath**, Aditya Dev, Ramasare Prasad, Ashwani Kumar Sharma, Shailly Tomar and Pravindra Kumar (2018) *In vitro* Metal Catalyzed Oxidative Stress in DAH7PS: Methionine Modification Leads to Structure Destabilization and Induce Amorphous Aggregation. *International Journal of Biological Macromolecules* 106, 1089-1106.
3. Poonam Kumari, Rutusmita Mishra, Neha Arora, **Apurva Chatrath**, Rashmi Gangwar, Partha Roy and Ramasare Prasad (2017) Antifungal and Anti-Biofilm Activity of Essential Oil Active Components against *Cryptococcus neoformans* and *Cryptococcus laurentii*. *Frontiers in Microbiology*, 8, 2161.
4. Rashmi Gangwar, Poonam Kumari, **Apurva Chatrath** and Ramasare Prasad. Characterization of Recombinant Manganese-superoxide dismutase (*NeMnSOD*) from *Nerium oleander*. (In communication)



CONFERENCES

1. **Apurva Chatrath**, Anchal Sharma, Poonam Kumari, Rashmi Gangwar and Ramasare Prasad. *In silico* molecular docking studies of azoles against lanosterol-14- α -demethylase protein (Erg11p) from *Candida tropicalis*. International Conference on Advances in Biosciences and Biotechnology, **1-3 February 2018**, IIIT Noida. (Poster Presentation)
2. **Rashmi Gangwar**, Poonam Kumari, **Apurva Chatrath** and Ramasare Prasad. Isolation and Characterization of Full-length Mn-Superoxide dismutase gene from Xerophytic plant *NeIIITR*. 9th International Meeting NextGen Genomics, Biology, Bioinformatics and Technologies (NGBT) Conference, **30 September- 2 October, 2019**, Mumbai, India. (Poster Presentation)
3. **Poonam Kumari**, Neha Arora, **Apurva Chatrath**, Rashmi Gangwar, Dinesh Kumar, Krishna Mohan Poluri and Ramasare Prasad. Deciphering the Biofilm Eradication Mechanism of Thymol against *Cryptococcus neoformans* Using Multiomics approach. 8th American Society of Microbiology (ASM) Conference on Biofilms, **7-11 October, 2018**, Washington DC, United States. (Poster Presentation)
4. **Poonam Kumari**, Neha Arora, **Apurva Chatrath**, Rashmi Gangwar, Vikas Pruthi and Ramasare Prasad. Anti-biofilm activity of Essential oil Active components against *Cryptococcus neoformans* and their safety prospects. American Chemical Society on Campus, **7 February 2018**, IIT Roorkee. (Poster Presentation) (BEST POSTER AWARD)
5. **Poonam Kumari**, Neha Arora, **Apurva Chatrath**, Rashmi Gangwar, Vikas Pruthi and Ramasare Prasad. Alterations of Cell Membrane Integrity and Extracellular Polysaccharides Matrix of *Cryptococcus neoformans* Biofilm on Exposure to Essential Oil Active Components. International Conference on Advances in Biosciences and Biotechnology, **1-3 February 2018**, IIIT Noida. (Poster Presentation)
6. Rajbala Yadav, **Apurva Chatrath**, Poonam Kumari, Awadhesh Kumar and Ramasare Prasad. *In silico* studies and functional validation of salt inducible *S6PDH* gene in rice using RNAi technology. International Conference on 'Molecular Signaling: Recent Trends in Biomedical and Translational Research' (ICMS: RTBTR-2014), **17-19 December 2014**, IIT Roorkee. (Poster Presentation)